UNIVERSITÀ DEGLI STUDI DI TRIESTE

XXVIII CICLO DEL

DOTTORATO DI RICERCA IN NANOTECNOLOGIE

NANO-ENGINEERED ADHESIVE BIOMATERIALS FOR BIOMEDICAL APPLICATIONS

(SSD BIO/10 – Biochimica)

DOTTORANDA

Francesca Scognamiglio

COORDINATORE DELLA SCUOLA

Prof. **Lucia Pasquato**

SUPERVISORE DI TESI

Dott. **Ivan Donati**

TUTORE DI TESI

Dott. **Andrea Travan**

ANNO ACCADEMICO 2014 / 2015

UNIVERSITÀ DEGLI STUDI DI TRIESTE

XXVIII CICLO DEL DOTTORATO DI RICERCA IN NANOTECNOLOGIE

NANO-ENGINEERED ADHESIVE BIOMATERIALS FOR BIOMEDICAL APPLICATIONS

Settore scientifico-disciplinare: SSD BIO/10

DOTTORANDA

FRANCESCA SCOGNAMIGLIO

COORDINATORE

PROF. LUCIA PASQUATO

SUPERVISORE DI TESI

DOTT. IVAN DONATI

TUTORE DI TESI

DOTT. ANDREA TRAVAN

ANNO ACCADEMICO 2014 / 2015

Acknowledgments

I would like to thank Prof. Sergio Paoletti,
my supervisor Dr. Ivan Donati, my tutor Dr. Andrea Travan,
Dr. Massimiliano Borgogna, Dr. Eleonora Marsich,
Dr. Michela Cok and Dr. Gianluca Turco
for what they taught me, for their help and support.
I thank Davide Porrelli, Pasquale Sacco, Lorena Tarusha,
Ilaria Geremia, Federica Vecchies and all the students of the Biomat group
for sharing with me this experience.
Thank you all for being much more than the research group where I did my PhD.

I thank my parents, Antonio, Elisa,
Gianluca and all my friends for being the most important part of my life.

Finally, I acknowledge all the people
I worked with and I encountered during this wonderful trip.

Table of content

Summary

This thesis is focused on the development of adhesive systems for biomedical applications and has been carried out in the framework of the European Project "AnastomoSEAL" (EU-FP7). Within this project, a bioactive membrane based on polysaccharides was developed for the prevention of anastomotic leakage (AL) after colo-rectal cancer (CRC) resection. The membrane was designed to be wrapped around the intestinal tissue in order to stimulate the healing of the surgical wound, thus accelerating its closure. The main components of the system were the two polysaccharides alginate and hyaluronan (HA), the former representing the physical matrix, the latter exerting a bioactive function in the terms of stimulating the healing of wounds. The main goals of this thesis were to manufacture and characterize the membranes and to design tissue-adhesives that could be implemented in the medical device. In the first part of the work, the procedure for the membrane preparation was set up, followed by the characterization of the product as to its mechanical, chemical and biological properties. The membranes were prepared by freeze-drying alginate-HA hydrogels crosslinked by calcium ions (Ca^{2+}). Several formulations of the membrane were screened to tailor its performance in the terms of mechanical resistance, stiffness and deformation. *In vitro* biological test pointed out the the non-cytotoxicity of the membranes, as well as the ability of the released HA to stimulate the healing of fibroblasts. Degradation tests and release studies were performed to predict the *in vivo* behavior of the membrane, pointing out that, in simulated physiological conditions, the release of HA occurs during the first hours, whereas a complete degradation of the membrane is achieved in 21 days. Sterilized membranes were also characterized to investigate the effect of terminal sterilization on the membrane properties; in particular, the effect of supercritical carbon dioxide ($scCO_2$) supplemented with H_2O_2 was studied. In parallel, adhesive strategies were designed and tailored to the peculiar features of both membrane and intestinal tissue.

The adhesive strategies developed in this thesis were based either on the use of exogenous compounds (*i.e.* H_2O_2), or on the use of molecules displaying bioadhesive properties. In the first case, adhesion studies proved the enhancement of the adhesion strength between membrane and tissue after the treatment with H_2O_2, and pointed out the ability of this compound to induce the formation of an adhesive interface made of gelatin, which was integrated in the structure of the tissue. In the latter case, bio-inspired adhesive strategies were designed considering the adhesion mechanism employed by natural organisms (*i.e.* mussels).

The key adhesive molecules of mussel's adhesive (*i.e.* catechol-based compounds) were implemented into the structure of the membrane by chemical modifications. *In vitro* adhesion tests showed an improved adhesion of the modified-membrane in simulated physiological conditions, which was confirmed *in vivo* by preliminary adhesion studies.

A second mussel-inspired adhesive strategy was based on the development of nanoparticles displaying a catecholic core, named melanin-like nanoparticles (MNPs). MNPs were characterized from a biological point of view and used to prepared adhesive coatings for the AnastomoSEAL membrane, whose adhesive properties were evaluated by *in vitro* adhesion tests. In conclusion, the tests performed allowed the development of a medical device endowed with adhesive components that enabled an efficient adhesion in a physiological environment.

Sommario

Il presente lavoro di tesi è incentrato sullo sviluppo di sistemi adesivi per applicazioni biomediche e si configura all'interno del Progetto Europeo "AnastomoSEAL" (EU-FP7). Questo progetto aveva come scopo lo sviluppo di una membrana bioattiva a base di polisaccaridi, per la prevenzione della deiscenza anastomotica, che può verificarsi successivamente alla resezione chirurgica del tratto di intestino affetto da carcinoma colo-rettale. La membrana è stata concepita per essere avvolta attorno al tratto di intestino interessato da sutura, al fine di stimolare e accelerare la chiusura della ferita chirurgica. Le principali componenti di questa membrana sono i polisaccaridi alginato e acido ialuronico (HA), i quali rappresentano rispettivamente la matrice fisica del sistema e la componente bioattiva che stimola il processo di guarigione delle ferite. I principali obiettivi di questa tesi riguardavano lo sviluppo della membrana e di sistemi adesivi che possono essere implementati nel dispositivo medico finale. Nella prima parte, è stata messa a punto la procedura per la preparazione delle membrane, le quali sono state caratterizzate dal punto di vista meccanico, chimico e biologico. Le membrane sono state ottenute mediante un processo di liofilizzazione di idrogeli a base di alginato-HA, reticolati mediante l'impiego di ioni calcio (Ca^{2+}). Sono state preparate membrane a diversa formulazione per modulare le proprietà in termini di resistenza a trazione, rigidità e deformabilità. Test biologici *in vitro* hanno dimostrato la non-citotossicità delle membrane e l'abilità dell'HA rilasciato dalla membrana di stimolare la migrazione e la proliferazione di fibroblasti. Studi di degradazione e di rilascio sono stati effettuati per predire il comportamento della membrana *in vivo* e hanno evidenziato che, in condizioni simil-fisiologiche, l'HA viene rilasciato durante le prime ore, mentre la completa degradazione della membrane avviene in circa 21 giorni. Le membrane sterilizzate sono state caratterizzate per valutare l'effetto della sterilizzazione terminale sulle proprietà della membrana; in particolare, è stato valutato l'effetto della sterilizzazione mediante CO_2 supercritica ($scCO_2$) in presenza di acqua ossigenata (H_2O_2). In parallelo, sono state sviluppate delle strategie adesive specifiche per il dispositivo medico finale, considerando le caratteristiche della membrana e del tessuto intestinale. Le strategie adesive sviluppate in questa tesi erano basate sull'impiego di composti esogeni (*i.e.* H_2O_2) o sull'uso di molecole con proprietà bioadesive. Nel primo caso, gli studi di adesività hanno dimostrato un aumento della forza adesiva, successivamente al trattamento con H_2O_2, indicando che questo composto consente di indurre modifiche del collagene tissutale portando alla formazione di

un'interfaccia adesiva costituita da gelatina. Nel secondo caso, sono state sviluppate strategie adesive inspirate a meccanismi di adesione impiegati da organismi naturali (*i.e.* mitili). Le molecole chiave delle sostanze adesive secrete dei mitili (*i.e.* molecole catecoliche) sono state implementate nella struttura della membrana, mediante modifiche chimiche. Test di adesione *in vitro* hanno dimostrato che in condizioni simil-fisiologiche, le membrane modificate presentano un'aumentata adesività, proprietà confermata da studi preliminari *in vivo*.

Una seconda strategia adesiva ha previsto l'impiego di nanoparticelle che presentano un struttura catecolica, denominate nanoparticelle *melanin-like* (MNPs). Le MNPs sono state caratterizzate dal punto di vista biologico e impiegate per la preparazione di rivestimenti adesivi per le membrane, valutate mediante test di adesione *in vitro*. In conclusione, i test effettuati hanno consentito lo sviluppo di un dispositivo medico integrato con componenti adesive che permettono un'adesione efficace in ambiente fisiologico.

List of publications

- **Scognamiglio F**, Travan A, Rustighi I, Tarchi P, Palmisano S, Marsich E, Borgogna M, Donati I, de Manzini N, Paoletti S. 2015. "Adhesive and sealant interfaces for general surgery applications". Journal of Biomedical Materials Research Part B: Applied Biomaterials 2015 Apr 1;n/a.

- Travan A, **Scognamiglio F**, Borgogna M, Marsich E, Donati I, Tarusha L, Grassi M, Paoletti S. 2015. "Hyaluronan delivery by polymer demixing in polysaccharide-based hydrogels and membranes for biomedical applications" (*submitted to "Carbohydrate Polymers"*).

- **Scognamiglio F**, Travan A, Borgogna M, Donati I, Marsich E, Bosmans J, Perge L, Foulc MP, Bouvy N, Paoletti S. "Enhanced bioadhesivity of dopamine-functionalized polysaccharidic membranes for general surgery applications" (*submitted to "Acta Biomaterialia"*).

- **Scognamiglio F**, Travan A, Blanchy M, Borgogna M, Donati I, Marsich E, Bosmans J, Foulc MP, Bouvy N, Paoletti S. "Sterilization of polysaccharide-based membranes by supercrtitical carbon dioxide" (*in preparation*).

- **Scognamiglio F**, Travan A, Borgogna M, Donati I, Marsich E, Paoletti S. "H_2O_2 caused improved adhesion between a polysaccharide-based membrane and the intestinal serosa" (*in preparation*).

- **Scognamiglio F**, Travan A, Borgogna M, Donati I, Marsich E, Paoletti S. "H_2O_2 caused improved adhesion between a polysaccharide-based membrane and the intestinal serosa" (*in preparation*).

- **Scognamiglio F**, Travan A, Borgogna M, Donati I, Marsich E, Paoletti S. "Melanin nanoparticles as adhesive coatings of membranes for wound healing applications" (*in preparation*).

- Borgogna M, Bosmans JWAM, Donati I, Marsich E, **Scognamiglio F**, Travan A, Bouvy N, Paoletti S. "Hyaluronan-based membranes for the healing of intestinal anastomoses" (*in preparation*).

List of abbreviations

AIMDD	active implantable medical devices		**iCMBAs**	injectable citrate-enabled mussel-insired bioadhesives
AL	anastomotic leakage		**IQ**	indo-5,6-quinone
ASTM	American Society for Testing Materials		**LDH**	lactate dehydrogenase
CRC	Colo-rectal cancer		**LDV**	laser doppler velocimetry
DHI	dihydroxyindole		**LSGS**	low serum growth supplement
DLS	dynamic light scattering		**L-DOPA**	L-3,4-dihydroxyphenylalanine
DMEM	Dulbecco's modified eagle's medium		**MALLS**	multi angle laser light scattering
DMSO	dimethyl sulfoxide		**MES**	2-(N-Morpholino) ethanesulfonic acid
D-Alg	dopamine-modified alginate		**MTT**	3-(4,5-Dimethylthiazol-2-yl)-2,5-Diphenyltetrazolium Bromide;
D-AlgM	dopamine-modified alginate membrane		**Mefps**	mytilus edulis foot proteins
ECM	extracellular matrix		**Mn**	numeric molecular weight
EDC	C1-ethyl-3-[3-(dimethylamino)propyl] carbodiimide hydrochloride		**MNPs**	melanin-like nanoparticles
FDA	Food and Drug Administration		**NHS**	N-hydroxusuccinimide
FBS	fetal bovine serum		**PDGF**	platelet-derived growth factor
GAGs	glycosaminoglycans		**PdI**	polydispersivity index
GDL	D-Gluconic acid δ-lactone		**PEG**	polyethylene glycol
GI	gastrointestinal		**PGSA**	polyglycerolcosebacate acrylate
HA	hyaluronic acid		**ppm**	parts per milion
HBSS	Hank's balanced salt solution		**RI**	refractive index
HDFa	human dermal fibroblasts adult		**SBF**	simulated body fluids
HEPES	4-(2-hydroxyethyl)piperazine-1-ethanesulfonic acid		**SEC**	size exclusion chromatography
H&E	hematoxylin and eosin		**$scCO_2$**	supercritical carbon dioxide
^{1}H-NMR	protonic nuclear magnetic resonance			

1. INTRODUCTION

1.1. COLORECTAL CANCER DISEASE

1.1.1. Incidence, mortality and survival

Colorectal cancer (CRC) is the third most common form of cancer and the fourth most common cancer cause of death in the world (1), accounting for 9.4% of all cancer incidence in men and 10.1% in women (2;3). The incidence of CRC varies in the different countries, although the highest rates are reported in Europe, Australia, New Zealand, Canada and United States, pointing out that it is a disease mainly affecting countries with a Western culture (2). Although a general increase of the survival rate has been reported since 1960s due to the accessibility to specialized health-care techniques (4), CRC still represents the worldwide main cause of morbidity and mortality (5). The rate of survival increases according to the stage at diagnosis: in general, the earlier the stage of cancer progression at the diagnosis, the higher the chance of survival. Indeed, it has been estimated that in the case of localized cancers, the survival rate reaches 90%, while it decreases to 70% and 10% in the case of regional and metastatic cancers, respectively (4;6). Despite the availability of modern diagnostic approaches and screening programs have improved the early cancer detection and treatment, no significant variation of the CRC incidence have been recorded over the years (3).

1.1.2. Risk factors of CRC

Risk factors such as the elderly, the occurrence of inflammatory bowel diseases, the heredity, the environmental parameters and the lifestyle have been associated to the incidence of CRC. The mean age of patients at the diagnosis is 73 years old, although already at the age of 70, at least 50% of the Western population develops some forms of CRC, spanning from early benign polyps to invasive adenocarcinomas (7;8). Adenomas often represent precursor lesions of colorectal cancer and almost 95% of sporadic CRC develops from these alterations (9) in a time-frame of 5 to 10 years (10;11). The early detection of adenomas, followed by their surgical removal can reduce the risk of CRC occurrence (12). Some forms of CRC are related to hereditary conditions such as the familial adenomatous polyposis (FAP) and the hereditary non-polyposis colorectal cancer, known also as the Lynch syndrome (13), which are caused by alterations of genes involved in the DNA repair mechanism (MLH1 and MSH2 genes) and

in the tumor suppressor gene APC, respectively (14). The occurrence of inflammatory bowel diseases such as the ulcerative colitis and Crohn's disease are also some of the factors that may increase the risk of developing CRC up to 20 folds (9;15). The lifestyle and environmental parameters can also influence the CRC development. Indeed, diets poor in fruits and vegetable or rich in fats as well as the high consumption of meat are considered some major risks for CRC, since in the digestive tract the accumulation of food metabolites can create a favorable environment for the development of a bacterial flora capable of degrading bile salts and lead to the formation of potentially carcinogenic nitric compounds (2;9;16;17).

The physical inactivity and the overweight or obesity conditions account from a fourth to a third of colorectal cancers. Although the underlying mechanism have not been elucidated yet, it is believed that the physical activity improves the metabolic rate and the gut motility and that it reduces the blood pressure and the insulin resistance-causing diabetes (1;3;18).

Smoking and alcohol consumption are also associated to the onset of CRC (19;20). Indeed, some alcohol metabolites such as acetaldehyde can exert a carcinogenic action. Similarly, smoking can cause DNA mutations, whose repair mechanisms are less efficient whether the alcohol consumption occurs. Moreover, alcohol can act as a solvent to favor the penetration of carcinogenic molecules into mucosa cells, thus enhancing the predisposition to tumor (21).

1.2. THE ANASTOMOTIC LEAKAGE

1.2.1. Medical need

Despite the availability of modern health care techniques and screening programs have allowed some improvements in the early diagnosis of CRC over the years, the curative management is mainly surgical and is based on the resection of the affected bowel, followed by the suture of the two extremities, in order to restore the normal transit (22;23). The site at which the bowel continuity is restored is called anastomosis and the most frequent post-operative complication of any bowel resection is the anastomotic leakage (AL), which occurs when no proper tissue regeneration takes place at the site of anastomosis (24;25) (figure 1).

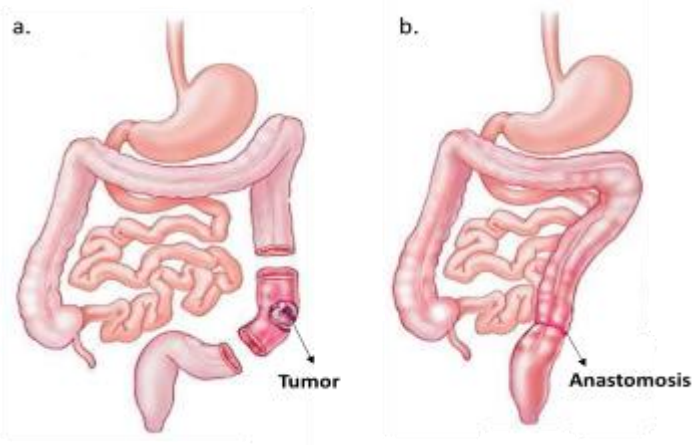

Figure 1. Intestinal bowel affected by cancer (a); anastomosis performed after CRC resection (b).

The general incidence of AL averages approximately around 10%, but it can be higher in the case of distal rectal cancers and much lower for cancers affecting the proximal colon tract (26). The rate of AL after rectal cancer surgery varies according to different countries, reaching the maximum value of 21% and leading to mortality in up to 39.3% of cases (27).

From a clinical point of view, the patients developing this complication need an additional number of radiographic studies and extra nursing along with long hospital stays that further increase the costs for medical care. Moreover, these patients often display a generalized peritonitis that turns out in the need of a re-intervention with a subsequent increase in morbidity and mortality (28-30).

The surgical intervention of CRC resection can be performed by hand-sewing or by mechanical stapling devices, through both laparoscopic and open surgery approaches, with no significant difference in the incidence of AL between the two techniques. However, some surgical aspects such as a technically difficult operation (*i.e.* a narrow deep pelvis, the

presence of a bulk tumor and a more advanced local stage of disease) or a reduced vitality of the treated tract, due to an excessive skeletonization of the proximal colonic stump, have been identified as possible causes of AL (31).

Both systemic and surgical aspects can contribute to the onset of AL, although this complication also occurs in patients with no apparent predisposition (32): parameters such as malnutrition, co-occurrence of metabolic diseases, organ failures, elderly, immunosuppression and neo-adjuvant therapies are considered some of the main risk factors (33;34). Other factors are male gender, smoking, obesity, alcohol abuse, the use of anti-inflammatory drugs, the preoperative transfusion and the contamination of the operative field (35-37).

1.2.2. Surgical-based treatment for treatment of anastomotic leakage (AL)

In spite of the strong social, economic and medical impact of AL, at present only some surgical solutions aimed at reducing its clinical impact are available for surgeons, in the specific case of mid or low rectal cancers or when a combination of high-risk variables for AL are present. For instance, after CRC resection, the realization of a defunctioning stoma (*i.e.* ileostomy) for fecal diversion accounts for a significant decrease of the severity and an easier management of AL (38). However, the presence of a temporary ileostomy can add other clinical complications, such as tendency to dehydration and the imbalance of electrolytes, especially in elderly patients, and it makes necessary a second operation during which the ileostomy is resected and a new anastomosis is performed. Moreover, the closure of a defunctioning stoma can result in a long-term anorectal disfunction (39). Defunctioning stomas are created in up to 73% of the patients treated for rectal cancer to avoid complications due to anastomotic dehiscence. Nevertheless, even in such situation, the leakage may occur in up to 32% of these patients. Thus, the use of a diverting stoma can reduce the risk of reoperation and post-operative death if leakage occurs, but it seems not to decrease the leakage rate (40).

In case of AL occurrence, the type of treatment depends on the severity of the clinical conditions and on the entity of the leakage (height and the flow volume of leakage). The treatment can range from percutaneous drainage to peri-anastomotic collection under ultrasound or CT-guidance to a major re-intervention. A portion of patients with AL can be managed conservatively, meaning to treat patients without performing any surgical intervention, but this approach often leads to a very long hospitalization. In a retrospective study conducted on 67 patients affected by AL after rectal cancer surgery, only 1.5% had a

conservative treatment, 1.5% underwent a surgical lavage and drainage operation with the creation of a diverting stoma not previously performed, while in 67.2% of patients a second resection with a new anastomosis was performed. In 11.9% of cases, there was a recurrent leakage rate. In the same paper, a more demolitive operation such as Hartmann's resection was needed in almost 30% of patients (41). This operation consists in the detachment of the former anastomosis, followed by the closure of the distal rectal stump and the creation of an end-colostomy. According to the age and general conditions of the patient, a subsequent new major abdominal operation called "reversal of Hartmann's" can be proposed, carrying again all the high morbidity and mortality risks mentioned for colorectal surgery, especially in old patients. The restoration of continuity after Hartmann's procedure can be done in up to 63% of cases, leading to a large number of patients to keep the colostomy all life long (41). Finally, in a very small group of patients developing a life-threatening peritonitis with sepsis and multi organ failures, an emergency life-saving surgery such as laparostomy can be necessary. In this case, the patient needs a longer hospital stay, meaning an enormous amount of resources. Following recovery, morbidity will be accompanied by restoration of bowel continuity and abdominal wall reconstruction after laparostomy.

These surgical methods are very invasive, debilitating and not fully efficient; therefore the prognosis and the health care of this pathology have not met any considerable improvement recently. **Nowadays, there are no efficient solutions for the prevention of the AL**, but only some surgical-based techniques to limit its consequences at the clinical level. Hence, this complication represents the major concern associated to the CRC resection. Given the serious impact on the patient's life and on the cost of the medical care associated to its occurrence, **the availability of devices and methods capable to prevent the AL and to limit its serious consequences appear as a strong need.**

1.2.3. Commercial products employed for the prevention of AL

Despite some surgical methods aimed at reducing the clinical impact of AL are being available nowadays, the high morbidity and mortality in patients undergoing AL justify the requirement of efficient solutions for decreasing the rate of failure (42). The absence of commercial products specifically tailored to the AL led clinicians to perform preclinical studies to test the effectiveness of biomaterials designed for general surgery and different applications, in the prevention of AL. In the last years, some biomaterials in the form of patches and membranes were tested in animals. For instance, in a porcine model, collagen-

based patches from small intestinal submucosa (SIS) have shown some beneficial effects in anastomotic sealing (42). However, the risk of animal source contamination and bowel obstruction, along with the occurrence of ulcers on the luminal surface remain serious concerns (43;44).

TachoComb® – Nycomed is a fibrin-collagen patch for topical hemostatic applications and whose effectiveness during the early healing period of colonic anastomoses was tested in rats. These patches were proved to support the anastomotic integrity, although they also caused an inflammatory reaction which may increase the time required for the healing process (45). Similarly, *TachoSil® – Nycomed*, a different collagen-based patch coated with the coagulation factors fibrinogen and thrombin, was used for the sealing of both colorectal (46) and gastrointestinal anastomoses (47). The first study was performed in a mice model and it pointed out a beneficial effect in terms of healing, although the underlying molecular mechanisms were not elucidated (46). In the second case, the material was tested on a porcine model, but the results did not point out any difference between sealed and unsealed controls (47). Conversely, autogenic grafts displayed bad anastomotic healing attributed to the avascularity of grafts and to aggravated adhesions between intestine and intra-abdominal organs (48).

ForeSeal® – Brothier, a bioabsorbable sleeve for lung staple-line reinforcement that can be used with surgical staplers, has shown hemostatic and healing properties, but clinical trials are only related to lung applications (49).

Hemo-ionic® – Brothier, an alginate-based material developed in the form of fibers, has been used as a non-resorbable haemostatic agent for rectal cancer surgery; this product may reduce the drainage volume but it did not show any clinical advantage over traditional techniques (50).

Another material developed for the general treatment of soft tissues is the copolymer poly(glycolic acid):trimethylene carbonate. This material has been used to produce the commercial product *Gore® Bio-A®*, a synthetic resorbable web in the form of sheets acting as a tissue reinforcement which, however, was not specifically designed for intestinal anastomosis.

The *ePTFE – Gore®*, an expanded poly(tetrafluoroethylene) sleeve, is a device displaying a good biocompatibility and handling, although these sleeves are non-resorbable, a feature that represents a limit for applications such as the prevention of AL, given the need to avoid a re-intervention (51).

Technical improvements to the surgical precedures have been reached by the use of synthetic, bioresorbable staple line reinforcements (*e.g. Gore® SeamGuard®*). However, their use has only slightly decreased the rate of leakage in these operations (42).

As shown by this literature overall, these biomaterials were not capable of satisfy entirely the clinical need of AL occurrence, thus pointing out the need of developing tailored biomaterials.

1.3. THE ANASTOMOSEAL PROJECT

1.3.1. General overview of the AnastomoSEAL project

The European project "AnastomoSEAL" was focused on responding to the widespread clinical need of preventing AL after CRC resection. Indeed, despite the efforts in identifying a possible treatment among the available ones, all the proposed solutions have shown some limitations and drawbacks and a biomaterial that is specifically tailored to the prevention of AL is still missing at the clinical level. A possible solution would be an external reinforcement of intestinal anastomosis through a material that can be wrapped around the intestine (44;46;52). Thus, an appropriate device to reach this objective would be a soft and pliable membrane that can be released *in situ* by the stapling device or applied exogenously to the staple line. Thus, the objective of the AnastomoSEAL project was the development of a bioresorbable biomaterial capable of stimulating the healing of the surgical wound, through the release of a bioactive component that accelerates tissue regeneration in terms of wound healing, during the critical period of tissue healing.

The wound healing occurs in all the organs and tissues of the body through a complex process, at the end of which the migration and proliferation of fibroblasts and the deposition of newly synthetized extracellular matrix (ECM) account for the closure of the wound margins accompanied by scar formation (53;54). Fibroblast cells composing the most external layer of the intestinal bowel are directly involved in tissue healing, since their migration and proliferation account for the closure of wounds. The activity of fibroblasts in terms of migration and proliferation can be stimulated upon exposure to trophic factors such as exogenous hyaluronic acid (HA), as shown by both *in vitro* and *in vivo* tests (55-59).

Given these premises, the proposed biomaterial was designed in the form of soft membrane (patch) mainly composed of the two polysaccharides alginate and HA, representing the physical matrix and the bioactive component, respectively. This patch was intended to be wrapped around the sutured part of the intestine where the HA, once released out of the membrane, stimulates the activity of fibroblasts composing the most external layer of the intestinal wall (serosa). This strategy was designed to promote the physiological process of tissue regeneration, thus preventing or limiting the risk of AL (figure 2).

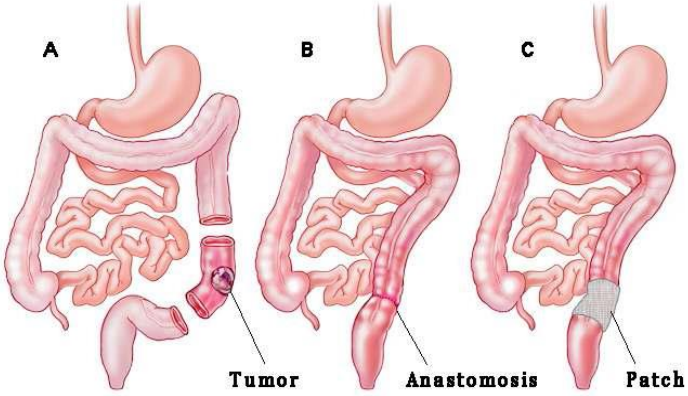

Figure 2. Colorectal cancer resection (A); anastomosis at the extremities of the resected bowel (B); patch wrapped around the anastomosis sealed with sutures (C).

In this perspective, this biomaterial is conceived as a delivery system, enabling the release of the bioactive molecule (HA) at the site of the wound. In order to achieve this goal, the biomaterial is required to adhere to the intestinal serosa and to remain *in situ* for the time-frame required to ensure the cicatrization and remodeling of the anastomosis. After having exerted this function, the biomaterial should undergo degradation within the human body, under the catalysis of hyaluronidase and the hydrolytic activity of body fluids (60). Hence, no second intervention would be required to remove the medical device from the site of implant.

1.3.2. The AnastomoSEAL Consortium

The AnastomoSEAL Consortium involved two academic and four industrial partners, integrating the research and technology development chain, from material design to pre-clinical testing.

Hereafter, the main roles of the partners within the project are described:

- *University of Trieste (UNITS).* UNITS was the coordinator of the project and it was responsible for its management. The main research activities focused on the study and development of biopolymer components and on the manufacturing of the patches, along with a chemical, physical and *in vitro* biological characterization of the materials.
- *University of Maastricht (UNIMA).* UNIMA was involved in the animal studies: its main role was to develop and coordinate the animal models, to test the patches *in vivo*, to perform all the animal experiments and to analyze tissues derived from these animal experiments.

- *SIGEA srl.* SIGEA is a company whose research and development activities are focused on polysaccharides development. Its contribution to the project was related to the production of the patches, according to biological screening feedback, to provide all the chemical background from laboratory tests necessary to the subsequent technological transfer for the industrialization of the membranes.
- *RESCOLL*. It is a private technology center of materials specialized in polymers, composites and surface treatment as well as adhesion and bonding technologies. The contribution within the AnastomoSEAL project was to develop adhesion strategies, to screen possible material reinforcements for the optimization of mechanical resistance of the matrix, to perform the mechanical characterization of adhesives over inert and biological substrates, as well as chromatographic, spectrometry and thermo-mechanical analyses. RESCOLL's activities were also focused on the development and validation of the sterilization process and on the study of the final product performance under accelerated aging simulating storage conditions.
- *FMC BioPolymer*. It is one of the leading manufacturers of biopolymers for pharmaceutical and biomedical applications. The Company manufactures ultrapure alginate as well as ultrapure chitosan and hyaluronan in NovaMatrix, a business unit of FMC BioPolymer. Two technology platforms developed by FMC BioPolymer/NovaMatrix were available to the *Consortium*: *i*) self-gelling alginate (an alginate system with controllable gelation kinetics); *ii*) ultrapure alginate foam with controllable degradation profiles; *iii*) industrial process technology and risk analysis aspects.
- *IMPULS*. It is a Polish company that commercializes innovative products for health-care. The contribution of IMPULS was focused on the following area: *i*) sterilization procedures on patches; *ii*) exploitation studies on both European and Russian markets; *iii*) industrial process technology and risk analysis aspects.

1.3.3. Advances of the AnastomoSEAL project

The proposed biomaterial is based on the polysaccharides alginate and HA, which have been widely used for wound healing applications (55;61-63). The use of the proposed material provides many advantages and benefits over the current surgical techniques for the prevention

and treatment of AL. The major innovative aspects achieved by this project can be outlined as follows:

i. development of an innovative material specifically designed for colorectal anastomosis applications;
ii. use of natural-derived degradable/resorbable polysaccharides. They represent an alternative to synthetic polymers or to proteins such as collagen that can be associated to a severe risk of biological contamination. Natural polysaccharides offer the advantages of being environmental-friendly, produced on large scale and in ultrapure medical grade form. Moreover, these compounds may display several properties such as biocompatibility, biodegradability, bioactivity and bioadhesivity to the target tissue (50;64-66);
iii. development of a patch with the following features: *i*) ease to handle during surgical procedures, *ii*) suitable for both open and laparoscopic techniques, *iii*) designed to have tear strength sufficiently high to support surgical positioning and physiological stresses on the site of implant, *iv*) endowed with adequate adhesive properties to be firmly held in position for the time required to achieve a successful healing;
iv. development of a biomaterial that has the potential to become the material of choice for a non-invasive technique in the prevention of AL.

1.3.4. Social and economical impact of the AnastomoSEAL project on European level

The AL associated to CRC resection leads to serious consequences on both the patients' life and on the costs for health care: the quality of life of a patient suffering from CRC is deeply modified when faced with this diagnosis and it worsens even more when complications occur. A study published in 2008 described how patients with AL had a poorer quality of life, lower body image, poor social activity and a significantly higher depression and anxiety (67). Patients requiring a stoma have to face problems including adapting to the new anatomy, managing the stoma and continuing normal activities in their socio-cultural environment (68). AL has also been associated with increased local recurrence and diminished survival after colorectal cancer surgery (69). The reduced incidence of the AL achieved by the use of the proposed medical devices would result in a short hospital stay, a quick return to daily activity and a good quality of life. It also could allow the patients to start the chemotherapy earlier and potentially prolong the long-term survival. The great impact on the quality of life of patients can be achieved in terms of patient's comfort, since the complications of the actual surgical

proceedings, the number of additional surgical procedures and all the related medical and psychological morbidities can be reduced.

Also the economic impact of the project is significant, especially in relation to the cost of health care and to the potential global growth of the european biomaterials industry. Indeed, the management of AL by the health care system is nowadays very onerous and the economical cost will increase in a linear fashion because of the aging of the population (70). Hence, by decreasing the number of patients suffering from this complication a subsequent decrease of the cost for health care can be achieved. Moreover, the proposed medical device can be exploited also for other applications in the fields of medical devices, considering that AL can occur in every kind of colorectal surgery as well as in the case of intestinal resections performed for inflammatory bowel diseases, diverticular disease, volvulus, perforation, strangulated hernia and ischemic colitis.

Finally, the proposed patch could be employed for other potential applications, in the field of bioactive biomaterials or drug delivery systems, by physical or chemical incorporation of pharmacologically active compounds, or used as a carrier in advanced therapy medicinal products, in combination with cells or plasma derived products. In those cases, the already proven success of the proposed construct in AL treatment would constitute a technological and economical benefit for more demanding applications.

1.3.5. Risk assessment and contingency planning

The proposed patch was mainly composed of alginate and HA. Both of these polysaccharides are approved for human uses and can be produced in large amounts with *Good Manufacturing Practices* (GMP) protocols. Therefore, all the possible risks were analyzed for each crucial research and development step of the project, with respect to the raw materials and to biomaterial processing. The risk assessment and foreseen actions are listed in Table 1.

Additional risks were related to the analysis of economical aspects, to the impacts of the product on the market and to the safety and efficacy of the medical device, based on indications of ISO 14971 that defines the international requirements of risk management for medical devices.

	Technological risk	Risk level	Preventing actions	Technological risk
1	Release of endotoxins from polysaccharides	Very low	Use of ultrapure GMP certified raw materials	
2	Release of toxic byproducts from the polysaccharide derivatives synthesis	Very low	Use of ultrapure GMP certified raw materials and production processes	
3	*In-vivo* biodegradation rate not matching tissue regeneration timing	Medium	Bibliographic study and *in-vitro* tests on the influence of polysaccharide concentration and reticulation on degradation rate	Redesign formulation and reticulation techniques. Modulate polymers crosslinking.
4	Insufficient adhesion of the patch to the intestinal tissue	Medium/High	Development of formulations with different amounts of HA	Use of additional biomimetic adhesive components (*e.g.* chitosan, bio-inspired glue)
5	Non-adequate mechanical properties	Medium	Research of the most suitable polysaccharide concentration and reticulation conditions	Use of biocompatible resorbable reinforcement fibers
6	Modification of chemical and physical properties of the biomaterial induced by sterilization	Medium	Monitor sterilization effect on different formulations; product characterization	Investigation of alternative sterilization techniques (*e.g.* β -radiation, supercritical CO_2)

Table 1. Technological risk assessment and contingency plan.

1.3.6. Regulatory issues for medical devices

In the European Union (EU), the regulatory issue relating to the safety and performance of medical devices has been regulated by three directives, since 1990s:

a. Council Directive 90/385/EEC on Active Implantable Medical Devices (AIMDD) (1990);
b. Council Directive 93/42/EEC on Medical Devices (MDD) (1993);
c. Council Directive 98/79/EC on In Vitro Diagnostic Medical Devices (IVDMD) (1998).

These Directives aim at guarantee a high level of protection for human health and safety. This regulation has been implemented by the Member States and undergone revision on the 26th of September 2012. The "COUNCIL DIRECTIVE of 20th June 1990 on the approximation of the laws of the Member States relating to active implantable medical devices" (90/385/EEC) stated that an active implantable medical device includes "*any active medical device which is intended to be totally or partially introduced, surgically or medically, into the human body or by medical intervention into a natural orifice, and which is intended to remain after the procedure*".

According to the guidelines and definitions of "*MEDICAL DEVICES: Guidance document - Classification of medical devices*" from EUROPEAN COMMISSION, DG HEALTH AND CONSUMER, the AnastomoSEAL product can be classified as a short term, surgically

invasive, non-reusable and for continuous use medical device (Class III). According to the definitions of concept of continuous use, invasiveness and permanence in the human body, a Class III medical device is considered as a surgically invasive one, intended for short-term use (between 60 minutes 30 days). Moreover, the device must exert a biological effect and be wholly or mainly absorbed or undergo chemical changes in the body.

1.4. POLISACCHARIDE-BASED BIOMATERIALS

Polysaccharides are a class of macromolecules whose chemical structures and physical properties make them suitable for the development of biomaterials for diverse purposes, ranking from tissue engineering to drug delivery applications (71;72). As a general consideration, their stereo-regular character confers to polysaccharides the ability to form helical conformations in solution. The stability of their ordered conformation depends on parameters such as temperature, ionic concentration and presence of uronic acid units or ionic substituents in their structure (73;74). The dissolution of polysaccharides in aqueous solutions depends on the pH and it is favoured by their polyelectrolyte character. The presence of –OH functional groups in their structure accounts for the formation of hydrogen bonds stabilizing the cooperative intra and interchain interactions and for the semi-rigid behavior in well-defined thermodynamic conditions (72). All polysaccharides also have a small hydrophobic character in relation to the CH groups (75;76). According to their charge, polysaccharides can be neutral or charge molecules. HA and alginate belong to the class of negatively charged polymers, given the presence of carboxylic groups; amino groups are instead present in chitosan, the only natural cationic polysaccharide.

As previously mentioned, the use of polysaccharides for the manufacturing of biomedical materials provides several advantages over synthetic polymers. For instance, biocompatibility, biodegradability, bioactivity and bioadhesivity are some of the most desired features. Biocompatibility is the ability of materials of not causing any adverse reaction once implanted in the human body (77;78); this feature can be enhanced either by varying the composition or by modifying the chemical structure of the polysaccharides composing biomaterials (79-81).

Biomaterials based on polysaccharides often undergo degradation in the human body. In the field of internal surgery, the availability of biodegradable biomaterials provides the advantage of avoiding a second intervention aimed at the removal of the medical devices from the site of implant, thus increasing the probability to have a successful medical outcome. For instance, in the case of AL prevention, both non-absorbable and absorbable materials are being studied (24), although the former materials seem to display several advantages over non-absorbable reinforcement (82). In the human body, the degradation of polysaccharide-based biomaterials occurs through the catalysis of hydrolases, as in the case of HA, while polymers such as alginate, for which there are no specific enzymes driving hydrolysis, undergo degradation given the contribution of both macrophages and bioerosion mechanisms, before excretion

through kidneys (60). Some natural polysaccharides can modulate biological responses. For instance, HA can positively influence the healing of wounds (83;84), while chitosan can exert an antimicrobial activity (85;86). These features have been exploited for the development of biomaterials devoted to topical applications, for which the stimulation of the wound healing and the absence of microbial infections are required (87;88).

The bioadhesivity of biomaterials is a requisite for materials that can exert their function whether an intimate contact with the target organ is achieved. Polysaccharides can favor this process given to their hydrophilic feature and partially to the presence of surface charges, although adhesive functionalities can be introduced in their chemical structure to enhance the adhesive properties (89). This analysis points out that the most suitable biomaterial for the proposed medical applications can be based on polysaccharides, such as alginate and HA.

1.4.1. Alginate

Alginate was first described in 1881, by the British chemist E.E.E. Standford (90). Alginate is a hydrophilic polysaccharide extracted from brown marine algae such as *Laminaria hyperborea* (91) or soil bacteria such as *Azobacter* and *Pseudomonas* (92;93). Alginate is a linear copolymer consisting of the two sugar residues 1-4 linked β-D-mannuronic acid (M) and α-L-guluronic acid (G). These monomers can arrange to form blocks in which homopolymeric regions (M or G-blocks) are interspersed with regions of alternating structure (MG-blocks) in the polymeric chains (94;95) (figure 3). The G-blocks are stiffer than M-blocks and display a more extended chain conformation, since the rotation around the glycoside bonds is impaired (96;97). Thus, the higher the G blocks content, the lower the intrinsic flexibility of alginate chains (98), while the viscosity of alginate solutions depends mainly on the molecular size (99).

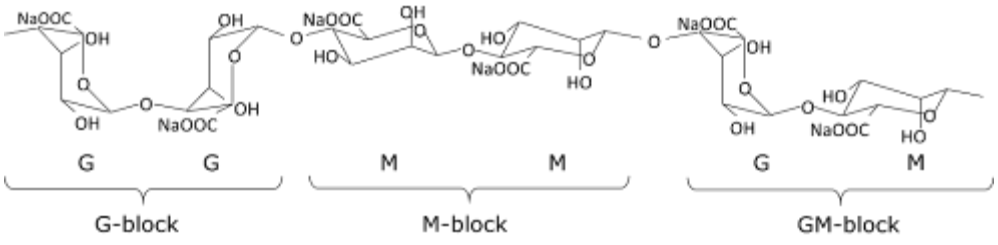

Figure 3. Chemical structure of G, M and GM blocks in alginate.

Alginate has attracted attention for its hydrogel forming ability through an ionic crosslinking mechanism. Indeed, alginates can bind divalent cations such as Ca^{2+}, Sr^{2+} and Ba^{2+} which

bind preferentially to the G-blocks in a highly cooperative manner (100). The binding of divalent cations accounts for the gel forming property of alginate (figure 4b) and this structure has been described by the "egg-box" model. In this model each divalent ion interacts with both two adjacent G-residues and with two G-residues in an opposing chain, leading to the formation of molecular junctions within the gel network (101) (figure 4a). However, these molecular junctions can be formed by involving not only the G-blocks of alginate but also the MG/MG and the GG/MG-blocks (102).

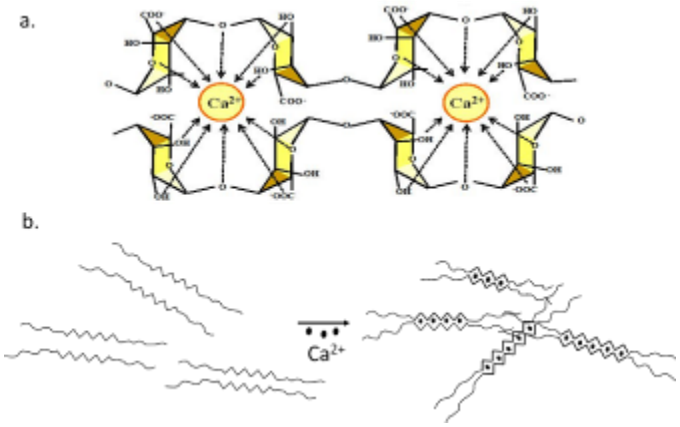

Figure 4. Probable calcium-binding site in a GG-sequence (a); ionic crosslinking of two homopolymeric blocks of G-residues in the egg-box model (b).

The selective binding of cations and the gel forming properties strongly depend on the composition (98) and sequence of alginate (95;103). Likewise, the properties of the gels depend on the molecular characteristics of the alginates, while the stability and the physical properties are related to the G content and to the length of the G blocks (104;105). Indeed, the higher the content of guluronate units, the stronger and more brittle will be the resulting gels; conversely, an increased number of mannuronate leads to the formation of softer and more elastic gels (95).

Alginate-based biomaterials can be manufactured into films (106;107), fibers (108;109), gels (102;110) and foams (111;112), according to their final applications. Alginates have long been known to possess hemostatic properties (113;114) and biomaterials based on them are being employed in several areas of drug delivery and tissue engineering (115). In the human body, alginate-based biomaterials are bio-eroded, partially degraded by macrophages and excreted through kidneys (60).

In the field of wound healing, biomaterials based on alginate offer many advantages such hemostatic properties and the gel-forming ability upon absorption of wound exudates (116;117). Alginate can be mixed with chitosan and silver nanoparticles for the manufacturing

of antibacterial wound dressing, in order to reduce the risk of bacterial infections. Indeed, the non-toxicity and biodegradability of alginate-based wound dressings with antiseptic properties are desirable features (72).

The bioactivity of these dressings is often sought in wound treatment. Literature evidences suggested that *Kaltostat*®, a bioactive alginate dressings, can improve the wound healing by stimulating the production of cytokines such as interleukin-6 (IL-6) and tumor necrosis factor-α (TNF-α) from monocytes; these are some of the pro-inflammatory factors that are beneficial to the healing process (61). In the field of internal surgery, alginate-based dressings have been recently shown to reduce postoperative drainage volume in patients undergoing elective rectal resection for cancer (50).

1.4.2. Hyaluronic acid (HA)

HA is a high molecular weight polysaccharide discovered in 1934 by Karl Meyer and John Palmer in the vitreous of bovine eyes (118). Nowadays, this polysaccharide can be produced on a large scale by *Streptococcus zooepidemicus* and *Streptococcus equi* with good yield and high purity (119). HA is a linear polysaccharide belonging to the family of glycosaminoglycans (GAGs), the main constituents of the extracellular matrix (ECM), and it is composed of D-glucuronic acid and D-N-acetylglucosamine linked together through alternating beta-1,4 and beta-1,3 glycoside bonds (120) (figure 5).

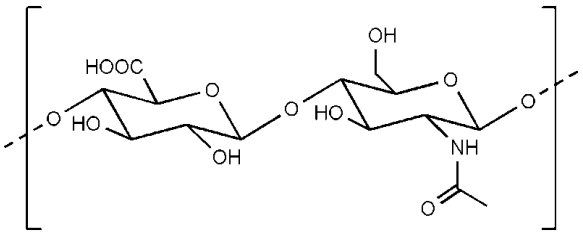

Figure 5. Repeating units of hyaluronic acid.

At physiological pH values, it has a polyanionic structure that imparts excellent hydro-coordinating properties and enables the retention of large amounts of water; given its highly hygroscopic behavior, hyaluronan is involved in the regulation of tissue hydration and osmotic balance (121).

HA is also involved in the regulation of several biological phenomena such as cell migration (56;58), differentiation (122;123), growth and adhesion (59;124), angiogenesis (125;126) as

well as the control of the immune response (127;128). In the human body, HA undergoes degradation through enzymatic catalysis (60).

HA is used as a linear polymer in solution at concentrations and molecular weights that depend on the final application. Given the good viscoelastic properties and semi-rigid character of HA, this polysaccharide has been first employed for viscosupplementation in joint diseases (129-131). In addition, its physicochemical properties, non-immunogenicity and high biocompatibility make this polysaccharide suitable for biomedical applications, such as bone, cartilage, skin defects and for the prevention of post-surgical adhesions (132-138).

Mixtures of alginate and HA have been investigated in order to combine the respective peculiar properties of these polysaccharides for various biomedical uses (63;139-142). For instance, alginate hydrogels containing HA have been prepared and proposed for cartilage transplant (143;144), articular surgery (145;146) and wound healing applications (55).

The wound healing ability of HA has been reported in several studies (147) and the interaction between HA and the cell receptor CD44 accounts for this mechanism. CD44 is a trans-membrane receptor widely expressed by most cell types (*e.g.* leukocytes, fibroblasts, endothelial and parenchymal cells) and it is upregulated upon tissue injury and inflammation (148;149). Many functions of CD44 receptor are mediated through interaction with its ligand HA (150). In the context of wound healing, the activation of the CD44 receptor in the presence of chemotactic agents such as HA, leads to the cytoskeletal organization of cells, thereby stimulating fibroblast's migration (151).

The wound healing stimulating ability of HA makes this polysaccharide a good candidate for the development of bioactive polysaccharide-based materials for tissue engineering applications. Several studies report this ability: crosslinked sponges composed of gelatin/HA showed improved wound healing properties over gelatin/alginate or chitosan/HA sponges (152;153). In another study, the administration of HA to the periodontal part was proved to stimulate the healing of the surrounding area (62).

In the field of internal surgery, the injection of autocrosslinked HA-based gels was proved to prevent an excessive scar formation in tendon and peripheral nerve of the hand and in the abdominal-pelvic area. In this last case, the prevention of post-surgical adhesions was also proved and attributed to the HA activity. To explain these results, it has been hypothesized that the HA-rich environment modulate the wound healing process of the peritoneum and is able to restore the gliding function of the tendon and peripheral nerve structures (63).

1.5. PATENTS ON POLYSACCHARIDE-BASED MEMBRANES

Among various polysaccharides, alginate fibers, gels and foams are known to be useful for the preparation of surgical dressings (129-131;154;155). Various types of dressings made of alginate fibers are patented. Most of them act as surgical absorbent hemostats, wound dressings and anti-adhesion barriers at the site of an intra-body trauma. In some patented works, alginate is used in combination with other polymers to obtain specific properties. The most relevant ones include the patent WO/2007/093805, where methods to create composite fibers and films of alginate with carboxymethylcellulose, pectin, hyaluronic acid, chondroitin sulfate, chitosan and other biopolymers are described. A patent by *Edwards et al.* (U.S. Pat. No. 6,809,231) concerns a wound dressing composed of cellulose and alginate, wherein the latter is crosslinked through a poly(carboxylic acid) ester bond to the cellulose of the material. Patent U.S. No. 7,226,972 describes the process to cross-link hyaluronic acid with other polymers as alginate to create biomaterials in the form of film or sheet. These patents prove the interest on polysaccharides such as alginate and HA for the development of biomaterials devoted to the biomedical field.

1.6. TERMINAL STERILIZATION OF BIOMATERIALS BASED ON POLYSACCHARIDES

The sterilization process is a fundamental step in the manufacturing of biomaterials and implantable medical devices. This process is generally carried out through physical or chemical treatments that enable the removal of organic macromolecules and microorganisms in order to prevent infections in patients (156;157). The sterilization procedure usually takes place at the end of the manufacturing chain and the methods used for sterilizing commercial biomedical materials must be approved by the Food and Drug Administration (FDA) (156). Several sterilization techniques are being used to this aim and the choice of the most suitable method is typically done according to the nature of the biomaterial, the impact on material properties and the type of potential contaminants (157). Regarding polymer-based biomaterials, it has been reported that the FDA approved terminal sterilization techniques (*e.g.* steam sterilization, γ-irradiation and ethylene oxide) might have a strong impact on their macromolecular structure, thus affecting the biomaterial properties and limiting the final medical application (156;158;159). For instance, γ-irradiation is well known to cause polymer degradation (158;160), while sterilization by ethylene oxide leads to the retention of toxic residues that can compromise the *in vivo* biocompatibility (161;162). To deal with the main drawbacks of the traditional sterilization methods, the use of supercritical carbon dioxide ($scCO_2$) has been proposed as an alternative sterilization technique (163). The main advantages in the use of the carbon dioxide (CO_2) for the sterilization of materials are related to its non-toxicity, non-inflammability and safety (159) and to the possibility of easily removing it by depressurization and degasing. In its supercritical state, CO_2 has a liquid-like density ($0.9 – 1.0 \times 10^3$ kg m^{-3}) (164), gas-like diffusivity ($10^{-7} – 10^{-8}$ m^2 s^{-1}) and viscosity ($3 – 7 \times 10^{-5}$ N s m^{-2}), and zero surface tension (161), features that enable its ease penetration through materials. Methods based on the use of $scCO_2$ have been reported as effective for sterilizing medical products and bioactive materials (165-167), while the combination of temperature, pressure and sterilization time was reported to influence the efficacy of the process (168). The efficiency of the sterilization can be improved through the addition of compounds such as hydrogen peroxide (H_2O_2), tert-butyl hydroperoxide, and paracetic acid (169;170), which ensures the inactivation of microorganisms, including bacterial endospores of different bacterial species (169;171-175). The use of such addictives allows the employment of milder conditions and shorter times of exposure (161;169;176-178). Despite the promising results regarding the application of $scCO_2$ for the sterilization of biomaterials,

little work has been done in evaluating the changes of the material features after sterilization. For instance, it has been shown that heat-sensitive biomaterials might undergo degradation upon exposure to high temperature and pressure (178); moreover, the use of compounds such as H_2O_2 may cause polymer oxidation and depolymerization (178;179), thus modifying the chemical and physical properties of the biomaterial. With regard to the biocompatibility of sterilized biomaterials, both *in vitro* and *in vivo* evaluations are needed to assess the possible cytotoxic effect that they can exert (171). Indeed, some residues of addictive molecules can be retained within the material structure and exert a toxic effect when released in the human body. Thus, a detailed characterization of the biomaterial is required to evaluate whether these modifications can affect its features along with the final application of the medical device.

1.7. WOUND HEALING PROCESS

Tissue repair and wound healing are complex physiological processes in which the damaged tissue repairs itself after an injury such as superficial cut, internal bleeding, or excision of a tumour (180). A wound is defined as a damage or distruption of the physiological and anatomical structures and functions (54). Wounds can be classified according to different criteria such as the aetiology, the degree of contamination, the morphological characteristics and the communication with hollow or solid organs (181-183). From a clinical point of view, the most common criterium of classification considers the time frame of healing, so that wounds are classified as acute or chronic (181;183;184). Acute wounds are able to repair themselves following the normal healing pathway, thus leading to the restoration of the functional integrity and of the anatomical structures. These wounds are considered as the result of either a traumatic event or a surgical intervention and the time course of healing usually ranges from 5 to 10 days (183;184). Chronic wounds are instead unable to heal following the phases of the normal healing process (183;185) because of the occurrence of pathological factors (182;186). For instance, hypoxia, tissue necrosis and excessive release of inflammatory cytokines are some of the negative factors affecting the healing process and they may retard or disturb one or more stages of tissue healing, thus perpetuating the non-healing state. The wound healing process takes place in all tissues and organs of the body, although the most understood mechanism regards the healing of skin wounds (54). Within this process, it is possible to recognise four different but overlapping phases such as *hemostasis*, *inflammatory response*, *proliferation* and *remodelling* (figure 6).

The *hemostasis* involves biological mechanisms whose principal aim is to stop bleeding from a wound, in order to protect the vascular system. A second goal is to provide a matrix for the migration of cells that are involved in the later phases of healing (54). During this phase, hemostatic events take place together with the activation of the coagulation cascade, so that the final stage regards the formation of a fibrin clot that limits the blood loss (187;188). The *inflammatory* phase is aimed at providing a barrier against micro-organisms. The inflammatory response is characterized by the release of cytokines and the activation of cells of the immune system (*i.e.* monocytes, macrophages, lymphocytes) acting against pathogens and accounting for the degradation of damaged tissue and the creation of healthy one (189). In the *proliferation* phase, the chemotactic agents released by macrophages and neutrophils draw fibroblasts at the wounded site where they proliferate and produce hyaluronan, fibronectin,

poteoglicans and type I and III procollagen composing the ECM (183;190-192). The HA produced during this phase contributes to stimulate cell migration and confers to the tissue the ability to resist to deformation by adsorbing water (193). Collagens are also synthetized by fibroblasts and impart integrity and strength to all tissues (194-196). At the end of this phase, abundant ECM accumulates and provides support to cell migration (191;197). The *remodelling* phase is characterized by the continuous synthesis and breakdown of collagen fibres, being responsible for the development of new epithelium and scar formation (54). These phenomena occur through the contribution of enzymes, cytokines and growth factors (180). During the remodelling phase, the highly disorganized collagen fibres become more oriented and they are cross-linked over time (54). The interactions between fibroblasts and the ECM allow the wound margins to get closer, leading to the formation of a mature scar displaying a high tensile strength (53;198;199).

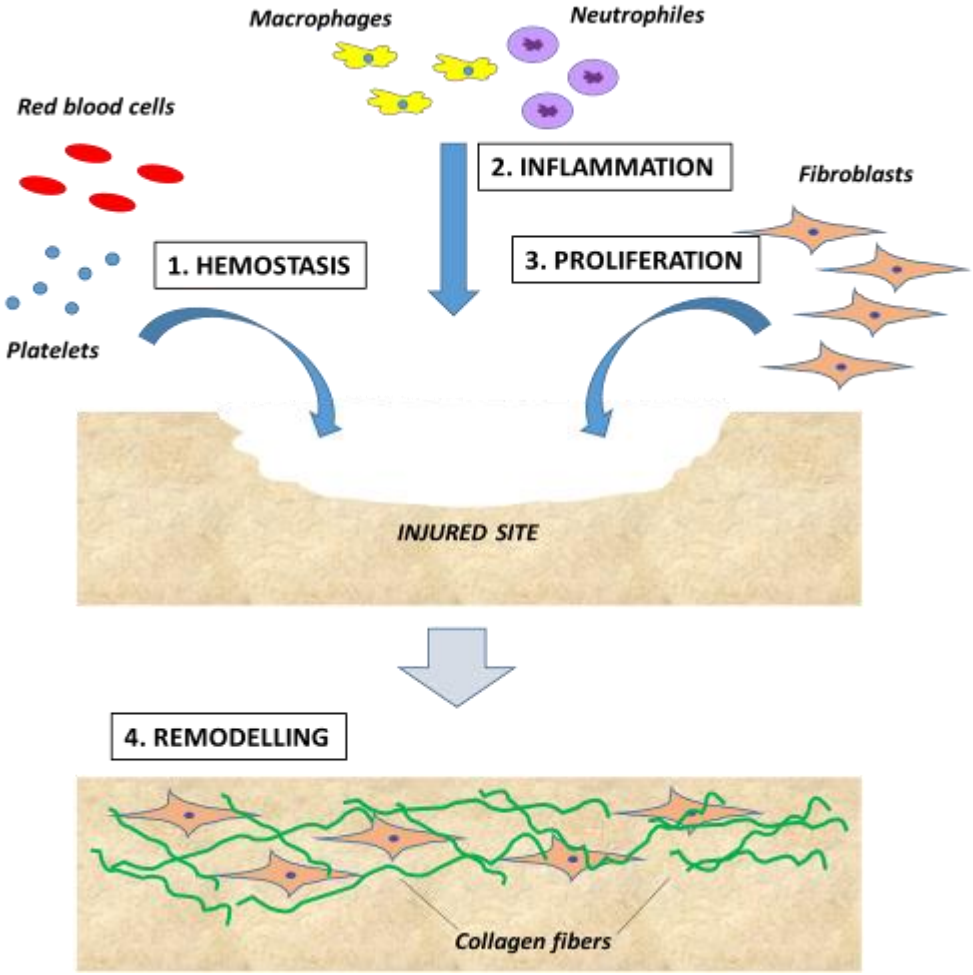

Figure 6. Wound healing process. The main cells involved in wound healing are platelets, red blod cells (*hemostasis*), macrophages, neutrophils (*inflammation*) and fibroblasts (*proliferation*). Newly deposited collagen fibers are reorganized at the end of the process (*remodelling*), leading to the complete closure of wounds.

1.7.1. Gastrointestinal healing

The wound healing process has been extensively studied in the skin, thus enabling the description of the canonical healing phases. Although the healing phases of skin have been ascribed also to the healing of the gastrointestinal (GI) tract (42;200), some differences can be outlined (201).

Significant differences between the healing of skin and of the GI tract regard the time frame of healing, the synthesis of collagen subtypes, the collagenase activity, the wound strength and tissue reactivity (201). In the GI tract, the healing of wounds is faster than in skin and parameters such as modifications of the vascular perfusion can represent potential risks threating a successful outcome (25;201). In the skin, fibroblasts synthetize type I and II collagen, while in the GI tract type I, III and V collagen are produced by both smooth muscle cells and fibroblasts (202). Moreover, the high activity of GI collagenases involved in the remodelling of the scar causes an excessive collagen lisys that decrease the anastomotic strength (203). The colon wall is made up of four layers: mucosa, submucosa, muscolaris mucosa and serosa (from the lumen to the outside part) and all these layers are involved in the anastomotic healing for the creation of a safe anastomosis (202). At this level, fibroblasts composing the most external intestinal layer play an active role in the healing of anastomosis, since they are activated after GI surgery, thus enabling collagen deposition (202) and the formation of a fibrotic cap at the serosa side, serving as a matrix for fibroblasts themselves (204).

1.7.2. Biomaterials for wound healing

In the wound management, the type of wound and the tissue properties often dictate the choice of the most suitable therapeutic approach. Several treatments are based on the use of biomaterials or drug-delivery devices that are able to influence one or more mechanisms involved in the healing cascade (54). For instance, novel therapeutic approaches aim at the topical application of growth factors (*i.e.* platelet-derived growth factor - PDGF) that can decrease the time course of healing by modulating the inflammatory response and accelerating the proliferative phase (205;206).

Biomaterials for the treatments of both superficial and internal wounds are available in the form of gauzes, synthetic dressings, hydrogels, hydrocolloids and foams (180). These biomaterials should display several requirements to exert their functions. For instance, biomaterials used for internal wounds should be hydrophilic, able to absorb exuded liquids,

should not favour microbial infections and should display a swelling behaviour that enables to fill voids within the damaged tissue. Moreover, to prevent adverse reactions, these biomaterials should be biocompatible and degrade on a time frame that matches with that of the wound healing process (*i.e.* few days) (207;208). Medical dressings can be designed and engineered in order to tune their features in the terms of antibacterial, anti-inflammatory, and adhesive properties, thereby tailoring the material to the final medical application (180).

Several medical approaches have been pursued to face the unmet medical need related to the inefficient wound closure. Advanced wound therapies focus on the delivery of drugs and healing factors at the wounded site, in order to stimulate a cellular response. These molecules can act as haemostatic, immunomodulatory, antibiotic, angiogenetic and cell growth agents and they are able to influence and accelerate the biological response of healing. As an additional advantage, these devices can be manipulated in order to enable a controlled spatial-temporal release of the bioactive agents (209;210). To achieve this goal, biomaterials such as bioactive hydrogels based on collagen, HA, chitosan, alginate, elastin and (poly)ethylene glycol (PEG) can be employed (211).

All these components provide benefits to the tissue. For instance, dressings based on alginate usually display a swelling ratio that enables the absorption of large volumes of exudate that are generally present in wounds (212), while both chitin and chitosan are known for their adhesive, antibacterial and fungicidal properties (65;213).

Collagen and hyaluronan are key components of the ECM and they are good candidate for the development of dressings that mimic the ECM and the surrounding environment (214). The bioactive properties of hyaluronan (with regard to the ability of stimulating the cell proliferation and migration) have been exploited for the development of systems that favor the migration of cells into the wound (193;215).

1.8. BIOADHESIVES FOR SURGICAL APPLICATIONS

1.8.1. Medical need and general requirements of bioadhesives

Bioadhesion is defined as the process whereby synthetic and natural macromolecules are able to adhere to a biological tissue for an extended period of time in the body (216). In the field of general surgery the use of adhesive and sealant interfaces are required for the replacement of sutures for wound closure (217), for hemostatic and sealing purposes (218;219) and for keeping in place implantable biomaterials (89;220).

Despite sutures are considered a mainstay for several treatments and procedures in general surgery, they also have some drawback mainly associated with a high infection rate, an extensive handling, a risk of blood-borne disease transmission and tissue reactivity (218;221). Moreover, the presence of sutures or staple materials in surgical wounds is considered to increase the risk of infections, which may retard wound healing, cause wound chronicity and threaten the patient's life (222;223). For these reasons, a general trend towards simpler, quicker and minimally invasive surgical procedures has encouraged the development of sutureless techniques based on the use of adhesive and sealant interfaces to restore soft tissue integrity and functionality.

Beside the use of adhesives for the substitution of sutures, these interfaces can be successfully employed as hemostatic agents. Hemostats work by causing blood to clot and are indicated to stop non-suturable or non-cauterizable bleeding particularly in anticoagulated or coagulopathic patients, so that their use appears as fundamental in the treatment of emergency hemostasis (218;219) as well as in sealing the leaks of gas or fluids (224).

Another common procedure in general surgery is the use of implantable biomaterials that should be maintained *in situ* in close contact with the target tissue; for instance, implanted devices like meshes, gauzes, webs or catheters need to be kept in place to properly fulfill their functions. Also in these cases, sutureless techniques offer considerable advantages (225;226).

Regardless the final goal, adhesive compounds must match several requirements in order to create safe and stable interfaces, taking into account clinical needs, biological effects and material features. An ideal bioadhesive should possess several properties: it should be biocompatible, non irritating, inflammatory, toxic or antigenic, and it should be easily applied or injected in a form of liquid or hydrogel on the target surface. Then, the reticulation process required for the adhesive consistency, should take place in the presence of body fluids in a conveniently short time, according to the requirements of the specific operation. After

reticulation, the adhesive should be as pliable as the tissue, in order to follow its physiologic expansion/contraction, while at the same time ensuring strong binding efficacy. For this reason, adequate mechanical properties are required for a proper elasticity/compliance of the interface. In some cases, the adhesive should progressively undergo biodegradation after having exerted its function. Moreover, each adhesive system must be effective once applied at the target site: the effectiveness of a given formulation stems from a compromise between cohesive and adhesive forces, the former being due to molecular forces within the interface (bulk-bulk bonding), the latter being due to attractive forces between the adhesive and the target surface (227). Cohesive interactions are required only to a certain extent since too much cohesion may result in a hardened material without significant affinity for a surface. On the other hand, adhesive interactions with the target tissue are a fundamental aspect that must be considered for each specific organ of the body (89).This wide range of functions is pursued by employing polymers capable of generating a three-dimensional network that binds to the target tissue. Commercial surgical adhesives and sealants are either based on natural compounds or on synthetic materials; the former are generally well accepted by tissues but often exhibit low adhesive strength while the latter typically display higher strength but lower biocompatibility. Depending on the nature of the polymers, the main classes of adhesives for general surgery include fibrin (228-230), gelatin (231), formulations based on proteins and polysaccharides (6;222), cyanoacrylates (232;233), polyurethanes (234;235) and polyethylene glycol (PEG) (236;237). These systems are often applied at the target site as exogenous compounds.

Taking into account the specific case of the AnastomoSEAL product, the adhesiveness of the membrane is required both in the short and in the long term: the short term adhesion enables the application of the material at the site of the implant without any slipping, thus preventing damages caused by surgical handling and positioning procedure. At the same time, the long term adhesion endowes to the membrane with the ability to withstand detachment caused by the action of biological fluids after implantation and it is required to ensure the release of HA at the anastomosis.

1.9. BIOMIMETIC ADHESIVE STRATEGIES

Despite a huge number of tissue adhesives are available nowadays at the clinical level, some issues related to the safety and performances have driven researchers to focus on the development of tissue adhesives with limited drawbacks (89;218). In general, good adhesion strength is associated to a certain extent of tissue toxicity, while biocompatible tissue adhesives often display a poor adhesion ability (89). Moreover, bonding in a wet physiological environment is one of the main challenges of bioadhesion (216;238), since the action of body fluids can affect the strength of chemical bonds *i.e.* the strength of the adhesive (218). Given these premises, biomimetic adhesive strategies that take inspiration from the key adhesive features and mechanisms employed by natural organisms such as geckos and mussels are being investigated for the development of novel adhesives. Among the most popular ones, the topography of gecko-foot and the molecular features of mussel's glues are being studied to develop novel adhesive materials (239-243).

1.9.1. Geckos-based adhesive strategies

The strategy employed by geckos to achieve adhesion relies on a physical mechanism related to the topography of their feet. Indeed, the gecko's foot pad is composed of keratineous structures known as *setae*; each *setae* displays several terminal projections (*spatula*) that are 200-500 nm in length (239;244;245) (figure 7). This fibrillar design accounts for adhesion to smooth and even inverted surfaces through a combination of mainly van der Walls and capillary forces (239;246;247).

Figure 7. Gecko's foot pad. The adhesion relies on physical mechanism due to a combination of Van der Walls and capillary forces.

Various techniques aimed at the achievement of these hierarchical structures have been employed to reproduce the topography of gecko's foot for the fabrication of bioadhesives to be employed in the biomedical field (248-250). For instances, *Kwak et al.* fabricated an

adhesive skin patch endowed with vertical pillars made of polydimethylsiloxane (PDMS). Although these patches displayed an initial lower adhesion over acrylic adhesives, there are several advantages such as the ability to restore adhesion, the improved biocompatibility and the reduced risk to be affected by surface contamination and oxidation were reported (251).

Another proposed medical device is an active endoscopic capsule endowed with gecko-patterned adhesive legs that extend from the capsule body and that enable the adhesion to the esophagus walls, thus withstanding the detachment caused by the peristaltic movements (252;253). Although geckos have inspired the development of many nano-structured adhesives, the adhesion mechanism employed by them is temporary and becomes ineffective under wet conditions (247). Only *Messersmtih et al.* developed a synthetic gecko-mimicking adhesive that can efficiently bind to inorganic surfaces under water, through the formation of reversible non-covalent bonds (254). However, biomedical adhesives are required to form covalent bonds to organic surfaces, in order to withstand detachment caused by the action of body fluids and by the movement of nearby tissues (89;255). In order to overcome the drawback regarding the in wet adhesion, *Mahdavi et al.* developed a nano-patterned polyglycerolcosebacate acrylate (PGSA), a biodegradable elastomer, coated with oxidized dextran and capable to covalent cross-link to wet tissue. Indeed, the presence of oxidized dextran enhances the adhesive binding of PGSA to tissue, since aldehyde groups can react with amino groups of tissue proteins thus strengthening the adhesion (255) (figure 8a).

A second strategy that has been adopted to improve adhesion in wet conditions was based on the combination between the micropatterned-structure of gecko's feet and the adhesive features of mussel's glue. *Lee et al.* prepared a polydimethylsiloxane (PDMS) endowed with a nanofabricated pillar that was dip-coated by a thin polymeric layer mimicking the adhesive functionalities of mussels. Thus, by combining the hierarchical topography of gecko's feet and the chemical features of mussel's glue the adhesive properties of the final system can be enhanced both in wet and in dry state (254) (figure 8b).

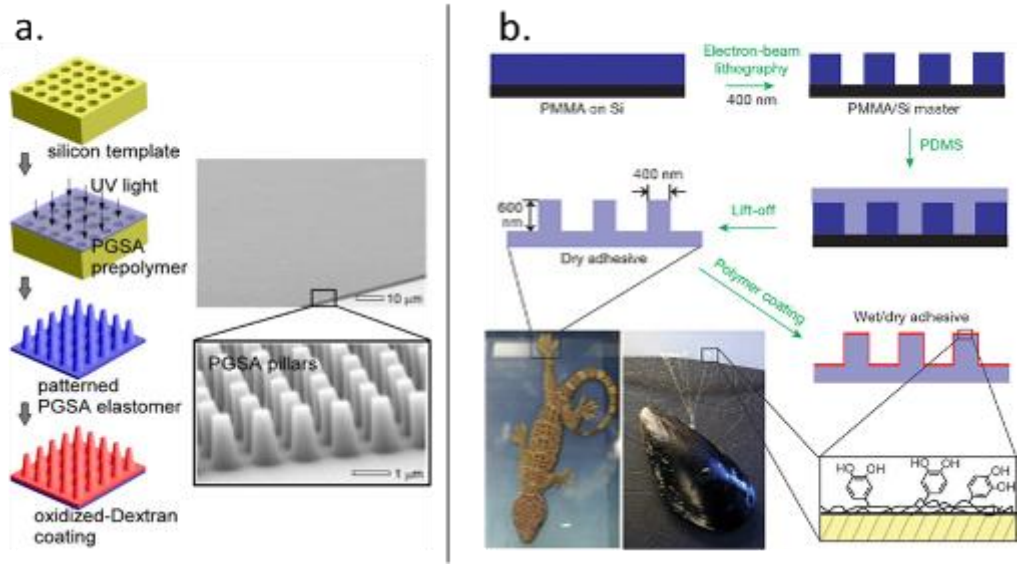

Figure 8. Nanopatterned PGSA coated with oxidized dextran coating. (a) The adhesive is obtained through several step process enabling the manufacture of gecko-like pillars coated with oxidized dextran. (*Reprinted with permission from PNAS "A biodegradable and biocompatible gecko-inspired tissue adhesive" (255); Copyright (2008) National Academy of Sciences, U.S.A.). doi: 10.1073/pnas.0712117105.*
(b) PDMS was casted on a substrate (PMMA) previously modified through electron-beam lithography to create an array of nanopillars. After curing, a catechol containing polymer was used to create an adhesive coating on PDMS. *Reprinted with permission from Macmillan Publishers Ltd: Nature (254), copyright (2007). Nature Publishing Group is acknowledged. http://dx.doi.org/10.1038/nature05968*

This literature overview clarify that the technological approaches exploiting gecko's adhesion mechanism for the fabrication of novel bioadhesives is promising and *in vivo* studies pointed out they are suitable for biomedical applications (255). However, the fabrication of these patterned adhesives is still expensive and some improvements have to be done in order to increase the adhesive strength (256).

1.9.2. Mussels-inspired adhesive strategies

Mussels are marine organisms able to attach to a wide range of surfaces such as sea rocks, wood and ship hulls and to resist detachment under the harsh conditions of the marine environment (218;256). The structural component providing attachment in mussels is the byssus that is composed of a bundle of threads that extends from the shell of the mussel and that displays an adhesive plaque at its distal end (257). Both the byssal and the adhesive plaque are protein-based structures secreted by mussels and undergoing rapid solidification

after secretion. The adhesive plaque is directly involved in the interaction with the substrates and it allows an effective adhesion under wet conditions (219;224) (figure 9).

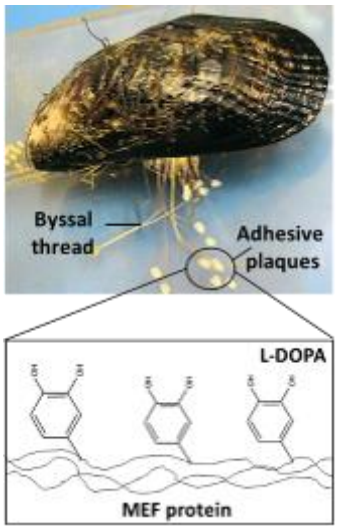

Figure 9. Mussel's adhesion. The adhesion occurs through the byssal thread that terminates with an adhesive plaque where MEF proteins are present. L-DOPA residues of MEF account for adhesion in wet and dry conditions.

The adhesive plaque is composed of proteins known as *Mytilus edulis foot proteins* (Mefp): to date, five Mefp have been identified and all of them share the presence of the aminoacid L-3,4-dihydroxyphenylalanine (L-DOPA) in their structure as a common feature (257;258) (figure 10).

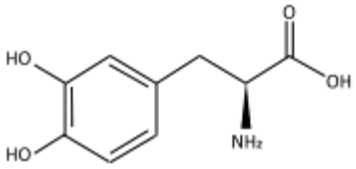

Figure 10. Chemical structure of L-DOPA.

Mefp-3 and Mefp-5 display the highest L-DOPA content among the Mef proteins (259;260) and they are mainly located near the interface between the plaque and the substrate (260;261). The presence of the catechol molecule L-DOPA within those proteins accounts for both cohesion and adhesion of mussels (262-264), which are required for the bulk elastic properties of the adhesive and for the physicochemical interactions formed at the interface, respectively (262-264). Indeed, the surface adhesion occurs through the establishment of covalent bonds between the oxidized hydroxyl groups of L-DOPA and nucleophiles (NH_2, SH, COOH and OH) exposed on both organic and inorganic surfaces; at the same time, the formation of covalent bonds between L-DOPA residues accounts for the formation of protein-crosslinking

(218). Based on the chemical reactivity of the key adhesive molecules of mussels, a number of mussel's inspired adhesive systems have been developed. The main strategies are based on the chemical coupling of the catechols (*i.e.* L-DOPA, dopamine and their derivatives) onto the backbone of polymers such as alginate (265), hyaluronic acid (266;267), and poly(ethylene glycol) (PEG) (225;268), for the development of nano-engineered adhesive polymers. The mechanism enabling the catechol-modified polymers to perform adhesion has been described in the literature. In particular, under oxidizing or alkaline conditions, L-DOPA residues are converted into ortho-quinone (o-quinone) moieties that may interact between them *via* aryl-aryl coupling to form intermolecular cross-linking (215;269). Alternatively, quinones can react *via* Michael Type Addition or Schiff base reaction with nucleophile groups (mainly NH_2 and SH) exposed on the tissue surface, thus leading to the formation of covalent bonds (270;271) (figure 11).

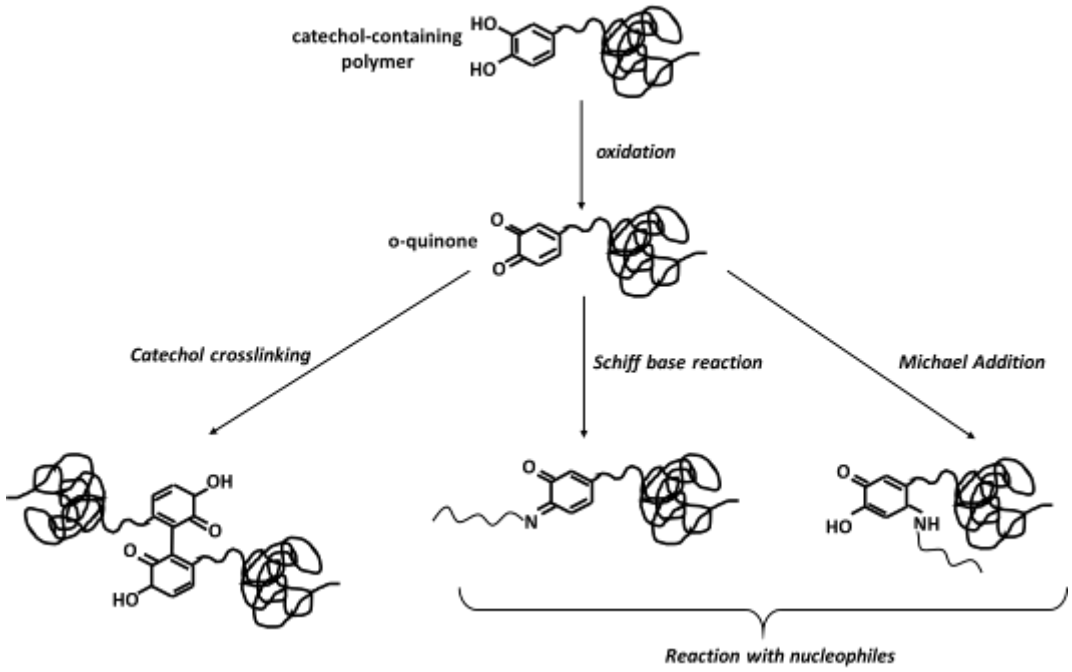

Figure 11. Chemical reaction involved catechol-containing polymers. The oxidation of dopamine leads to the formation of o-quinones that can form covalent crosslinking between catechols; alternatively, the formation of covalent bonds occurs through Schiff base reaction and Michael Addition (adapted from (218)).

Hydroxyl groups (OH) of the catechol rings of L-DOPA residues can also interact with hydrophilic surfaces through hydrogen bond formation (257;272). The hydrogen binding ability of DOPA-containing polymers accounts for the mucoadhesive properties of such compounds (273-275). Thus, the main mussel-inspired adhesive strategies, are based on the coupling of catechols with polymers. A novel emerging strategy exploiting mussel's adhesion

is based on the synthesis and purification of catechol-based nanoparticles to be used as adhesive coatings.

1.9.3. Nanostructured dopamine containing polymers

The use of DOPA-modified polymers has been described for the development of adhesive biomaterials, since the presence of catechols in both natural and synthetic polymers endowes them with adhesive, coating and anchoring features that enable their binding to diverse surfaces (276-281). Beside L-DOPA, other catechol-based molecules such as dopamine or 3,4-dihydroxyhydrocinnamic acid can be used for the functionalization of polymers, since these compounds were found to possess adhesive properties similar to those of DOPA (238;282-284). In the field of adhesive materials, DOPA residues were implemented in the structure of synthetic polymers such as polypeptides (238;285-288), poly(ethylene glycol) (PEG) (237;289) and polystyrene (290;291) to enhance adhesion. For instance, *Yu et al.* developed a polypeptide composed of L-DOPA and L-lysine that was able to adhere to different substrates and that displayed resistance to moisture environment (292). *Brubaker et al.* synthetized a catechol derivatized PEG adhesive (cPEG) in the form of hydrogel for the immobilization of pancreatic islet beta cells to extrahepatic tissues, for the treatment of diabetes type I mellitus. The adhesive features of this system were proved *in vivo* and ascribed to the presence of catechols (238). Similarly, an injectable nanocomposite tissue adhesive in the form of hydrogel was obtained by combining a dopamine-modified four-armed PEG with a synthetic nanosilicate (283). Natural polymers have also been functionalized with catechols. For instance, *Lee et al.* described the synthesis of an adhesive hydrogel based on dopamine-conjugated hyaluronic acid mixed with thiol end-capped pluronic F127 copolymer whose adhesive features were tested on mouse skin (293). Similarly, a composite adhesive in the form of hydrogel was prepared from a mixture blend of catechol-functionalized chitosan and thiol-terminated Pluronic F127. The adhesion properties were proved on mouse subcutaneous tissues, thus pointing to the adhesive binding ability and to the hemostatic properties of the system (294). A two-components bioadhesive for bone applications has been developed by *Hoffman et al*: the adhesive was based on a mixture of the polysaccharides chitosan and starch, the latter oxidized to provide aldehyde groups on starch. These reactive groups enabled the interaction with both aminogroups of chitosan and tissue proteins, thus accounting for the formation of adhesive bonds and internal crosslinking within the adhesive. Starch was then conjugated with DOPA to further enhance the adhesive ability to tissues (295). Recently,

Mehdiazadeh et al. developed injectable citrate-enabled mussel-insired bioadhesives (iCMBAs) based on citric acid, PEG and dopamine/L-DOPA, whose adhesive properties were proved *in vivo* and showed up to 10 times increase over commercial fibrin glue (296). *In vivo* studies proved the effectiveness of iCMBAs in stopping bleeding and in closing wounds on the dorsal part in rat, without the use of stiches or staples.

This literature survey shed light on the wide interest in developing such a water resistant tissue adhesives.

1.9.4 Catechol-based nanoparticles

Besides the development of polymers modified at the nanometer scale, the synthesis of nanoparticle suspensions has been reported for adhesive purposes (297;298). Recently, the synthesis of nanoparticles based on dopamine was described in the literature (299). Although little is known about the adhesive properties of these nanoparticles, it is likely that adhesive coatings based on these nanoparticles confer adhesive binding ability to biomaterials, since they display a catecholic core that is involved in the formation of the adhesive bonding with the tissues. The synthesis of nanoparticles containing catechols is generally carried out by inducing the oxidation of a catechol containing solution (*i.e.* aqueous dopamine solution). This process involves the polymerization of dopamine molecules under oxidizing conditions through a mechanism that resembles the biological pathway of melanin biosynthesis (figure 12).

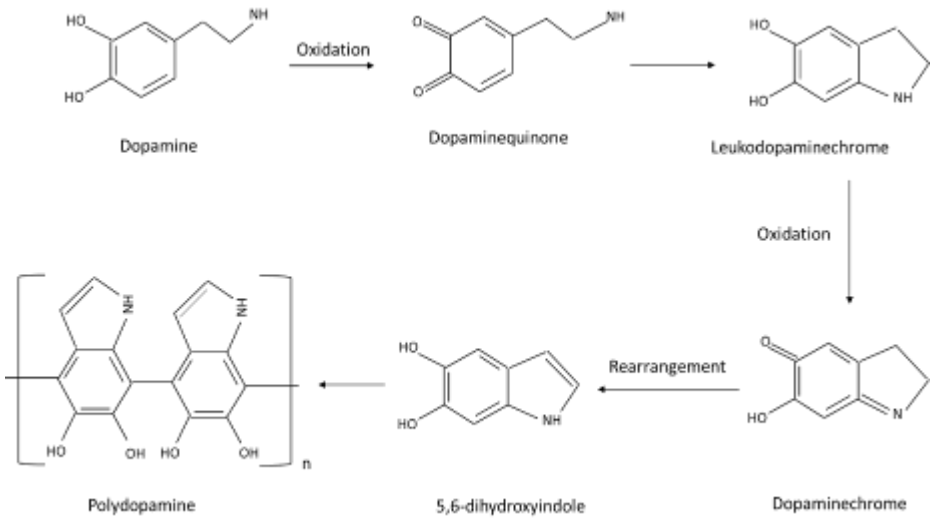

Figure 12. Dopamine polymerization mechanism. The oxidation of dopamine induces crosslinking among molecules leading to the formation of polydopamine that is structurally similar to melanin.

These reactions lead to the formation of insoluble nanoparticles whose molecular structure is similar to that of melanin: for this reason they are called melanin-like nanoparticles (MNPs) (299). In particular, it has been reported that the oxidation of catechols (*i.e.* DOPA or dopamine) in the presence of oxidizing agents such as sodium hydroxide leads to the formation of the 5,6-dihydroxyindole (DHI), the monomer precursor of melanin (300-302). These monomers can interact with themselves to form oligomeric structures in which from two to eight DHI monomers are present (303). The oligomers assemble together to form nanometric aggregates (2-20 nm) that are stabilized by π-π stacking interactions and covalent bonds (304). The polymerization of the nanoparticles occurs through the association of the aggregates together with the inclusion of monomeric species and free oligomers, a mechanism that enables the growth of the nanoparticle size over time (305) (figure 13).

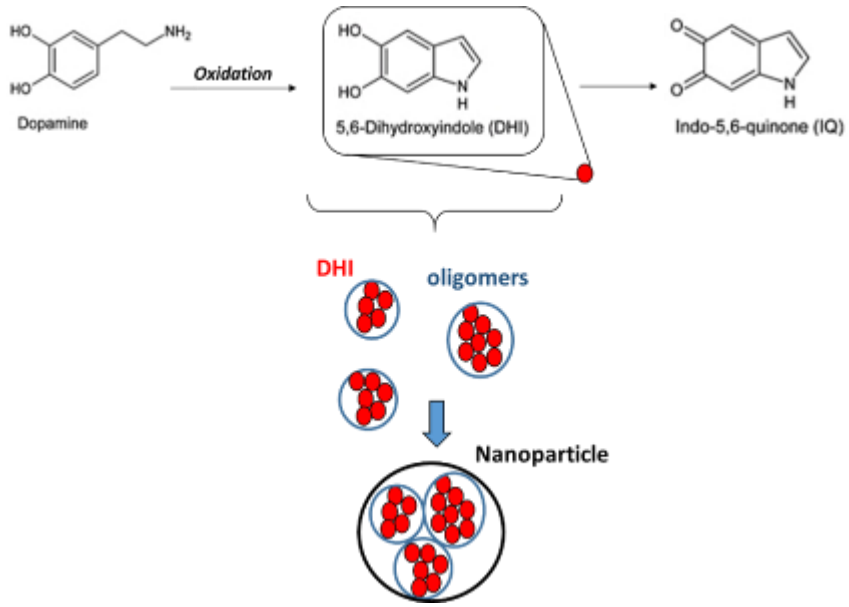

Figure 13. Mechanism of dopamine-based nanoparticle formation. Under oxidizing conditions, dopamine is converted in 5,6-dihydroxyindole (DHI) and indo-5,6-quinone, the monomer precursors of melanin. Monomers interact to form oligomeric species that aggregates to give the nanoparticle.

MNPs can fulfill a wide range of functions, since they can serve as drug delivery system (306;307), free radical scavengers (299), protector agents against ɣ-irradiation (308), films for structural color material (309;310) and contrast agents for magnetic resonance imaging (311) and for optoacoustic tomography (312). In the field of bioadhesion, little work has been done in investigating the role of MNPs as adhesives, although the presence of reactive o-quinones exposed on the surface of MNPs can account for the formation of covalent bonds with amines or thiols of tissue proteins, thus ensuring a firm adhesion (238;313).

The use of MNPs for adhesive purposes provides several advantages over catechol-functionalized polymers. First, the chemical modification of polymers can modify the properties of the native molecules, which may lead to unpredictable outcomes. As a second main point, nanoparticle suspensions are suitable for the development of uniform coatings and the high active surface of nanoparticles together with the presence of a higher number of quinone reactive groups exposed on their surface can ensure the establishment of an increased number of covalent interactions, thus strengthening the adhesive bonds.

2. AIMS

The overall scope of this research work was to develop a bioactive adhesive biomaterial for wound healing applications.

More in detail, the specific aims of this thesis were to:

- develop membranes based on the polysaccharides alginate and HA that could stimulate the healing of wounds and perform the mechanical, chemical and biological characterization of the biomaterial properties;

- design and manufacture adhesive systems based on the modification at the nanoscale of the structural component of membranes and tissue, or on the use of nanoparticle suspensions;

- evaluate the tissue adhesiveness of the proposed adhesive systems and characterize them as to their mechanical and biological properties.

3. MATERIALS AND METHODS

3.1. Materials. Sodium alginate from *Laminaria hyperborea* (Alginate Pronova UP LVG, molecular weight, MW∼120 000; fraction of guluronic G residues, F_G = 0.69; fraction of guluronic diads, F_{GG} = 0.59; number average of G residues in G-blocks, $N_{G>1}$ = 16.3) and sodium hyaluronate (HA) Pharma grade (MW∼ 800 000) were kindly provided by Novamatrix/FMC Biopolymer (Sandvika, Norway). HA (MW∼240 000, Phylcare Sodium Hyaluronate extra LW) was kindly provided by Sigea S.r.l. (Trieste, Italy). Calcium carbonate ($CaCO_3$), D-Gluconic acid δ-lactone (GDL), glycerol, C1-ethyl-3-[3-(dimethylamino)propyl]carbodiimide hydrochloride (EDC), N-hydroxusuccinimide (NHS), fluoresceinamine, 4-(2-hydroxyethyl)piperazine-1-ethanesulfonic acid (HEPES), LDH (lactate dehydrogenase) TOX-7 kit, mitomycin C, 2-(N-Morpholino)ethanesulfonic acid (MES), sodium chloride (NaCl), sodium bicarbonate ($NaHCO_3$), hydrochloric acid (HCl), calcium chloride ($CaCl_2$), glutaraldehyde, glucose, ethanol and Hanks' Balanced Salt solution (HBSS) sodium hydroxide (NaOH), dimethyl sulfoxide (DMSO) and 3-(4,5-Dimethylthiazol-2-yl)-2,5-Diphenyltetrazolium Bromide (MTT), ethanol, hexamethyldisilazane (HMDS), Iodure Potassium (KI), Sodium Hydroxide (NaOH), Ammonium Molybdate $(NH_4)_2MoO_4$, Potassium Hydrogen Phtalate ($C_8H_5KO_4$) were obtained from Sigma-Aldrich Chemical Co. U.S.A. Dopamine hydrochloride (DOPA-HCl, heat-inactivated fetal bovine serum were supplied either by Sigma-Aldrich Chemical Co. U.S.A., Acros or Alfa-Aesar.

Primary human dermal fibroblasts (HDFa) were purchased from Invitrogen™ Life Technologies; Medium 106, Low Serum Growth Supplement (LSGS) from Gibco™. Mouse fibroblast-like (NIH-3T3) cell line (ATCC CRL1658), Dulbecco's Modified Eagle's Medium high glucose (DMEM) and Fetal Bovin Serum (FBS) were purchased from EuroClone (Italy).

Intestine explants were harvested from freshly sacrificed pigs at local slaughterhouse.

3.2. Preparation of membranes

All membranes were prepared according to the following procedure: the polysaccharides were dissolved in deionized water and glycerol was added as a plasticizer (final concentration = 5% v/v). Then, $CaCO_3$ and GDL were added and the mixture was poured into rectangular moulds for the *in situ* gelation of the solution. The ratio $CaCO_3$ / GDL was 0.5 for each formulation studied; suspensions of $CaCO_3$ corresponding to $[Ca^{2+}]$ 20 or 50 mM were used.

Subsequently, the hydrogels were cooled by immersion in a liquid cryostat; ethylene glycol in water (3:1) was used as refrigerant fluid. Temperature was decreased stepwise from +20°C to -20°C by 5°C steps with 30 min intervals for equilibration. Finally, the frozen hydrogels were dried under vacuum using a Single-Chamber Freeze-Dryer (Christ Alpha 1-2 LDplus). Several membrane formulations were prepared by varying the compositions: the list of formulations employed is reported hereafter:

- Formulation A: Alginate 15 g/L, $CaCO_3$ 20 mM, GDL 40 mM, glycerol 5% v/v;
- Formulation B: Alginate 15 g/L, HA (800 kDa) 15 g/L, $CaCO_3$ 20 mM, GDL 40 mM, glycerol 5% v/v;
- Formulation C: Alginate 20 g/L, HA (240 kDa) 15 g/L, $CaCO_3$ 20 mM, GDL 40 mM, glycerol 5% v/v;
- Formulation D: Alginate 15 g/L, HA (240 kDa) 15 g/L, $CaCO_3$ 20 mM, GDL 40 mM, glycerol 5% v/v;
- Formulation E: Alginate 15 g/L, HA (240 kDa) 15 g/L, $CaCO_3$ 50 mM, GDL 100 mM, glycerol 5% v/v.

3.3. Preparation of membrane containing dopamine-modified alginate

The preparation of membranes containing dopamine-modified alginates (D-AlgM) was performed following the procedure described in the section 3.2. *("3.2. Preparation of membranes"*), under nitrogen flush (formulation D: Alginate 15 g/L, HA (240 kDa) 15 g/L, $CaCO_3$ 20 mM, GDL 40 mM, glycerol 5% v/v). In this case, dopamine-grafted alginate was used instead on unmodified alginate. After freeze-drying, the modified membranes were stored in oxygen-free pouches.

3.4. Synthesis and characterization of MNPs

MNPs (melanin-like nanoparticles) were prepared as described in the literature (299). Briefly, 180 mg of dopamine hydrochloride were dissolved in 90 ml of deionized water and NaOH 1M (760 μL) was added to solution at 50°C under vigorous stirring. After 5 hours, melanin-based nanoparticles (MNPs) were retrieved by centrifugation (20000 xg) and washed three times in deionized water. An additional centrifugation was carried out at 4000 xg, in order to remove larger particle size and MNPs were dispersed in aqueous solution at the final concentration of 1 mg/ml (w/v). pH was measured during MNPs formation. UV-visible spectra were acquired with a spectrophotometer in the range of 280 - 730 nm (Infinite M200 PRO NanoQuant, Tecan) after MNPs purification.

3.5. Preparation of MNPs-coated membranes

The preparation of MNPs-coated membranes (formulation D: Alginate 15 g/L, HA (240 kDa) 15 g/L, $CaCO_3$ 20 mM, GDL 40 mM, glycerol 5% v/v) was performed following the

procedure described in the section 3.2. (*"3.2. Preparation of the membranes"*). In this case, after freeze-drying, the coating was obtained by spreading the nanoparticle suspension over the lyophilized membranes (25 μg/ml MNPs / cm^2 membrane).

3.6. Mechanical characterization of the membranes (uniaxial tensile test)

The membranes were cut in dog-bone shapes according to ASTM D638-10 standards (type 1 samples); their mechanical properties were studied using a Universal Testing Machine (Mecmesin Multitest 2.5-i) equipped with a 100 N load cell. Tensile tests were performed at a crosshead speed of 5 mm/min. The cross section of the samples was measured with a caliper. Tensile stress was calculated dividing the load by the average original cross sectional area in the gage length segment of the specimen. Young's Modulus (*E*) was calculated as the slope of the linear portion in the stress-strain curve, considering the deformation range of 1%-3%. For each formulation, five replicates were used and the data were averaged and standard deviations calculated.

3.7. Swelling test

Circular samples of the membrane (formulations A and D; Ø = 20 mm) were weighted at the dry state. The samples were soaked with 4 ml of SBF and the weight of the hydrated membranes was measured after drying the samples on a filter paper. Data were expressed as the ratio between the weight of the wet membranes and the weight of the dry membranes, as a function of the time. Three parallel replicates were averaged and standard deviations calculated.

3.8. Degradation studies

Circular samples of the membrane (Ø = 20 mm) were soaked with 10 ml of Hank's balanced salt solution (HBSS) at room temperature and daily the samples were collected, dried for 1 minute on filter paper, weighted and then immersed in fresh HBSS. The weight variation was recorded as a function of solution shifts. As a reference, the 100% of the weight was considered as the weight of the samples after 4 hours of immersion in HBSS. Six parallel replicates were averaged.

3.9. Release studies

Membranes composed by alginate and HA were incubated in 10 ml of HBSS for selected time intervals. After incubation, the supernatants were collected and dialyzed for two days against 0.1 M HCl (4 shifts) and deionized water until the conductivity of the solution was below 4 μS. Then, the solution was collected and the pH adjusted at approximately 7.2. The supernatants were dried, weighted and analyzed by NMR according to the procedure described by *Geremia et al* (140).

3.10. Cell cultures

Primary human dermal fibroblasts isolated from adult skin (HDFa) were purchased from Invitrogen™ Life Technologies. The cells were cultured in Medium 106 and supplemented with Low Serum Growth Supplement (LSGS), both provided by Invitrogen™ Life Technologies, 100 U/ml penicillin, 100 μg/ml streptomycin. The cells were maintained at 37 °C in a humidified atmosphere of 5 % CO_2 at 37 °C.

Mouse fibroblast-like (NIH-3T3) cell line (ATCC CRL1658) were cultured in Dulbecco's Modified Eagle's Medium high glucose (DMEM) supplemented with 10% Fetal Bovin Serum (FBS), 100 U/ml penicillin, 100 μg/ml streptomycin. These products were purchased from EuroClone (Italy).

3.11. *In vitro* biocompatibility of the liquids extracted from the membranes (LDH assay)

The biocompatibility of the biopolymeric membranes (formulation A and D) was evaluated through a quantitative analysis of the effect of the liquid extracts of the materials, according to the ISO 10993-5:2009 International Standard; the lactate dehydrogenase (LDH) assay was used. Since the extracting conditions should simulate or exaggerate the clinical use conditions, the following procedure was developed. UV-sterilized specimens of membranes have been soaked and incubated in the extraction culture medium for 72 hours at 37 °C. The ratio between weight of the patch and volume of the medium was maintained constant and selected in order to reach a polymer concentration (on the basis of the release studies) of 0.5 % w/V, which avoided biased results due to excessive viscosity of the extraction medium.

The *in vitro* biocompatibility of the compounds was evaluated by means of the LDH assay. HDFa were trypsinized and seeded on a 24-well sterile plate at final concentration of 40000 cells per well. Aliquots of 500 μl of liquid extract of the membranes were added to the wells. Untreated cells and cells treated with Triton X-100 0.1% were considered, respectively, as a

negative and positive control. The LDH assay was performed 24 and 72 hours after the treatment: the level of cytotoxicity was evaluated by comparing the LDH values measured for the samples and those corresponding to the total amount of intracellular LDH calculated by inducing cellular lysis. For each series, four replicates were tested. 45 µl of both cell medium from tested samples and cellular lysates were added to LDH mix (30 µl LDH assay substrate, 30 µl LDH cofactor, 30 µl die solution) and the incubation was allowed 30 minutes in dark. The enzymatic reaction was stopped by adding 1/10 HCl 1N to each sample. The plate was read at 490 nm and 690 nm with a spectrophotometer (Infinite M200 PRO NanoQuant, Tecan). Evaluation of cytotoxicity was calculated according to the formula: LDH released (%)=[(A-B)/(C-B)]·100, with A: LDH activity in the culture medium of treated cells, B: LDH activity of culture medium from untreated cells and C: LDH activity after total cell lysis at 24 and 72 hours.

3.12. *In vitro* biocompatibility of the liquid extracted from membranes sterilized by means of $scCO_2$ (LDH assay)

The LDH assay was performed on primary human dermal fibroblasts (HDFa) to evaluate the biocompatibility of the $scCO_2$ sterilized membranes, by following the procedure described in the section 3.11. ("*3.11. In vitro biocompatibility of the liquids extracted from the membranes (LDH assay)*"). The sterilized and non-sterilized membranes (1 g) were incubated in 10 ml of cell medium for 72 hours. After this period, cell medium was harvested and membranes were discarded and 500 µl of the supernatant were added to each well. This procedure aimed at the evaluation of cytotoxic effect of substances released by membranes. Untreated cells and cells treated with Triton X-100 0.1% were considered, respectively, as a negative and positive control.

3.13. *In vitro* biocompatibility of MNPs (LDH assay)

The biocompatibility of MNPs was evaluated by means of the lactate dehydrogenase (LDH) assay. The experiment was performed at the conditions reported in the section 3.11. ("*3.11. In vitro biocompatibility of the liquids extracted from the membranes (LDH assay)*"). For this test the cells were treated with cell culture medium (negative control) MNPs (5 µg/ml and 50 µg/ml) and TritonX-100 0.1% (positive control).

3.14. *In vitro* wound healing (scratch assay)

The scratch assay was performed to evaluate the ability of the HA released from the membranes to stimulate the closure of a scratch on a confluent cell plate; this assay is a well-developed method to measure cell migration *in vitro*, enabling the study of cell-matrix and cell-cell interactions also during the wound healing process (112). For this test the plasticizer (glycerol) was removed from the formulation, in order to avoid biased results due to the increased viscosity of the aliquots of liquid extract. The kinetic of the closure of the gap is monitored and measured by using a microscope equipped with a camera, and a software for image analysis. HDFa cells were seeded at a density of 250000 cells per well in 6-well plate and incubated at 37 °C for 16 hours, in order to enable cell adhesion on the cell plate. Cells were treated with the liquid extract of the membranes (3 ml). 24 hours after the treatment a scratch was performed in each well using a sterile 200 µl plastic tip and the scratch closure was followed over time through an optical microscope (Optech IB3 ICS) equipped with a Pentax K100D camera and the images of the scratch were acquired over time to monitor the wound closure. The analysis was performed using the software Image J: the opened area was outlined per each scratch and the percentage of closure over time was plotted. The results are reported as percentage of closure of the gap area between day n and day 0. For each sample, data are expressed as mean ± standard deviation. In order to discriminate the contribution of cell migration to the scratch closure, cells were also treated for 24 hours with a non-toxic concentration of mitomycin C (1 µg/ml), a drug that blocks the proliferation of cells at G_0 phase, to inhibit cell proliferation.

3.15. *In vitro* cell adhesion

The membranes (formulation D) were immobilized on the bottom of the well of a 6-well sterile plate by means of a ring CellCrown (Scaffdex) to enable the complete immersion in cell medium. 230 000 cultured cells (primary fibroblasts) were resuspended in 400 µL of medium and then seeded on each membrane specimen. After 1.5 h, 2 ml of medium were further added to the wells. After 24 h, the membranes were removed from the cell culture medium and prepared for SEM analysis according to the following steps. The membranes were rinsed twice for 30 minutes with 10 mM Hepes buffer, 0.1 M NaCl, 10 mM $CaCl_2$, 5 mM glucose, pH 7.4. Then, the samples were fixed by using 10% glutaraldehyde in 10 mM Hepes, 0.1 M NaCl, 10 mM $CaCl_2$, 5 mM glucose for 1 hour and finally washed with deionized water 3 times for 10 minutes. The membranes were dehydrated by sequential

immersions in ethanol 70%, 95% and 100%. Before SEM analysis, the dehydrated samples were gold-sputtered.

3.16. Scanning Electron Microscopy (SEM)

Morphological analyses of samples were performed using a Leica-Stereoscan 430i Scanning Electron Microscope (SEM). The following samples were employed for the analysis: gold-sputtered membranes (with and without cells) and MNPs-coated membranes, MNPs-treated and bacteria (*E. coli*, *S. aureus*).

3.17. Mechanical adhesion tests

Adhesion tests were performed by means of a Universal Testing Machine (MultiTest 2.5-i) equipped with a 100 N cell load. Test conditions were inspired by ASTM F2258-05 standards. The membranes (2.5cm X 2.5cm) were glued onto the lower holder with a cyanoacrylate glue (Loctite® Superglue) while the intestine tissue was clamped on the upper holder. Before the test, 100 µl of deionized water or H_2O_2 at different concentrations were spread on the surface of the membrane, while the tissue was kept moist with gauze soaked in HBSS. Then, the tissue was brought in tight contact with the patch (compression force = 5 N) for 10 minutes and then pulled off at a crosshead speed of 50 mm/minute. The force-displacement curves were recorded. Data were averaged over at least 5 replicates. The detachment force was defined as the highest force required for the complete detachment.

3.18. Sterilization of membrane with gaseous H_2O_2

The gaseous H_2O_2 sterilization was carried out through a custom made equipment developed by "Impuls" using the following parameter: 250 ppm geaseous H_2O_2, 30% - 50% humidity.

3.19. Sterilization of membrane with $scCO_2$

Membranes (3 cm X 5 cm) were exposed to $scCO_2$ under controlled conditions and in a 100 ml stainless steel reactor (NWA, Lörrach, Germany). Four sets of conditions were employed.

	Pressure (bar)	**Temperature (°C)**	**H_2O_2 content (ppm)**	**Exposure time (hour)**
Set 1	270	40	200	1
Set 2	270	40	1000	1
Set 3	270	40	200	3
Set 4	270	40	1000	3

The high pressure vessel was disinfected with sodium hypochlorite prior to use. H_2O_2 was added to the vessel by using a sterile medical cotton. A standard CO_2 cylinder was used and the gas was pressurized by a high-pressure syringe pump (NWA, PM-101) equipped with a EUROTHERM 2216E heating unit. The reactor temperature was controlled by a digital GTH 1150 thermometer (Greiser Electronic). The internal pressure of the reactor was controlled by a transducer (DS Europe LP632) connected to a pressure control unit (DS Europe AN341).

3.20. Quantification of residual H_2O_2

For the quantification of the residual H_2O_2, a solution containing KI (33 g), NaOH (1 g), $(NH_4)_2MoO_4$ (0.1 g) (solution A) and a solution contining $C_8H_5KO_4$ (10 g) (solution B) were prepared in distilled water (final volume of 500 ml). Sterilized and non-sterilized membranes (100 mg) were left in distilled water (100 ml) for 30 minutes; solution A and B were then mixed together with the membrane containing solution (ratio 1:1:1). The absorbance was measured at 351 nm. For the calibration curve, 60 µl of 30% w/v H_2O_2 were added to 100 mL of distilled water (H_2O_2 concentration = 200 mg/L); this solution was used as a stock to prepare standard samples.

3.21. Dissolution of membranes sterilized by means of $scCO_2$ and membranes treated with H_2O_2

The $scCO_2$ sterilized membranes were transferred in a dialyzing tube (Mw cut-off 10.000) and the dialysis was carried out against aqueous HCl 0.1 M (4 shifts) and against deionized water until the conductivity was below 4 µS. The pH was adjusted to 7.2 and the solution was freeze-dried. The same procedure was employed for alginate membranes (formulation A) (100 mg) treated with 100 µl of H_2O_2 30% w/w for 30 minutes at room temperature and rinsed with water. As a control, an alginate membrane treated with distilled water was used and processed in the same way.

3.22. SEC-MALLS analyses of membranes treated with H_2O_2

Determinations of molecular weights were carried out by combining Size Exclusion Chromatography (SEC) with Multiangle Laser Light Scattering (MALLS) as described by Vold et al (314). The setup consisted of a Waters SEC (Waters 2695 Separations module), a MALS-detector (DAWN HELEOS; Wyatt Technology Corp., U.S.A) and an Optilab rEX RI-detector (Wyatt Technology Corp., U.S.A). The SEC columns used were G6000PWXL,

5000PWXL, and 4000PWXL (Tosoh Bioscience LLC, U.S.A.), and mobile phase was 0.05 M Na2SO4 and 0.01 M EDTA. The flow rate was 0.5 ml/min. The injected mass was 3 mg, and the sample concentration was adjusted to obtain the best possible light scattering signal without influencing the refraction index (RI) profile (overloading). Samples were filtered through a filter 0.45 μm prior to injection. Data from the light scattering and the differential refractometers were collected and processed using Astra (v. 5.3.4.14) software (Wyatt Technology Corp., U.S.A.). The constants used were refractive increment index $(dn/dc)_{\mu}$ of 0.150 ml/g (314) and second virial coefficient A2 of 5.0×10^{-3} ml•mol/g^2.

3.23. Size Exclusion Chromatography (SEC) on membranes sterilized by means of $scCO_2$

The setup for estimation of molecular weight of polysaccharides from dissolved membranes consisted of a Waters SEC (Waters 2695 Separations module) and an Optilab rEX RI-detector (Wyatt Technology Corp., Santa Barbara, CA, U.S.A.). Two SEC columns Agilent PL aquagel-OH 8μm 50 x 7.5 mm were used at 40°C; the flow rate was 1 ml/min and the mobile phase was 0.2 M NaCl in distilled water. Software for analysis from Wyatt Technology Corp. was Astra V SP. Pullulan at different molecular weight was used for the calibration curve.

3.24. Synthesis of dopamine-modified alginates

The synthesis of dopamine-modified alginate (D-Alg) is based on previously published articles (315-317). The syntheses were carried out under nitrogen flushing to avoid oxidation of dopamine. Sodium alginate (final concentration 1% w/V) was dissolved in 100 mM MES buffer pH 6.2 and 0.5 M NaCl. NHS and EDC were added to the solution at the same concentration of DOPA-HCl and stirred for 30 min. DOPA-HCl was added at different final concentration (12.5 mM, 25 mM, 50 mM and 75 mM) to the solution in order to enable the synthesis of D-Alg with different substitution degrees, and stirred for 1 hour. The solution was precipitated in ethanol (10X the volume of the alginate solution) and the precipitate was thoroughly washed several times with ethanol (2X the volume of the initial alginate solution) to eliminate unreacted molecules. The precipitate was then dried.

3.25. *In vitro* adhesion studies with membranes containing dopamine-modified alginate and MNPs coated membranes

Adhesion studies were performed by employing an experimental setup adapted from Bernkop-Schnürch and colleagues (318). Briefly, membranes were cut (1 cm X 1 cm), and attached to the external part of freshly harvested pig intestine that was kept moist with HBSS solution at pH 7.5. The tissue was fixed on a plastic cylinder (diameter 2.5 cm; height 11 cm) and incubated at 4°C for 16 hours. The cylinder was then immersed into a beaker containing 500 ml of HBSS at room temperature and gently shacked to mimic the action of the body fluids. For each series, ten specimens were tested and the number of detached samples was recorded with 30 minutes interval. Three independent experiments were averaged and the results are reported as mean ± standard deviation. This test was employed to evaluate the adhesion ability of membranes prepared with dopamine-modified alginates and MNPs-coated membranes, both containing HA. As a negative control, unmodified alginate-HA membranes were used.

3.26. ^{1}H-NMR studies on dopamine-modified alginates

Samples were prepared as described by *Grasdalen et al.* (179;319). The ^{1}H-NMR spectra were recorded at 90°C with a JEOL 270 NMR (6.34 T). The chemical shifts are expressed in ppm downfield from the signal for 3-(trimethylsilyl)-1-propanesulfonate.

3.27. UV spectroscopy studies on dopamine-modified alginates

The degree of substitution of D-Alg was determined from the molar extinction coefficient of dopamine and the absorbance of the sample. The D-Alg solution (1 g/L in citric acid/phosphate buffer pH 5.5) was analyzed by UV-spectroscopy (JASCO UV/Visible Spectrometer V6530) at λ = 280 nm. The molar extinction coefficient of dopamine in citric acid/phosphate buffer (pH 5.5) at 280 nm determined from a standard calibration curve was equal to: $\varepsilon_{280\,nm} = 0.0128$ L mol^{-1} cm^{-1}. The determination of degree of substitution was performed in triplicate.

3.28. *In vitro* biocompatibility of dopamine-modified alginates (MTT assay)

The biocompatibility of the compounds was evaluated through a quantitative and a qualitative analysis, both according to the ISO 10993-5:2009 International Standard. In the first case, the MTT assay was performed, while in the second case, an optical analysis of cell morphology

was employed. Primary human dermal fibroblasts (HDFa) and a mouse embryonic cell line (NIH-3T3) were cultured in Medium106 and DMEM respectively, at 37°C and 5% pCO_2. Medium106 and DMEM were supplemented with 0.5% LSGS and 10% FBS respectively, both with the addition of 0.25% penicillin/streptomycin. Cells were plated on a 96-well sterile plate at final concentration of 5000 cells in each well. The dopamine-modified alginate was dissolved in cell medium at different concentrations (0.2 %, 0.1 %, 0.5 %, 0.02 % w/V) and 100 µl of sample were added to the wells. As a positive control of cell viability, cells treated with Triton X-100 (final concentration 0.01 % V/V) were considered. Cells growth in plain medium were used as negative control. The MTT assay was performed 24, 48 and 72 hours after treatment: 100 µl of MTT solution (0.5 mg/ml) were added to each well and incubation was allowed for 4 hours at 37 °C. After the incubation, the MTT solution was removed and 50 µl of DMSO were added to each well for the dissolution of the formazan crystals. The absorbance of each well was read at 570 nm with a spectrophotometer (Infinite M200 PRO NanoQuant, Tecan). The percentage of viability of the negative control was set at 100% and relative viability was calculated for all samples. For each series, eight replicates were tested and averaged.

3.29. *In vivo* adhesion studies on minipigs

In vivo tests were carried out in pigs devoted to laparoscopic skill-training for surgical residents. The experimental protocol was compliant with the Dutch Animal Experimental Act and approved by the Animal Experimental Committee of Maastricht University Medical Center. After laparotomy, the membranes (3 cm X 6 cm) were placed around the intestine which was then repositioned in the abdominal cavity and the abdomen was sutured in two layers. After 7 hours, the animal was sacrificed, the treated intestine was macroscopically evaluated and the part of the intestine in direct contact with the membrane was harvested for histological analysis. This test was employed to test the *in vivo* adhesiveness of membranes containing dopamine-modified alginate and membranes sterilized by means of $scCO_2$ (*set3*).

3.30. Histological analyses

Tissue samples were fixed in formalin 4% v/v for 24 hours and then embedded in liquid paraffin. Sections of 4 µm were cut, de-paraffinized in xylene and rehydrated in graded ethanol to distilled water, followed by hematoxylin-eosin staining.

3.31. Attenuated Total Reflectance Fourier Transform Infrared Spectroscopy (FTIR-ATR) on MNPs

Fourier transform infrared spectra of MNPs were collected using a Spectrometer Nicolet 6700 (Thermo Electron Corporation, Madison WI, U.S.A.) with a DTGS KBr detector. The following setup was used throughout the measurements: number of sample scans 16, resolution 6 cm^{-1} from 500 cm^{-1} to 4000 cm^{-1}.

3.32. Dynamic Light Scattering (DLS) and ζ-potential measurements

The hydrodynamic size and surface ζ-potential of the MNPs suspension (50 μg/ml) were assessed at 25 °C by a a Zetasizer Nano ZS (Malvern Instruments), consisting of a photodiode detector and a 4 mW He–Ne laser (λ = 633 nm). The hydrodynamic diameter was calculated from the ζ-average translation diffusion coefficient through the Stokes–Einstein equation. The laser doppler velocimetry (LDV) was employed to determine the ζ-potential values of all the MNPs suspensions. All the measurements on MNPs suspensions were performed at least in triplicate. The analyses of MNPs at the final concentration of (50 μg/ml) were redispersed in the following working solutions: NaCl 1.5 mM, 150 mM, 500 mM, HCl 50 mM (pH 2), MES buffer 50 mM (pH 5), Hepes buffer (pH 7), PBS 10 mM (pH 8), NaOH (pH 10), deionized water (pH 6), Lurian Broth (LB) 1X and Medium106 respectively.

3.33. Bacterial growth inhibition assay

The antibacterial activity of MNPs was evaluated using *Escherichia coli* (ATCC® 25922™), *Staphylococcus aureus* (ATCC® 25923™) strains. 20 μl of bacteria preserved in glycerol were added to 5 ml of LB broth and incubated overnight at 37°C. After 24 hours, 500 μl of bacterial suspension was diluted in 10 ml of broth and grown up for 90 min at 37°C in order to restore an exponential growth phase. Bacterial concentration was measured by means of optical density (OD) at 600 nm. Bacteria were resuspended with LB broth (2×10^5 bacteria ml^{-1}). MNPs-treated bacteria were treated with MNPs at different concentrations (200 μg/ml, 50 μg/ml, 20 μg/ml). As a negative control, latex Beads (Sigma) were used. In the case of membranes, coated (25 μg MNPs / cm^2) and uncoated samples (ϕ = 6 mm) were rehydrated in water and incubated with the bacterial suspension (2×10^5 bacteria ml^{-1}) in a final volume of 500 μL. All bacterial samples were incubated at 37 °C for 24 hours in shaking conditions. At the end of incubation, bacterial suspension was serially diluted in

PBS buffer (from 10^{-1} to 10^{-7}) and 25 µl of each suspension was plated on LB agar. After overnight incubation at 37 °C, the colony forming units (CFUs) were counted. Outcomes were compared with the suspension of bacteria grown in liquid medium as control.

3.34. Preparation of bacteria for SEM

E. coli and *S. aureus* (2×10^5 bacteria ml^{-1}) were incubated with MNPs (50 µg/ml and 200 µg/ml) and with LB medium (negative control) for 1 hours at 37°C, under shaking. Bacteria were rescued on a nitrocellulose filter paper with pore size of 0.2 µm. The filters were washed in PBS 1X for three times and gradually dehydrated in ethanol (30%, 50%, 70%, 95%, 100%), each step for 10 minutes. To dry the filters, samples were immerse in 2 ml of HMDS until amalysis.

3.35. UV spectroscopy studies on dopamine-modified alginates

UV-visible spectra of MNPs (100 µg/ml in water) was acquired in the range of 200 – 800 nm with a *UV-1800 Spectrophoometer Shimadzu*.

3.36. Statistical analyses

Data are expressed as means and standard deviations. Statistical analyses were performed using Student's t test, and a p-value < 0.05 was considered statistically significant.

4. EXPERIMENTAL SECTION

4.1. PREPARATION AND MECHANICAL, CHEMICAL AND BIOLOGICAL CHARACTERIZATION OF POLYSACCHARIDE-BASED MEMBRANES FOR WOUND HEALING

4.1.1. LIST OF ABBREVIATIONS

- GDL D-Gluconic acid δ-lactone;
- HA hyaluronic acid;
- HDFa human dermal fibroblasts adult;
- LDH lactate dehydrogenase;
- SEM scanning electron microscopy.

4.1.2. AIMS

In this section, polysaccharide-based membranes for wound healing applications were prepared and characterized. Mixtures containing alginate and HA were employed for the preparation of calcium-reticulated hydrogels that underwent freeze-drying for the manufacturing of surgical membranes. The main aims of these studies were to:

- set up the procedure for membrane manufacturing;
- evaluate the mechanical properties of the membranes to predict the behavior of the biomaterial during a surgical procedure, considering their potential use for intestinal applications (anastomosis wound healing);
- prepare different formulations of membranes and evaluate the effect of the composition on their mechanical properties;
- evaluate degradation and release profiles in simulated physiological conditions;
- investigate the biological effect of the membranes on fibroblast cells in terms of biocompatibility and bioactivity (*i.e.* ability to stimulate the migration and proliferation of cells).

4.1.3. RESULTS AND DISCUSSION

4.1.3.1. Manufacturing of membranes based on alginate and HA

Polymer-based biomaterials in the form of membranes, meshes and dressings represent ideal supports for the development of bioactive surgical devices (320). In particular, in the field of wound treatment, the use of membranes based on both natural and synthetic polymers has been reported (321;322). Given these premises, in this research work alginate-HA membranes for intestinal wound healing applications were manufactured through a freeze-drying procedure, starting from aqueous solutions containing the two polysaccharides. In particular, alginate and HA were dissolved in deionized water in the presence of glycerol as a plasticizer. A $CaCO_3$ suspension was added to the solution as an inactive source of Ca^{2+} ions. The further addition of GDL decreased the pH of the solution, leading to the release of Ca^{2+} ions that enabled hydrogel formation. The mechanism of hydrogel formation is sketched in figure 14.

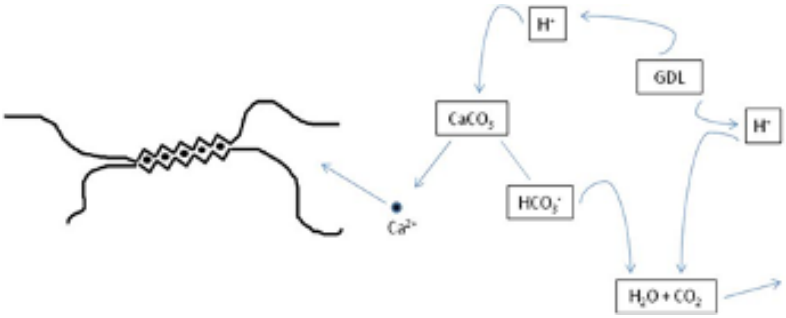

Figure 14. Formation of alginate hydrogels in the presence of Ca^{2+} ions.

After gelation, freeze-dried membranes were obtained through a procedure based on a temperature-controlled freeze-drying; this procedure enabled to obtain pliable membranes with a homogeneous mesh (figure 15a). A morphological analysis of the membrane at the microscopic scale was carried out by SEM microscopy (figure 15b and c) which highlighted their homogeneous polymeric texture. Cross section micrographs displayed an average thickness of approximately 300 μm (figure 15c); such a limited thickness matches with the thickness range of the main commercial surgical membranes for internal use (323).

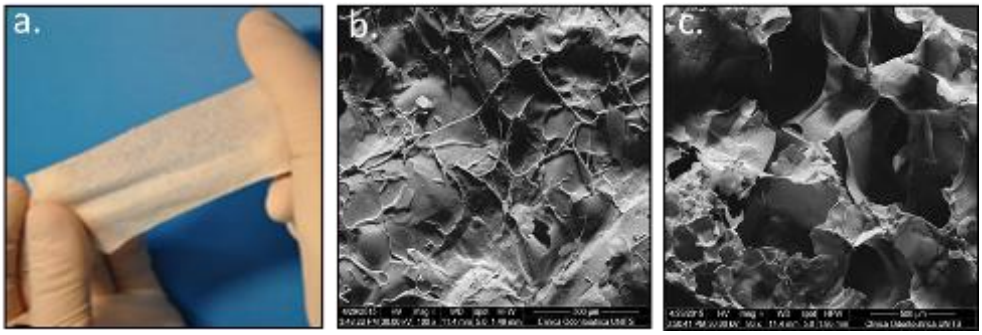

Figure 15. Images of alginate-HA freeze-dried membranes (Formulation D): macroscopic view (a); top view at SEM (b); cross section at SEM (c).

4.1.3.2. Mechanical characterization of membranes

During a clinical procedure, it is important to handle, position and adapt a surgical membrane to the target site without breaking or tearing the material. The polysaccharide-based membrane described in the section 4.1.3.1 ("*4.1.3.1. Manufacturing of membranes based on alginate and HA*") were specifically designed and developed as an implantable device to be wrapped around the intestine (anastomotic site), in order to stimulate the wound healing. In this perspective, it should be considered that these membranes were conceived to withstand the maximum mechanical stress during the positioning of the device on the target body site, *i.e.* at the dry state. After implantation, the membrane was designed to undergo a progressive degradation under the effects of body fluids and enzyme catalysis.

For these reasons, the mechanical performances of the membranes (at the dry state) were investigated in terms of stiffness, resistance and pliability by means of uniaxial tensile tests, considering the Young's Modulus, the stress and the strain at break of several membrane formulations. In particular, we investigated the effect of polymer concentration, amount of reticulating agent (Ca^{2+} amount) and molecular weight of HA on the mechanical behavior of the membranes, considering membranes of alginate alone (Formulation A) as a reference. The formulations investigated for this analysis are listed the table 2.

Formulation	**Alginate concentration (g/L)**	**HA concentration (g/L)**	**MW HA (kDA)**	**$CaCO_3$ concentration (mM)**	**GDL concentration (mM)**	**Glycerol concentration (v/v)**
A	15	-	-	20	40	5
B	15	15	800	20	40	5
C	20	15	240	20	40	5
D	15	15	240	20	40	5
E	15	15	240	50	100	5

Table 2. List of the formulations of membranes evaluated in term of mechanical properties.

Tensile tests were performed according to the ASTM-D638-10 standards with type 1 specimens ("dog-bone shape"). The mechanical behavior of the different membrane formulations is reported in figure 16.

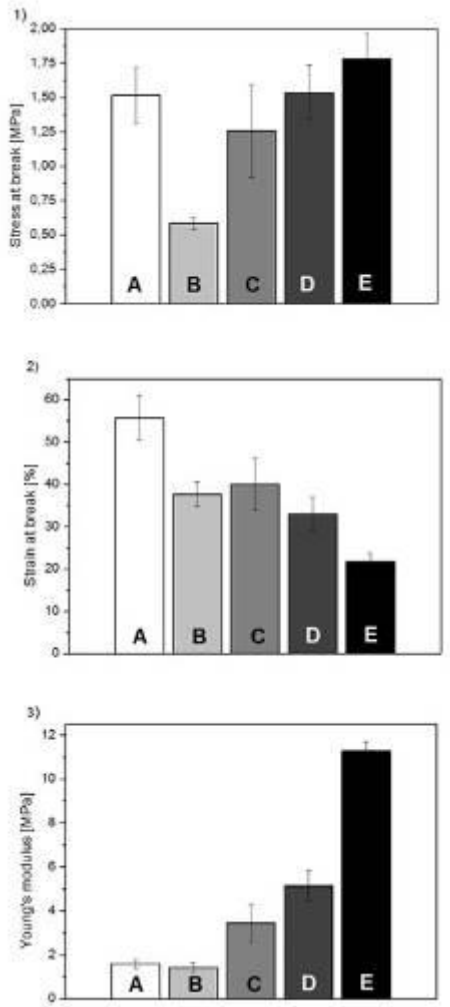

Figure 16. Mechanical properties of freeze-dried membranes of different compositions: 1) Stress at break, 2) Strain at break, 3) Young's Modulus. Membrane formulations: A) Alginate 15 g/L, $CaCO_3$ 20mM, GDL 40mM, glycerol 5% v/v; B) Alginate 15 g/L, HA (800 kDa) 15 g/L, $CaCO_3$ 20 mM, GDL 40 mM, glycerol 5% v/v C) Alginate 20 g/L, HA (240 kDa) 15 g/L, $CaCO_3$ 20 mM, GDL 40 mM, glycerol 5% v/v; D) Alginate 15 g/L, HA (240 kDa) 15 g/L, $CaCO_3$ 20 mM, GDL 40 mM, glycerol 5% v/v; E) Alginate 15 g/L, HA (240 kDa) 15 g/L, $CaCO_3$ 50 mM, GDL 100 mM, glycerol 5% v/v.

Despite the absence of covalent crosslinks to stabilize the physical matrix of the membrane, all the membranes displayed a tensile strength in the range of 0.5 – 1.8 MPa, in line with commercial collagen-based membranes for surgical use (324).

Considering membranes of alginate alone (Formulation A) as a reference, when HA with molecular weight 800 kDa was added, the stress at break decreased from 1.5 ± 0.2 MPa to 0.6 ± 0.1 MPa (Formulation B) and the strain at break decreased from 55 ± 5% to 37 ± 3%, while the Young's Modulus remained approximately unaltered. At variance, when HA with a lower molecular weight (240 kDa) was added (Formulation D), the stress at break remained around 1.5 MPa, the Young's Modulus increased from 1.5 ± 0.2 MPa to 5.2 ± 0.4 MPa and the strain at break decreased from 55 ± 5% to 33 ± 4%. These results point out that, at a fixed alginate concentration, the addition of low molecular weight HA (240 kDa) increases the membrane stiffness with respect to high molecular weight HA (800 kDa). This could be ascribed to the fact that the low molecular weight HA could be better integrated within the reticulated polysaccharidic structure; conversely, high molecular weight HA causes a more pronounced destabilization of the alginate matrix.

Comparing membranes with a fixed concentration of alginate (15 g/L) and HA 240 kDa (15 g/L) (Formulation D), when the concentrations of $CaCO_3$ (and GDL) increased by 2.5-fold (Formulation E), the Young's Modulus increased from 5.2 ± 0.7 MPa to 11.3 ± 0.4 MPa, the stress at break slightly increased from 1.5 ± 0.2 MPa to 1.8 ± 0.2 MPa, while the strain at break decreased from 33 ± 4 % to 22 ± 2 %. Moreover, increasing the concentration of both $CaCO_3$ and GDL increases material stiffness and resistance, while the deformation ability decreases. Indeed, higher amounts of $CaCO_3$ increase alginate crosslinking, which accounts for the mechanical resistance and stiffness of the membranes.

Considering the effect of the alginate content in membranes prepared with 15 g/L HA (240 kDa), 20 mM $CaCO_3$ and 40 mM GDL (Formulation D), an increase of alginate concentration from 15 g/L to 20 g/L (Formulation C) caused a decrease of the Young's Modulus (from 5.2 ± 0.7 MPa to 3.5 ± 0.9 MPa), a slight decrease of the stress at break and an increase of the strain at break (from 33 ± 4% to 40 ± 6%). Given the equal concentration of Ca^{2+}, if a larger number of alginate chains occurs, there are less crosslinking points between alginate chains, which causes a decrease of membrane stiffness and a slight increase of its maximal elongation.

Overall, this analysis indicates that by varying parameters such as the concentration of the main components (*i.e.* polysaccharides, $CaCO_3$, GDL), the mechanical properties of the membranes can be tailored. The mechanical characterization of the membranes indicated Formulation D as the best compromise among resistance (stress at break), stiffness (Young's modulus) and compliance (strain at break); for this reason, this membrane was selected for

further investigations in terms of polysaccharides release, degradation and biological behavior.

4.1.3.3. Rehydration studies on membranes

Rehydration studies were performed to evaluate the swelling behavior of the alginate-HA membranes (Formulation D) over time. As a reference, alginate membranes (Formulation A) were considered (figure 17).

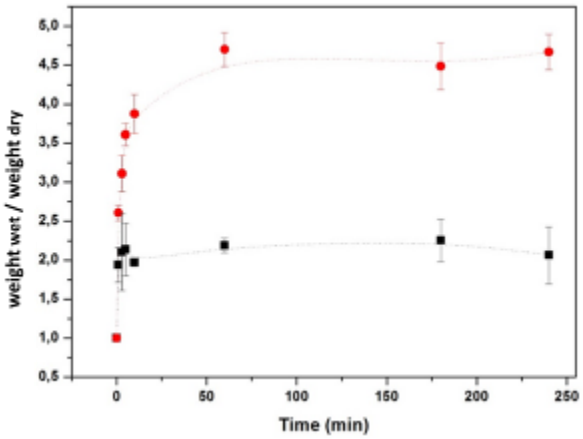

Figure 17. Rehydration kinetics of alginate (Formulation A; black squares) and alginate-HA membranes (Formulation D; red squares) in SBF solution. Data are reported as ratio between the weight of hydrated membranes and that of dry membranes.

The results showed that in both cases, the freeze-dried membranes rapidly absorb liquids after immersion in the medium. The weight of alginate membranes (Formulation A) underwent a two-folds increase after 1 minute incubation, with no significant variation over time. Conversely, in the presence of HA the weight of the membranes (Formulation D) gradually increases during the first 15 minutes of immersion, after which the swelling profile reaches a plateau. This behavior can be ascribed to the hydrophilic features of the HA that tends to absorb the surrounding fluids. After 4 hours of incubation, the equilibrium of water absorption was reached. Overall, these results show that the presence of HA enhances the swelling behavior of the membranes.

4.1.3.4. Polysaccharide release and membrane degradation

The evaluation of both polysaccharide release and degradation kinetics was tackled to predict the *in vivo* behavior of the membranes. The release profile of the two polysaccharides was

studied by means of NMR according to a procedure described by *Geremia et al* (140). The membranes (Formulation D) were incubated in HBSS and the release of the two polysaccharides was measured as a function of time and expressed as percentage at given time with respect to the initial amount of the polymers within the membrane (time zero), as shown in Figure 18A.

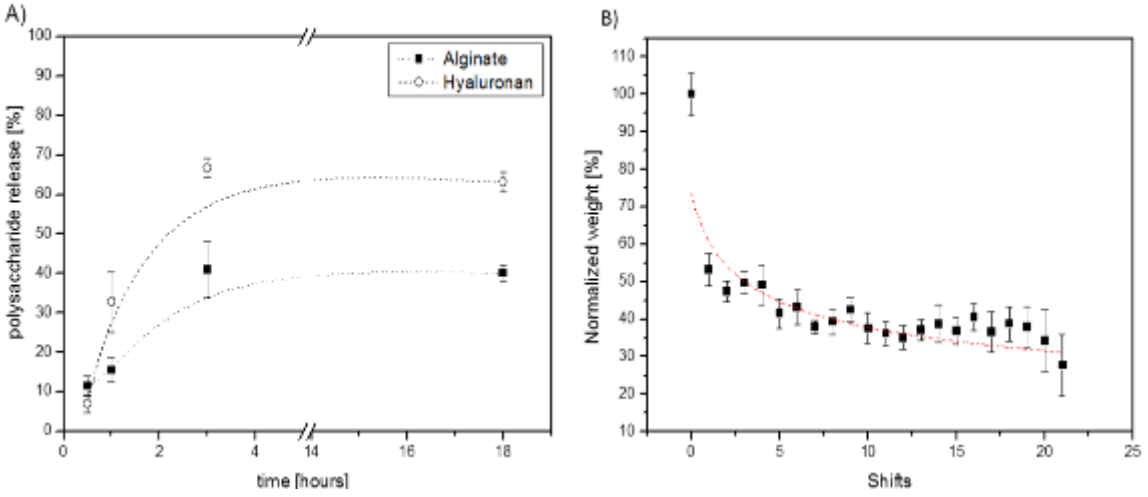

Figure 18. Polysaccharide release and degradation profiles in HBSS of the alginate-HA membrane (Formulation D). A) Polysaccharide release from alginate-HA membranes as a function of immersion time (square symbols: alginate release; round symbols: HA release); B) Degradation profile of the membrane in HBSS upon daily solution shift. Dashed and dotted lines were drawn to guide the eye.

It should be considered that these polymeric membranes were designed to enable the *in situ* release of the bioactive component (HA) at the injured site. Once the HA has been delivered at the target site, the membranes have to progressively degrade within the body. The results show that both polysaccharides start to be gradually released during the first 3 hours of immersion, after which both release profiles reach a plateau. The HA display a faster release kinetics than alginate: considering the initial content of both polysaccharides, approximately the 66% of HA and the 33% of alginate are released during the first 3 hours of immersion. In this time frame, the dissolution of alginate can be ascribed to the presence of surface domains where the reticulation of the alginate chains was partially affected by the accumulation of HA. These results are in line with the study of *Lindenhayn et al.* showing that more than 40% of the HA entrapped in alginate beads with higher degree of reticulation is released during the first 3 days in cell culture medium (325). The fast release of the HA represents a positive feature for the membrane, since the HA has to be effectively provided on the wounded site to stimulate tissue healing, immediately after the wound has been closed by sutures.

In parallel, the degradation profile of alginate-HA membranes was studied by immersing the samples in HBSS solution at 37 °C and measuring the mass upon daily shifts of solution. The results are coherent with the analysis of the polysaccharide release (figure 18B): the membrane underwent an initial rapid loss of weight which is consistent with the release of HA and of a small fraction of alginate from the membrane, observed during the first hours of immersion (figure 18A). Then, the degradation rate decreases, with a gradual weight reduction for the successive 3 weeks. After that time, only small fragments of the membrane could be found in solution.

4.1.3.5. *In vitro* biocompatibility

The *in vitro* biocompatibility of alginate (Formulation A) and alginate-HA membranes (Formulation D) was investigated on human dermal fibroblasts (HDFa cells), by testing the effect of the liquid extracted from the membranes. The analysis of the *in vitro* biocompatibility was carried out through the quantification of lactate dehydrogenase (LDH). The LDH is a cytosolic enzyme that is released in the culture medium upon cellular membrane permeabilization caused by the effect of cytotoxic substances and materials. In this test, the effect of the liquid extracted from the membranes was evaluated (figure 19).

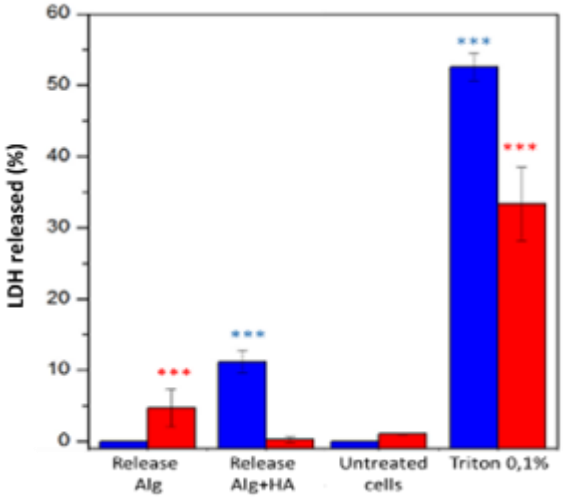

Figure 19. *In vitro* biocompatibility (LDH test) of primary human dermal fibroblasts (HDFa) treated with the liquid extracted from the alginate (Alg, Formulation A) or alginate-HA (Alg+HA, Formulation D) membranes, 24 hours (blue bars) and 72 hours (red bars) after incubation (***: p-value < 0.001).

The LDH data pointed out that, after 24 hours of treatment, the release of LDH slightly increases in the case of cells treated with the liquid extracted from the alginate-HA membrane (11.16 % ± 1.61 %), with respect to the control (untreated cells) (p-value < 0.001). At

variance, in the case of alginate membranes, a slight increase of LDH release was observed after 72 hours incubation (4.69 % ± 2.62 %) (p-value < 0.001). On the contrary, the enzyme release quantified in the medium of cells treated with the cytotoxicity control (Triton X-100) was significantly higher (p-value < 0.001). The slight increase of LDH release observed in the case of cells treated with the liquid extracted from the membranes can be ascribed to the increased viscosity of the cell medium, caused by the release of polysaccharides and glycerol. However, an optical evaluation of the treated cells points out no signs of cell suffering.

The biocompatibility of the membrane was also highlighted by a SEM investigation of primary human dermal fibroblasts (HDFa) seeded on the alginate-HA membranes: 24 hours after seeding, fibroblasts were able to colonize the material and to spread firmly on it; many cells appear flattened with long cytoplasmic extensions (figure 20). A deep physical integration of the cells with the polysaccharide matrix was observed, suggesting the existence of strong biological interactions between cells and substrate.

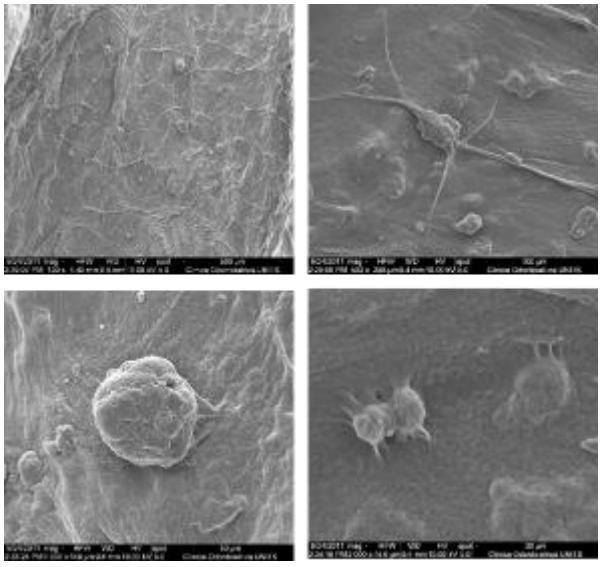

Figure 20. Primary human dermal fibroblasts (HDFa) on alginate-HA membrane (Formulation D).

These biological results suggest a possible use of this membrane also for tissue engineering applications, given its ability to support cell adhesion and proliferation.

4.1.3.6. *In vitro* wound healing

The wound healing assay was performed in order to evaluate the ability of the HA released from the membrane to stimulate the healing process. To this end, primary human dermal fibroblasts (HDFa) were treated with the liquid extracted from the membrane (Formulation

D). In order to highlight the contribution of HA to stimulate the wound healing, cells treated with cell culture medium and with the liquid extracted from alginate membranes (Formulation A) were considered.

For all the samples, a scratch was performed on a confluent cell plate and the gap closure was monitored over time (figure 21C, 21D, 21E, 21F). The results are expressed as the percentage of scratch closure as a function of incubation time (figure 21A and 21B). This approach mimics the physiological response of tissue healing, after a wound has been made on an intact tissue. Since the wound closure is due to a combination of both the cell migration and proliferation, in order to highlight the two contributions, the scratches were performed in the absence (figure 21A) or presence (figure 21B) of mitomycin C, a compound able to impair cell proliferation.

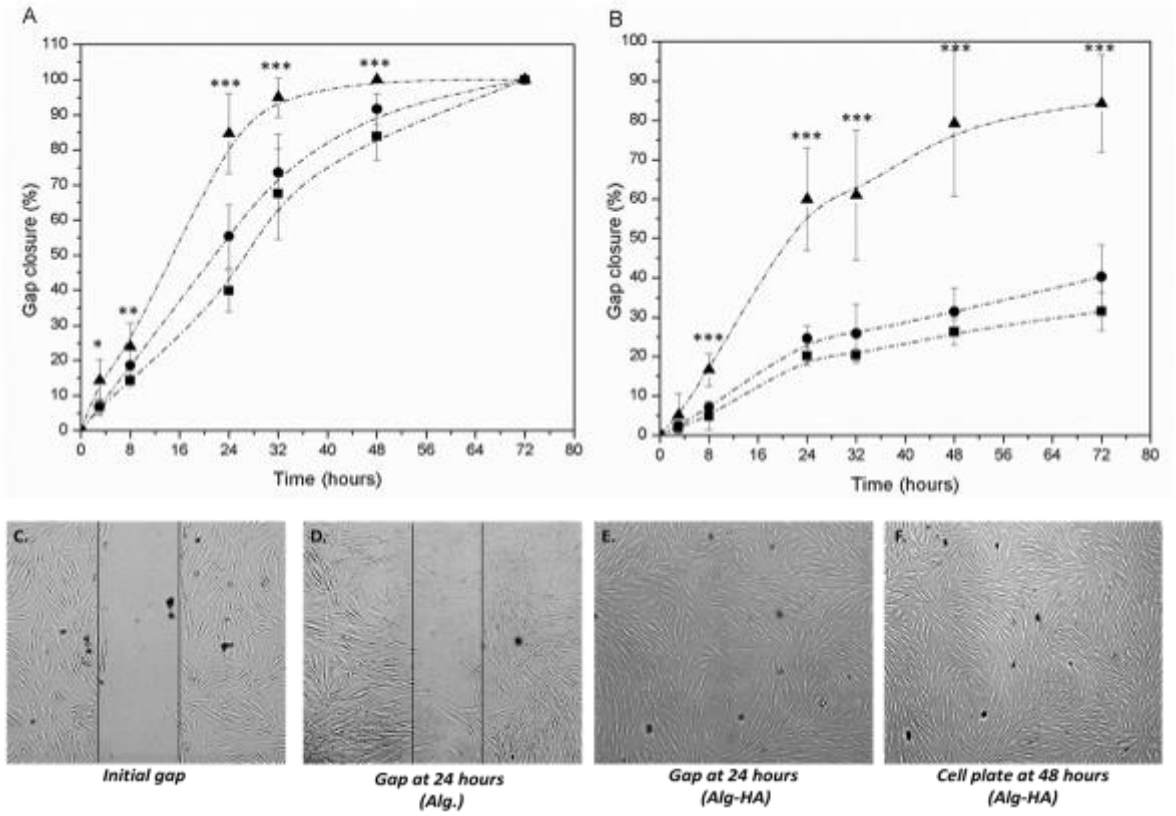

Figure 21. Effect of the membranes on the closure of gaps within HDFa cells cultured for the scratch tests in the absence (A) or presence (B) of mitomycin C. Triangles: alginate-HA membrane (Formulation D); circles: alginate membrane (Formulation A); squares: untreated cells (control). (*: p-value < 0.05; **: p-value < 0.01; ***: p-value < 0.001).

The results show that the kinetics of scratch closure of both cells treated with the liquid extracted from alginate membranes and untreated cells display a similar profile; conversely, in

the presence of the HA, the wound closure is accelerated. In this latter case, a complete gap closure was achieved after 32 hours, whereas in the same time frame, only a 70% of closure was observed for non-treated cells and cells treated with alginate membranes (figure 21A). When cell proliferation was impaired by mitomycin C (figure 21B), in the case of cells treated with alginate-HA membranes, the gap closure was 60% after 32 hours and 80% after 72 hours, while in the absence of HA the gap closure was less than 40% at 72 hours. These data point out that the main mechanism involved in the wound closure is the cell migration; however, since in the presence of mitomycin C a complete gap closure was not reached, a minor contribution of HA to cell proliferation seems to be involved. This biological study proved that the HA effectively released from the membrane provides a significant support to the physiological healing process.

4.1.3. CONCLUSIONS

In this section, a bioactive membrane based on polysaccharides and designed for the stimulation of wound healing was manufactured and characterized.

The main points addressed by this study are reported as follows:

- membranes based on alginate and HA can be manufactured starting from Ca^{2+}-reticulated hydrogels, through a freeze-drying procedure that enables to obtain pliable and soft membranes with a homogeneous texture;
- the mechanical properties of the membranes were evaluated by studying the influence of polysaccharides concentration, molecular weight and amount of reticulating agent (Ca^{2+}). Considering the final medical application, this analysis pointed out that the best performing candidate was Formulation D (Alginate 15 g/L, HA (240 kDa) 15 g/L, $CaCO_3$ 20 mM, GDL 40 mM, glycerol 5% v/v), since it combines the required resistance (stress at break), stiffness (Young's Modulus) and compliance (strain at break);
- the polysaccharide release profiles of alginate and HA were investigated in physiological solutions, pointing out that most of HA is released during the first 3 hours of immersion. This finding represents a positive feature of the membrane since this bioactive component should be immediately provided on the wounded site to stimulate tissue healing.

- *in vitro* biological tests proved the biocompatibility of the membranes on human dermal fibroblasts (HDFa), which were also able to colonize the substrate and integrate within the polysaccharide matrix.
- scratch assays demonstrated the excellent capability of the HA released from the membrane to support *in vitro* the physiological healing process.

Overall, these novel alginate-HA membranes represent a promising solution for several medical needs, in particular when the *in situ* administration of HA from a resorbable device is required. This strategy appears well suited for both the treatment of topical wounds as well as to promote the healing of internal tissues that have undergone surgery.

4.2. STERILIZATION OF POLYSACCHARIDE-BASED MEMBRANES BY MEANS OF SUPERCRITICAL CARBON DIOXIDE ($scCO_2$)

4.2.1. LIST OF ABBREVIATIONS

- FDA Food and Drug Administration;
- HA hyaluronic acid;
- HDFa human dermal fibroblasts adult;
- LDH lactate dehydrogenase;
- P.I. polydispersity index;
- $scCO_2$ supercritical carbon dioxide;
- SEC size exclusion chromatography.

4.2.2. AIMS

In this section, membranes based on polysaccharides were sterilized by means of $scCO_2$, in the presence of H_2O_2. Four sets of conditions were employed and the effects of temperature, time of exposure and amount of H_2O_2 on the properties of the membranes were investigated. In particular, the main aims of this study were to:

- investigate *in vitro* biocompatibility of the $scCO_2$-sterilized membranes;
- evaluate the extent of alginate degradation after sterilization;
- determine the effect of $scCO_2$ sterilization on the mechanical properties of the membranes;
- characterize the physico-chemical and biological properties of $scCO_2$-sterilized membranes in the presence of H_2O_2;
- perform preliminary *in vivo* studies to evaluate the effects of the sterilized material on the intestinal tissue.

4.2.3. RESULTS AND DISCUSSION

4.2.3.1. Evaluation of residual H_2O_2

FDA approved terminal sterilization techniques (*i.e.* steam sterilization, γ-irradiation and ethylene oxide) might have a strong impact on the macromolecular structure of polysaccharidic biomaterials (156;158;159;163), leading to side effects such as polymer

degradation (158;160) or retention of toxic residues that can compromise the *in vivo* biocompatibility of the sterilized biomaterial (161;162). To deal with these main drawbacks, the use of supercritical carbon dioxide ($scCO_2$) has been proposed as an alternative sterilization technique (163).

For the sterilization of the polysaccharidic membranes (Formulation D) by means of $scCO_2$, four sets of conditions were considered, by varying the amount of H_2O_2 (200 ppm or 1000 ppm) used and the exposure time (1 hour or 3 hours) (table 3).

	Pressure (bar)	**Temperature (°C)**	**H_2O_2 content (ppm)**	**Exposure time (hours)**
Set 1	270	40	200	1
Set 2	270	40	1000	1
Set 3	270	40	200	3
Set 4	270	40	1000	3

Table 3. Conditions employed for the sterilization of polysaccharidic membranes by means of $scCO_2$.

The efficiency of sterilization by means of $scCO_2$ can be enhanced in the presence of addictive molecules such as H_2O_2 (169), although these compounds can damage biomaterials based on polysaccharides and exert a cytotoxic effects toward eukaryotic cells (171;178). In this perspective, the quantification of the H_2O_2 within the membrane after sterilization can provide useful insights to predict whether potential adverse *in vivo* reactions might occur after implantation. To this aim, a colorimetric assay was performed to quantify the H_2O_2 within the sterilized membranes (figure 22).

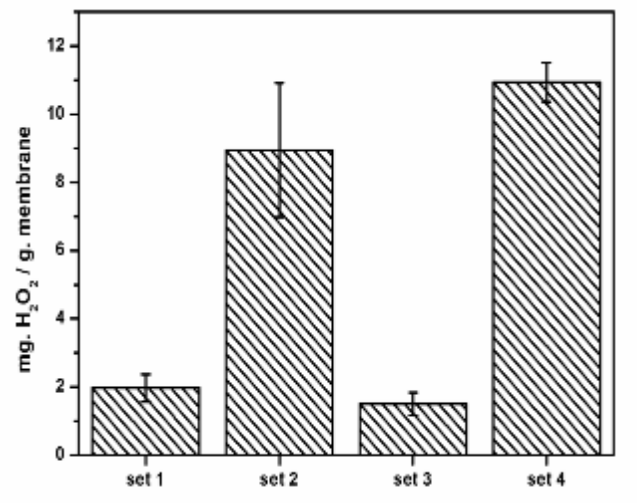

Figure 22. Quantification of residual H_2O_2 upon sterilization according to *set1*, *set2*, *set3*, *set4* conditions.

The analyses pointed out that the amount of H_2O_2 retained after sterilization increased by increasing its initial concentration (comparison between *set1-2* and *set3-4*; p-value < 0.01),

while no significant influence of the exposure time was noticed when the same amount of H_2O_2 was used (comparison between *set1-3* and *set2-4*; p-value > 0.05). Overall, the concentration of H_2O_2 employed for the sterilization, rather than the time frame of the procedure, affects the amount of H_2O_2 in the sterilized membranes.

4.2.3.2. Influence of the sterilization on alginate

The membranes sterilized according to the conditions of *set1*, *set2*, *set3*, *set4* were employed for SEC analyses to evaluate whether the sterilizing conditions cause the degradation of the polysaccharide matrix, taking into account the structural component of the membrane (alginate). For this reason, alginate alone membranes (Formulation A) were considered. The results are reported in table 4.

Type	Exposure time (hours)	H_2O_2 content (ppm)	Mn	P.I.	Mn reduction (%)
Non-sterilized	--	--	195.680	1.70	--
Sterilized (*Set1*)	1	200	170.998	1.89	13
Sterilized (*Set2*)	1	1000	31.449	2.40	84
Sterilized (*Set3*)	3	200	128.427	1.89	34
Sterilized (*Set4*)	3	1000	30.306	1.60	85

Table 4. SEC data of alginate membranes (Formulation A). Sterilization conditions, numeric molecular weight (Mn), polydispersity index (P.I.) and reduction of numeric molecular weight (%) are reported.

The results point out that, for all tested conditions, the $scCO_2$ sterilization causes a degradation of the polysaccharide matrix of membrane, since a reduction of the numeric molecular weight (Mn) of alginate was observed. The extent of such a degradation is mainly related to the amount of H_2O_2 used during sterilization (comparison between the *set 1-2* and *set 3-4*). In particular, the use of 200 ppm H_2O_2 has a minor impact on alginate degradation (13% degradation), while 1000 ppm H_2O_2 strongly decreases its molecular weight (85% degradation). These experimental evidences indicate that the conditions of *set2* and *set4* might not be suitable for the terminal sterilization of such biomaterials, while the sterilization performed according to the conditions of *set1* is suitable for the alginate structure. However, it has been demonstrated that times of exposure shorter than 3 hours do not ensure the sterilizing effect (165). Therefore, considering these results and data from the literature, the sterilization of the membranes for further analyses was carried out for 3 hours by using 200 ppm H_2O_2 (*set3*), since only this condition was found to cause an acceptable reduction of alginate molecular weight (34%).

4.2.3.3. Mechanical characterization of sterilized membranes

The alginate-HA membranes (Formulation D) were sterilized by means of $scCO_2$ (*set3*) and their mechanical performances were evaluated in terms of stiffness, resistance and pliability. This test was performed since the sterilizing procedures can affect the mechanical properties of polysaccharide-based biomaterials, making them less resistant and more prone to failure during surgical handling. For comparison, membranes sterilized by two approved terminal sterilization techniques, *i.e.* H_2O_2 in gaseous phase the γ-rays (>25 KGy) were considered (figure 23).

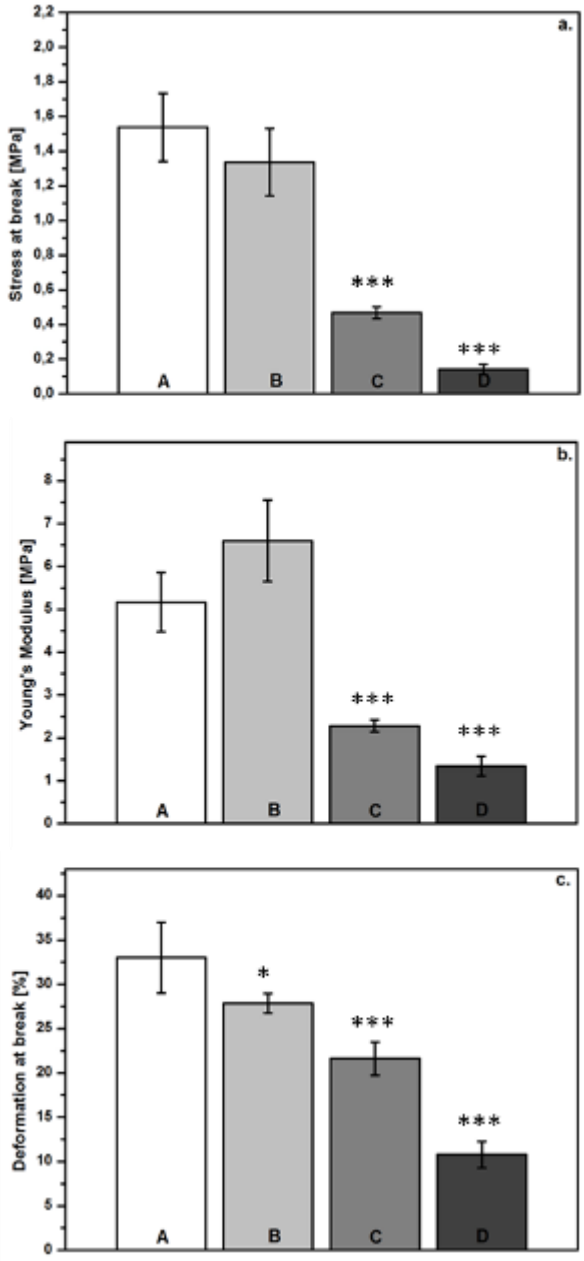

Figure 23. Mechanical properties of alginate-HA membranes (Formulation D) before and after sterilization. (A) non-sterilized membranes, (B) membranes sterilized by $scCO_2$ (*set3*), (C) gaseous H_2O_2 and (D) γ-radiation.

Stress at break (a), Young's Modulus (b) and deformation at break (c) are reported. (*: p-value < 0.05; ***: p-value < 0.001).

These data indicate that $scCO_2$ sterilization (*set3*) has a lower impact on the mechanical properties of polysaccharide-based membranes with respect to γ-irradiation and gaseous H_2O_2, for which a significant reduction of Young's Modulus (figure 23a), stress (figure 23b) and deformation at break (figure 23c) were observed (p-value < 0.01). At variance, in the case of $scCO_2$-sterilized membranes only a slight reduction (15%) of the deformation at break was noticed (p-value < 0.05), while the Young Modulus and the stress at break remain approximately unaltered. These results are in line with the studies of *Bernhardt et al* who demonstrated that the sterilization of alginate powder by means of $scCO_2$ has a lower impact on the mechanical properties of the resulting hydrogels with respect to steam sterilization and γ-irradiation (171). Similarly, *Donati et al* showed that the mechanical properties of biomaterials for biomedical applications (*i.e.* bisGMA-TEGDMA thermoset materials) and bioactive coatings sterilized by $scCO_2$ in the presence of H_2O_2 undergo only little variations after sterilization (165). Overall, these results indicate that sterilization by means of $scCO_2$ at the conditions of the *set3* can be an acceptable solution to preserve the mechanical properties of the alginate-HA membranes developed in this research work.

4.2.3.4. *In vitro* cytotoxicity of sterilized membranes

To evaluate the potential *in vitro* cytotoxicity of the $scCO_2$-sterilized membranes (*set3*), the LDH assay was performed on fibroblast cells (HDFa). $ScCO_2$ sterilized membranes (*set3*) were left in cell medium for 72 hours; the release of membranes was then incubated with cells and the analysis performed 24 and 72 hours after incubation. As a positive control of cell death, cells treated with a toxic compound (Triton-X100) were considered. The result points out that 24 and 72 hours after treatment, the release from sterilized membranes slightly affects cell viability, as the percentage of LDH released was as low as 16.6 ± 9.0 % (figure 24). Neverthless, the ISO 10993-5:2009 method for the evaluation of the cytotoxicity of a compound, states that a reduction of cell viability lower than 30% can be considered as a non-cytotoxic effect (171).

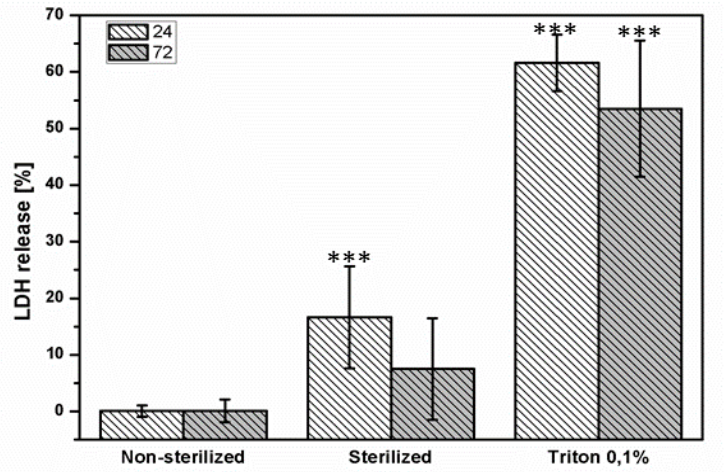

Figure 24. LDH cytotoxicity assay of alginate-HA membranes (Formulation D) before and after $scCO_2$ sterilization (*set3*) on HDFa cells. The positive and negative control of cell viability are represented by cells treated with Triton 0.1% and cell treated with the release of non-sterilized membranes, respectively.

Despite a certain extent of cell death that was observed in the case of cells treated with the sterilized membranes (7.50 % – 16.64 %) the level of cytotoxicity for the treated cells differs from that of the positive control (Triton-X100 0.1%). This effect can be ascribed to the presence of some toxic residuals of H_2O_2 that are retained into the membranes after sterilization and that can trigger a toxic response once released in cell culture medium. This hypothesis is consistent with the findings of *Ikarashi et al* who reported that the cytotoxic effect of several medical materials sterilized by vapour phase H_2O_2 was caused by the residual H_2O_2 (326). In a different work, sterilization of materials with $scCO_2$ in the presence of a solution containing H_2O_2 and acetic anhydride did not elicit a cytotoxic effect on bone-derived human mesenchimal stem cells. Thus, it is likely that the potential cytotoxic effect caused by the contact with a sterile biomaterial can be related to both the conditions employed for sterilization and to the features of the material itself. It should also be noticed that *in vitro* tests on cell cultures differ from real *in vivo* environment, where these residuals can be continuously diluted in body fluids; therefore, the effect of cell death is enhanced *in vitro* with respect to *in vivo* conditions.

4.2.3.5. *In vivo* evaluation of tissue reactions

A preliminary *in vivo* test in a pig model (non-dedicated animals) was performed for the evaluation of possible tissue reactions due to the presence of residual H_2O_2. For this evaluation, the $scCO_2$-sterilized membranes (*set3*) were wrapped around the intact intestine (*i.e.* in the absence of anastomosis) and kept in place for 7 hours after implantation (figure

25a). At the positioning, the sterilized membranes could successfully withstand the surgical handling and showed a good pliability and adaptability to the intestinal walls. No adverse tissue reactions (*i.e.* tissue bleaching) were observed when the contact between the membrane and the intestinal serosa was established. Upon animal sacrifice, the tract of the intestine previously wrapped with the sterilized membrane was harvested and embedded in paraffin. Paraffin sections were cut and subsequently stained with hematoxylin and eosin for the morphological analysis (figure 25b).

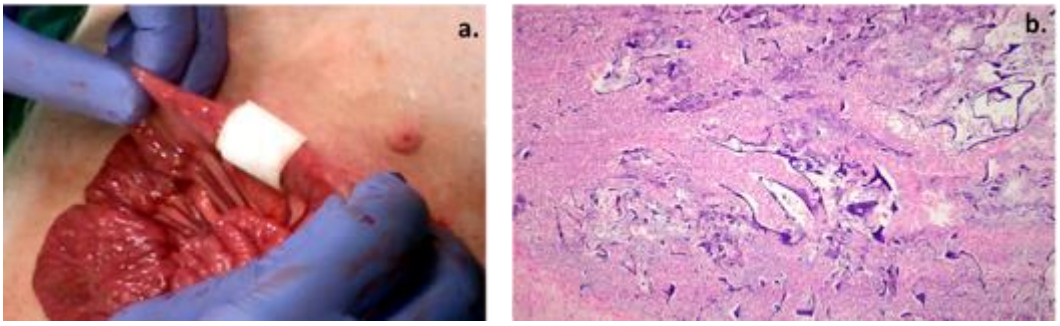

Figure 25. Membranes positioning at the pigs intestine (a) and histology of treated tissue (b).

The histological assessment showed a normal extracellular organization along with no signs of inflammation or early adverse tissue reactions. These morphological analyses point out that the sterilization based on $scCO_2$ may be promising for the terminal sterilization of these membranes, although an *in vivo* evaluation over prolonged time of exposure is required to confirm these preliminary results.

4.2.4. CONCLUSIONS

In this work, the effect of $scCO_2$ sterilization on the properties of membranes based on polysaccharides was investigated. Parameters such as temperature, time of exposure and amount of H_2O_2 were optimized to limit the impact of the sterilization procedure on the membranes. The test performed on sterilized membranes pointed out that:

- the amount of H_2O_2 within the membrane after sterilization is dependent on the amount of H_2O_2 employed for the sterilization, while no influence of the exposure time was noticed in the presence of equal amounts of H_2O_2;
- an overall reduction of the molecular weight of alginate occurred depending on the amount of H_2O_2 employed;

- sterilization performed for 3 hours by using 200 ppm H_2O_2 (*set3*) was found the most suitable, since the combination of these parameters were found to be less detrimental to alginate integrity and to ensure, at the same time, the sterilizing effect;
- sterilization by means of $scCO_2$ (*set3*) has a lower impact on mechanical properties of the sterilized membranes, with respect to γ-irradiation and H_2O_2 gas plasma sterilization.
- the H_2O_2 released from the membranes causes a slight *in vitro* cell cytotoxicity after 24 hours of incubation. No significant variation was observed at 72 hours;
- a preliminary *in vivo* test pointed out the absence of early adverse tissue reactions after the contact between membrane and pig's intestine. However, long term *in vivo* studies are required in order to provide enough evidence for a safe use of $scCO_2$.

4.3. H_2O_2-MEDIATED BIOADHESION OF THE POLYSACCHARIDE-BASED MEMBRANE TO THE INTESTINAL SEROSA

4.3.1. LIST OF ABBREVIATIONS

- SEC size exclusion chromotography;
- MALLS multiangle laser light scattering.

4.3.1. AIMS

In this section, the short-term adhesion of alginate membranes to intestinal explants of pigs was investigated. The main aims of these studies were to:

- develop an adhesive strategy based on the use of H_2O_2 applied as an exogenous compound to enhance the tackiness of membranes to the intestine;
- evaluate the structural modifications induced on both tissue and membranes upon exposure to H_2O_2 and investigate the molecular mechanisms driving the adhesion.

4.3.2. RESULTS AND DISCUSSION

4.3.2.1. Adhesion studies based on the use of H_2O_2

The rationale of this study was to induce the formation of an adhesive layer between an alginate-based membrane (Formulation A) and the intestinal tissue explants by treating both surfaces with H_2O_2. This oxidizing agent was employed to induce a molecular modification of the outer collagen of the tissue (serosa), in order to induce the formation of an adhesive layer of gelatin, while at the same time, promoting a partial oxidation of the polysaccharide alginate to enable the formation of reactive aldehyde groups. This approach is sketched in figure 26.

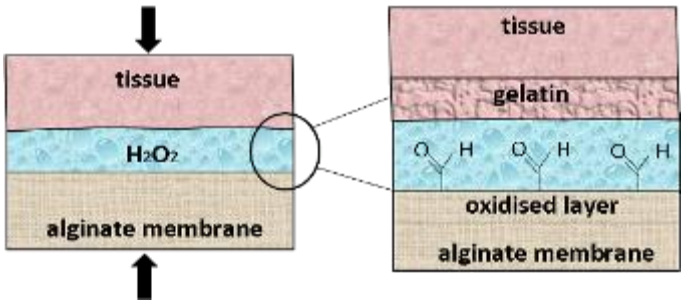

Figure 26. Formation of an adhesive interface between an alginate membrane and the intestinal serosa (tissue): surface modifications induced by treating the surfaces with H_2O_2.

To simplify the analysis regarding the contribution of the polysaccharide and tissue modifications in enhancing the adhesiveness of the biomaterial-tissue system, membranes devoid of HA were considered. To evaluate the detachment forces between the two surfaces, an experimental setup that mimics the *in vivo* interaction between membrane and tissue was considered taking into account that a possible site of application is represented by the intestine. In that configuration, the membranes were first placed in tight contact with the explanted pig intestine and the two surfaces were then pulled apart and the detachment force was measured (figure 27a). H_2O_2 was added on the membrane surface before forcing the contact with the tissue, while deionized water was used as a control liquid. The results show that the force required for the detachment of the membrane upon the treatment with H_2O_2 increases with respect to the membranes treated with water, pointing out the formation of an adhesive interface (figure 27b).

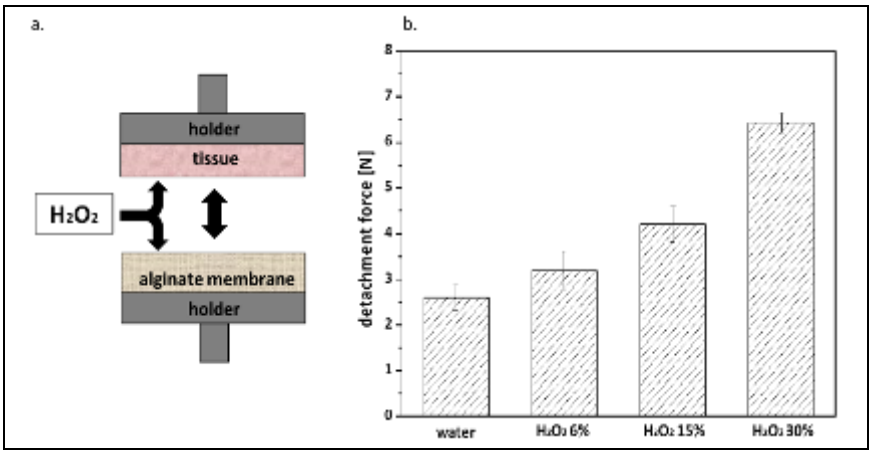

Figure 27. Adhesion tests between the alginate membrane (Formulation A) and the intestinal tissue (tissue): a) sketch of the experimental setup; b) detachment forces measured in the presence water or with increasing concentration of H_2O_2.

This behavior can be explained considering that H_2O_2 can exert its oxidative action through the modification of the chemical structure of the membrane and of the macromolecular components of the tissues. In principle, these modifications can determine the formation of an adhesive interface. In particular, H_2O_2 has been reported to drive the degradation of alginate molecules, causing the formation of aldehydes groups capable to establish covalent bonds mainly with amino groups of tissue proteins (179). At the same time, collagen denaturation triggered by H_2O_2 was previously reported to occur *in vivo* in tissues like cartilage (327), leading to the formation of a gelatin-like structure that displays adhesive features. Moreover,

the extent of such modifications can be related to concentration of H_2O_2 used: the higher the concentration of H_2O_2, the higher the extent of alginate and tissue modifications that result in the enhancement of the adhesion forces. Indeed, figure 27b shows that increasing the concentration of H_2O_2 leads to an enhancement of the adhesion force between membrane and tissue, with a maximum detachment force obtained with 30% v/v H_2O_2.

Once verified the formation of an adhesive interface by means of adhesion tests, molecular analyses were carried out to establish the contribution of gelatin formation and alginate oxidation upon contact with H_2O_2. In order to focus on the adhesive features of the gelatin layer formed on the surface of tissue after contact with H_2O_2, two alternative substrates (glass and stainless steel) were employed for the adhesion tests and compared with the alginate-based membrane. Tissue specimens were treated with 30% v/v H_2O_2 prior to contact with these substrates and the detachment forces were measured; the results showed that adhesion forces increase in all cases regardless the chemical nature of the interacting substrates, which highlights the adhesive role played by the gelatin layer (figure 28).

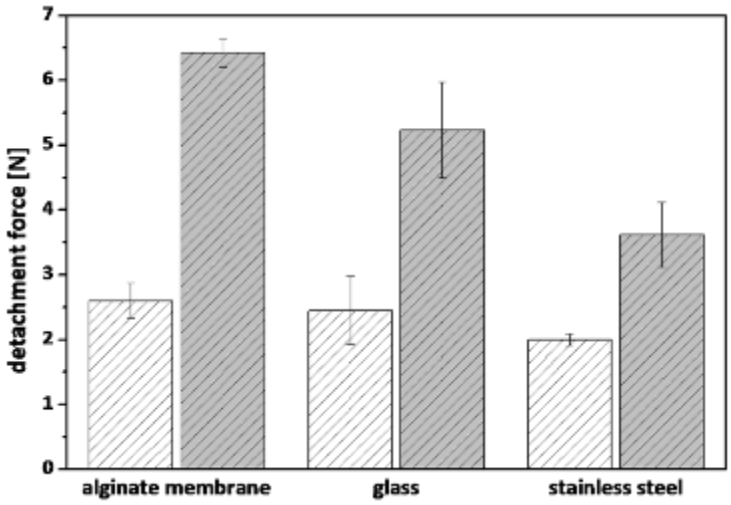

Figure 28. Adhesion tests between the intestinal tissue and various substrates (glass, stainless steel), in the presence of deionized water (white bars) and H_2O_2 (grey bars). As a reference substrate, the values obtained with the alginate membrane (Formulation A) are reported in the same graph.

4.3.2.2. Molecular Characterization of membranes treated with H_2O_2

After the analysis of the effects of H_2O_2 on the intestinal serosa, a study of the molecular modifications of the alginate-based membrane was carried out. With reference to the effect of oxidative species on alginates, the rupture of the glycoside bonds between monomers determines the shortening of the alginate chains and the formation of reactive aldehyde groups

by reducing C-1 ends (179); these groups may be involved in the formation of covalent bonds with amino groups of cell surface proteins (328;329).

In order to evaluate if the treatment with H_2O_2 causes the degradation of alginate, SEC-MALLS measurements were performed. The analysis pointed out a slight reduction of the molecular weight for the H_2O_2-treated sample (78.000 g/mol) with respect to the control sample (95.000 g/mol), stressed by the shift of the refractive index (RI) curve at higher retention times (figure 29).

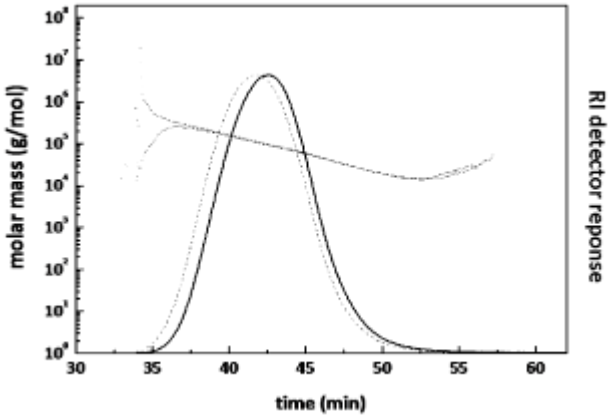

Figure 29. SEC-MALLS analyses of untreated alginate (dotted line) and alginate treated with H_2O_2 (solid line).

4.3.3. CONCLUSIONS

Adhesive interfaces between the alginate-based membrane and the intestinal tissue can be obtained by means of exogenous compounds applied between tissues and biomaterials. In this section, the use of H_2O_2 to drive the adhesion between the two surfaces has been investigated. The main conclusions addressed by this study are:

- H_2O_2 improves the adhesion between an alginate-based membrane and the intestinal serosa, through a mechanism that involves chemical/macromolecular modifications of both tissue and membrane;
- H_2O_2 drives the formation of an adhesive layer of gelatin on the surface of the tissue; this layer plays a major role in increasing adhesion forces;
- alginate undergoes a slight decrease of the molecular weight after the treatment with H_2O_2; however, this phenomenon does not seem to have significant effect in enhancing the adhesion strength, pointing to the main role of gelatin in adhesion mechanism.

Overall, this study describes a strategy to create adhesive interfaces between biomaterials and collagen-containing tissues and it can be exploited to enhance the adhesion of polysaccharide-based membranes to intestinal serosa, thus favoring an intimate contact between biomaterial and tissue.

4.4. ENHANCED BIOADHESIVITY OF POLYSACCHARIDIC MEMBRANES FUNCTIONALIZED WITH DOPAMINE.

4.4.1. LIST OF ABBREVIATIONS

- D-Alg dopamine-modified alginate;
- D-AlgM dopamine-modified alginate membrane;
- HA hyaluronic acid;
- HDFa human dermal fibroblasts adult;
- ^{1}H-NMR protonic nuclear magnetic resonance;
- H&E hematoxylin and eosin;
- MTT 3-(4,5-Dimethylthiazol-2-yl)-2,5-Diphenyltetrazolium Bromide;
- NIH-3T3 murine fibroblast cell line.

4.4.2. AIMS

In this section, an adhesion strategy based on the grafting of adhesive functionalities on alginate composing membranes was devised. This strategy enabled to enhance the long-term adhesiveness of the membrane to the intestinal epithelium in wet conditions. The main aims of this study were to:

- synthetize engineered polysaccharides (*i.e.* alginate grafted with dopamine moieties);
- set-up and optimize the manufacturing of membranes with dopamine-modified alginate;
- evaluate the adhesion of the membrane endowed with dopamine moieties in both simulated physiological conditions and *in vivo*;
- characterize the adhesive system as to its mechanical, adhesion and biological properties.

4.4.3. RESULTS AND DISCUSSION

4.4.3.1. Synthesis of dopamine-modified alginates

The adhesive substances secreted by mussels are protein-based compounds whose key adhesive molecules are L-DOPA residues. These molecules display a catecholic core that accounts for the attachment of mussels in wet environment, through the establishment of covalent bonds to both organic and inorganic surfaces (218). Given these premises, in this

research work catechol molecules displaying chemical features similar to those of L-DOPA (*i.e.* dopamine residues) were grafted on alginate in order to endow the structural component of the membrane with adhesive functionalities. EDC and NHS were added to the solution to activate the carboxyl groups of alginate, thereby enabling the coupling of alginate with the amino group of dopamine moieties. The reaction is shown in figure 30.

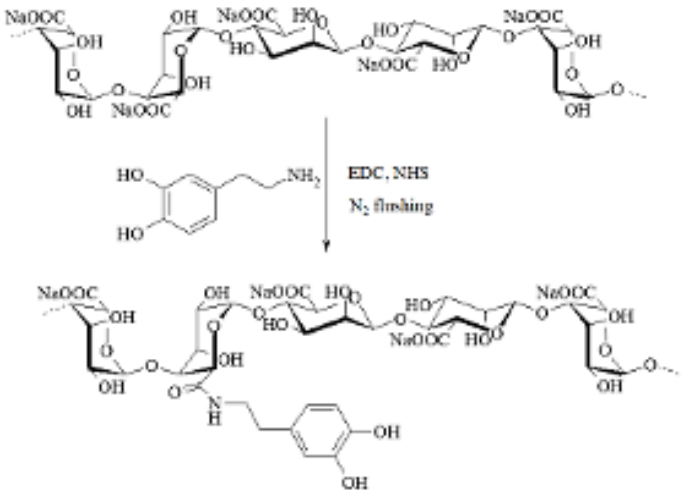

Figure 30. Grafting of dopamine on alginate backbone after activation with EDC, NHS of the carboxyl group of alginate.

Four formulations of dopamine-modified alginate (D-Alg1, D-Alg2, D-Alg3 and D-Alg4) were synthetized by varying the initial concentration of dopamine in solution. For each formulation, the degree of substitution was evaluated by means of ^{1}H-NMR that pointed out the successful grafting of dopamine on the alginate backbone (figure 31), and confirmed by UV spectroscopy. These analyses showed that the degree of substitution of D-Alg increases by increasing the initial concentration of dopamine employed for the synthesis (table 4).

Formulation	**Dopamine concentration (mM)**	**Degree of substitution (%) UV-visible spectroscopy**	**Degree of substitution (%) ^{1}H-NMR spectroscopy**
D-Alg1	12.5	0.62 ± 0.02	< 1
D-Alg2	25	1.68 ± 0.22	1.15
D-Alg3	50	2.48 ± 0.01	1.83
D-Alg4	75	3.42 ± 0.42	2.80

Table 4. Dopamine-modified alginates. For each formulation, the initial dopamine concentration (in solution) and the degree of substitution (measured by UV-visible and ^{1}H-NMR spectroscopy) are reported.

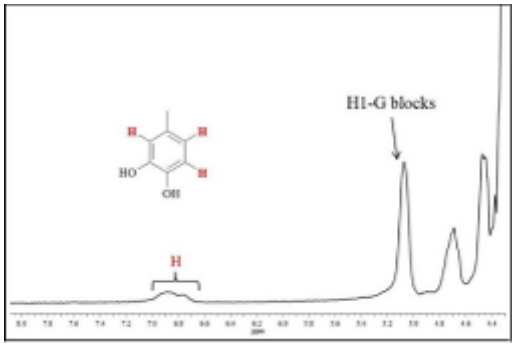

Figure 31. ^{1}H-NMR spectrum of dopamine-modified alginate.

Dopamine-modified alginates were employed for the preparation of calcium-reticulated hydrogels, which were freeze-dried to obtain the membranes (D-AlgM), as reported in the Materials and Methods section ("*3.3. Preparation of membrane containing dopamine-modified alginate*").

4.4.3.2. *In vitro* adhesion studies of membranes

In vitro adhesion studies were performed to evaluate the adhesiveness of the membranes in simulated physiological conditions and to highlight a possible correlation between the amount of grafted dopamine and the adhesion ability of D-AlgM to tissue. To this aim, an experimental setup was devised taking inspiration from the procedure described by Bernkop-Schnürch and colleagues (318). In the experimental set-up, fresh porcine intestine was harvested and wrapped around a plastic cylinder to put the mucosa in contact with the support and to expose to HBSS solution the external part (serosa). The membranes were then applied on the serosa side (figure 32).

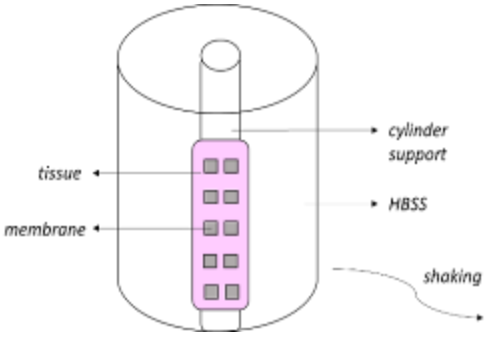

Figure 32. Experimental setup of *in vitro* adhesion studies. The tissue is wrapped around a cylinder, to expose the serosa tissue. Membrane specimens are applied on it and the system is immersed in HBSS and put under shaking.

The membrane-tissue system was completely immersed in HBSS under gentle shaking to mimic the action of abundant body fluids within the abdominal cavity. The time required for the detachment of the membranes from the intestinal tissue was recorded (figure 33).

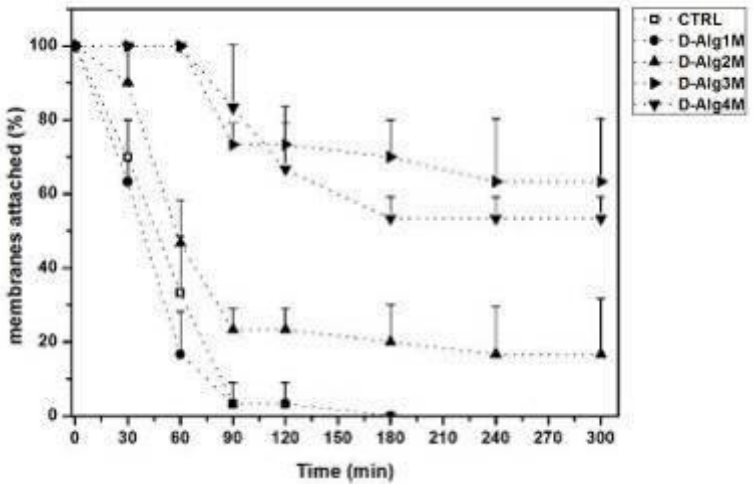

Figure 33. *In vitro* adhesion behaviour of membranes attached on explanted pig's intestine: the chart describes the detachment kinetics of the D-Alg membranes with respect to the control material (membrane without dopamine).

The test showed that the detachment of the D-Alg membranes occurs with a kinetic that reflects the substitution degree: in particular, the higher the latter, the higher the percentage of D-Alg membranes attached to the intestine. The behaviour of the membranes based on D-Alg1 was comparable to that of the membranes devoid of dopamine (control membranes). At variance, when higher dopamine contents were used, the detachment profiles of the membrane (D-Alg2M, D-Alg3M and D-Alg4M) showed an enhanced adhesiveness. Hence, the D-Alg1 formulation was not considered for further investigations.

Considering the experimental setup, it is reasonable to assume that this adhesion process could be enhanced *in vivo*, since the oxidizing environment in the human body might accelerate the oxidation of the hydroxyl groups of the catechol rings of dopamine, thus boosting the adhesion process. Finally, it should be considered that these test conditions put the membranes in contact with a volume of fluid higher than those generally found in the intraperitoneal cavity. For such reasons, this *in vitro* model is supposed to overestimate the rate of the detachment process with respect to *in vivo* conditions.

4.4.3.3. Mechanical characterization of membranes

The mechanical properties of the D-Alg membranes were tested at the dry state under uniaxial tensile conditions, in order to evaluate the effect of different substitution degrees on the mechanical performances of the modified membranes. Figure 34 shows the values of stress and strain at break of the membranes.

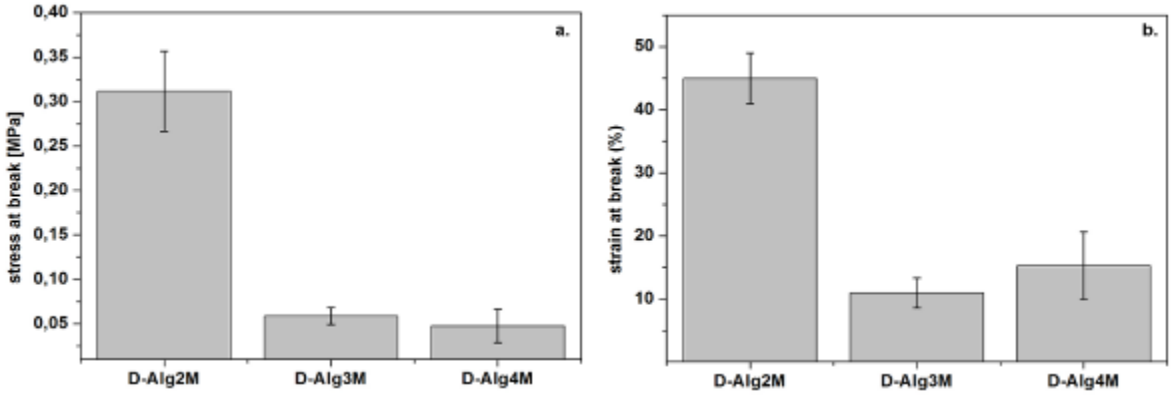

Figure 34. Mechanical properties of membranes based on dopamine-modified alginates (D-Alg): a) stress at break, b) strain at break.

The results show that the amount of grafted dopamine affects the tensile properties of the D-Alg membranes in the terms of mechanical resistance and deformation. This analysis pointed out that the parent membranes (*i.e.* having the same composition of D-Alg membranes, except for the polysaccharide being unmodified), displayed higher strength at break (1.31 ± 0.19 MPa) with respect to the D-Alg membranes. Moreover, the higher the substitution degree of D-Alg membranes, the lower the ultimate tensile strength of the membranes (figure 34a). This behaviour can be related to the fact that the chemical modification of alginate is known to influence its Ca^{2+}-coordination ability, which affects the reticulation process (330;331). In fact, given the key role played by guluronic acid sequences in determining such egg-box structures, it is reasonable to expect that an in principle random distribution of the dopamine residues on the alginate chains may affect a non-negligible number of such residues, thus preventing them from participating to the calcium-mediated interchain cross-links.

Considering the results from the *in vitro* adhesion test and the mechanical characterization, the D-Alg2 membranes were considered as the best performing, since they combine good mechanical resistance and improved adhesiveness. Thus, this membrane formulation was selected for the *in vitro* biocompatibility studies and for the evaluation of the *in vivo* adhesiveness.

4.4.3.4. *In vitro* biocompatibility (MTT assay)

To investigate the influence of the dopamine-modified alginate on cell viability, a colorimetric assay (MTT) was carried out on primary fibroblasts (HDFa) and on a fibroblast cell-line (NIH-3T3). The modified alginate (D-Alg2) was dissolved in cell medium at various concentrations and the cell viability was evaluated at 24, 48, and 72 hours after the treatment. As a positive control of cell viability, cells treated with a detergent that induces cell lysis (Triton X-100) were used. The results are reported in figure 35.

In the case of NIH-3T3 (figure 35a), there is no significant reduction of cell viability when comparing treated cells to control cells (p-value > 0.05), which indicates the non-cytotoxicity of the tested compound at each time intervals considered; the same results were obtained for HDFa primary fibroblasts at 24 hours. However, at 48 and 72 hours after treatment a slight reduction (12-16%) of the viability of treated cells could be observed at each concentration compared to untreated cells (p-value < 0.01) (figure 35b). As a mean of comparison, the viability of cells treated with the positive control (Triton) was reduced of more than 50% for both NIH-3T3 and HDFa cells. A qualitative evaluation of cell viability was performed by a visual analysis of the cell cultures through a microscope, in order to provide additional information on the potential cytotoxic effect of the modified alginates (figure 35c and 35d).

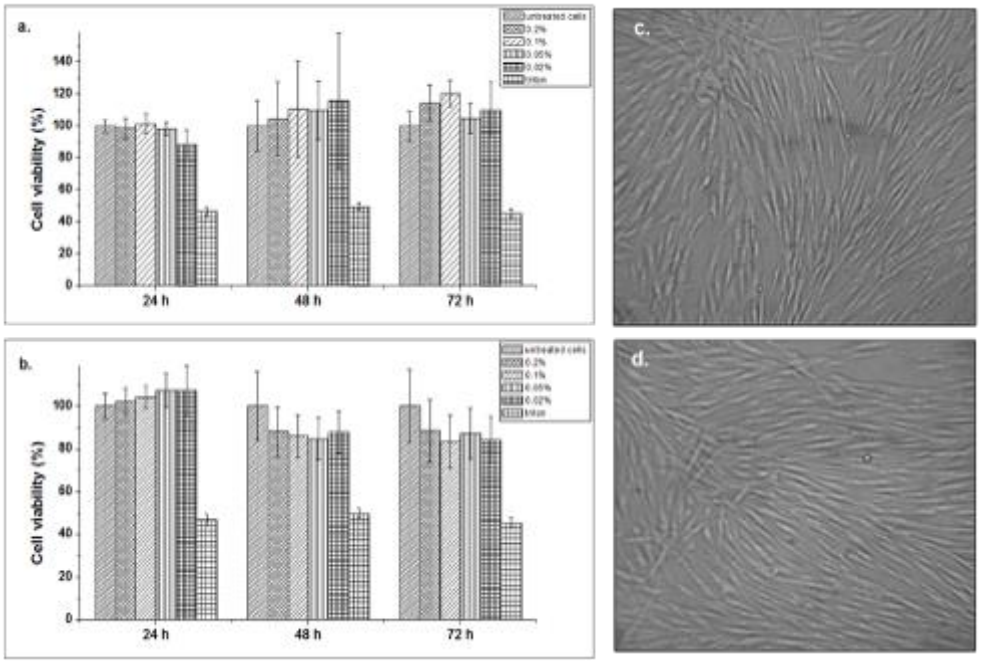

Figure 35. Cell viability (MTT test) of NIH-3T3 (a) and HDFa cells (b) treated with dopamine-modified alginate (D-Alg2) at various concentrations (0.2 %, 0.1 %, 0.05 % and 0.02 %). Optical images of untreated HDFa cells after 72 hours of culture (c) and cells treated with a dopamine-modified alginate at 0.2% (d).

Despite the slight decrease in the cell viability, it should be considered that, according to the ISO 10993-5:2009 method for the evaluation of the cytotoxicity of a compound, only a 30% or higher percentage of reduction of cell vitality is considered as a cytotoxic effect. Moreover, optical images of untreated cells (figure 35c) and of cells treated with dopamine-alginate after 72 hours of culture (figure 35d), points out no visible signs of cell suffering such as change of cell morphology, cell detachment, chromatin aggregates and apoptotic bodies, thus supporting the non-cytotoxic effect of the compound.

4.4.3.5. *In vivo* adhesion studies

The adhesiveness of the dopamine-modified membranes (D-Alg2M) was evaluated *in vivo* on a pig model. As a control, membranes prepared with non-modified alginate (Formulation D) were used. The materials were wrapped around the pig's intestine and kept in place for 7 hours after the operation. In both cases, the membranes displayed a good initial adhesion when in contact with the moist tissue and a good ability to adapt to the anatomy of the intestinal walls as neither alteration of the intestinal motility nor stenosis of the treated tract were observed. Interestingly, an increased stickiness was qualitatively observed in the case of the dopamine-containing membrane upon contact with the intestinal serosa. After 7 hours, the pig's abdomen was re-opened and the dopamine-containing membrane (D-Alg2M) was still found in place, appearing as a flexible and soft layer surrounding the intestinal walls. Moreover, the material could not be manually detached and a slight brownish colour was observed, indicating that a possible oxidation of the modified-polysaccharide occurred within the body (figure 36). At variance, the unmodified membrane was not found in place anymore when the abdomen was re-opened, pointing out an insufficient long-term adhesiveness of the material in such conditions.

Figure 36. *In vivo* adhesiveness of dopamine-containing membrane (D-Alg2M): the white arrows indicates the dopamine-containing membrane adhering to the intestinal serosa after 7 hours of implantation.

After the animal sacrifice, the tract of the intestine in contact with the dopamine-containing membrane was harvested and stained with hematoxylin and eosin for the morphological analysis. Hematoxylin and eosin are basic and acid dyes that are able to stain the cellular structures through charge interactions in a non-specific manner; so these compounds were employed to stain the negatively charged polysaccharides of the membrane in contact with the tissue (figure 37).

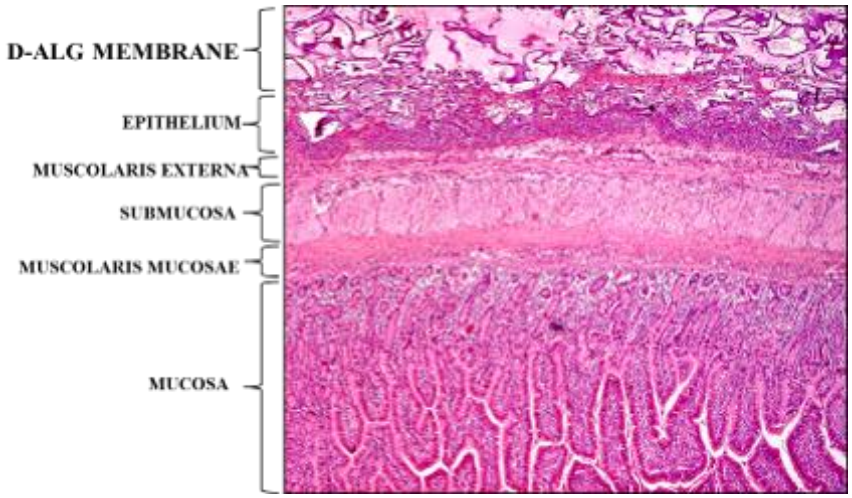

Figure 37. Histological analysis of the intestine-membrane interface (H&E staining).

The histological assessment pointed out the absence of early adverse tissue reactions upon the contact with the modified-membrane (figure 37) and the presence of the D-Alg2M membrane appearing as a purple layer grafted on the intestinal epithelium (serosa), showing the deep compenetration between the material and the intestinal epithelium.

4.4.4. CONCLUSIONS

In this study, the long term adhesiveness of polysaccharidic membranes to the intestinal epithelium was improved by exploiting a bio-inspired adhesive strategy. Dopamine moieties were chemically grafted on alginate, in order to endow the membrane with adhesive functionalities enabling an improved bioadhesion in wet conditions. The main points addressed by this study were the followed:

- alginate modified with dopamine moieties (D-Alg) can be synthetized by chemical coupling. The linear correlation between the initial concentration of dopamine and the substitution degree of the modified polymers was pointed out by ^{1}H-NMR and UV spectroscopy;

- the grafting of dopamine on alginate significantly improves the adhesiveness of the biomaterial to the intestinal tissue, as proved by both *in vitro* and *in vivo* tests;
- the mechanical properties of the D-Alg membranes are affected by the grafted dopamine residues, which can be ascribed to the inability of guluronic sequences of modified-alginate to coordinate Ca^{2+} ions, thus leading to the formation of weaker junctions within the hydrogels;

Overall, these engineered membranes enhanced adhesiveness in wet environment and showed good *in vitro* biocompatibility, thereby holding great promise for the development of adhesive biodegradable biomaterials for general surgery applications.

4.5. DEVELOPMENT OF ADHESIVE COATINGS BASED ON MELANIN NANOPARTICLES FOR POLYSACCHARIDE-BASED MEMBRANES

4.5.1. LIST OF ABBREVIATIONS

- DHI 5,6-dihydroxyindole;
- IQ indo-5,6-quinone;
- MNPs melanin-like nanoparticles;
- PdI polydispersivity index.

4.5.2. AIMS

The development of adhesive coatings for soft membranes represents an alternative to the functionalization of polysaccharides with chemicals. In this section, adhesive coatings based on melanin-like nanoparticles (MNPs) were prepared and characterized. The main aims of this study were to:

- synthetize and characterize MNPs suspensions (size dimension and surface charge);
- evaluate the stability of MNPs at different pH and ionic strength;
- set-up the manufacturing of membranes coated with MNPs and evaluate the adhesive properties in simulated physiological conditions;
- investigate the biological properties of MNPs in terms of *in vitro* biocompatibility and antimicrobial activity.

4.5.3. RESULTS AND DISCUSSION

4.5.3.1. Synthesis and characterization of MNPs

MNPs are catechol-based nanoparticles whose reactivity might offer novel solutions for the development of novel adhesive systems. Indeed, these nanoparticles expose reactive o-quinone groups on their surface, which enable the formation of covalent bonds with amines or thiols of tissue proteins; this property might be exploited to prepare adhesive coatings for implantable biomaterials (238;313). The use of MNPs for adhesive purposes provides several advantages over catechol-functionalized polymers. First, the chemical modification of polymers can modify the properties of the native molecules, which may lead to unpredictable

outcomes. As a second main point, nanoparticle suspensions are suitable for the development of uniform coatings and the high active surface of nanoparticles together with the presence of a higher number of quinone reactive groups exposed on their surface can ensure the establishment of an increased number of covalent interactions, thus strengthening the adhesive bonds.

The synthesis of MNPs was performed through the addition of NaOH to an aqueous solution of dopamine, as described in the literature (299). Dopamine-containing solutions are colorless at slightly acidic pH. The addition of NaOH triggers the formation of MNPs: the color of the solution immediately turns to pale yellow and then to black. At the same time, the pH of the solution decreases from basic to acidic values over prolonged polymerization time (figure 38a).

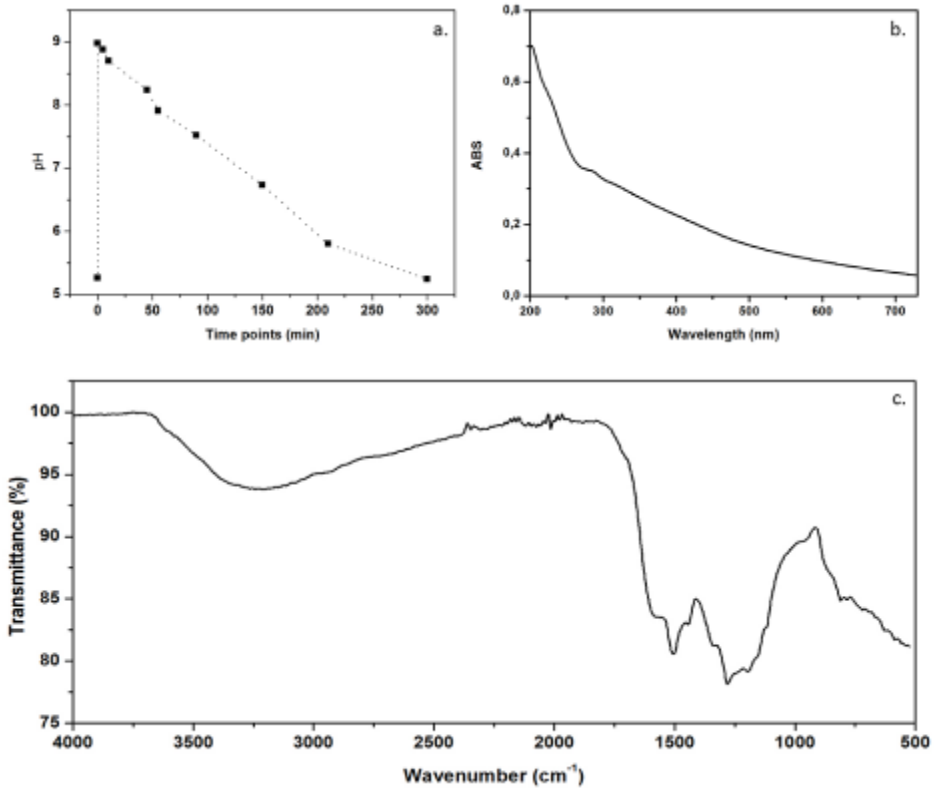

Figure 38. pH variation over MNPs formation (a); UV-visible spectrum of MNPs (b); FTIR spectrum of MNPs (c).

The decrease of the pH over time can be ascribed to the deprotonation of the amino group of dopamine (299). The addition of NaOH induced the synthesis of MNPs through the spontaneous oxidation of dopamine, leading to the formation of 5,6-dihydroxyindole (DHI) that can be further oxidized to indo-5,6-quinone (IQ). DHI units can assemble together to

form oligomers which are further linked through π-π stacking interactions and covalent bonds, leading to the formation of the nanoparticles (304) (see the section "*1.9.4 Catechol-based nanoparticles*"). The chemical reactions that take place after the addition of NaOH and the main intermediates that form during the synthesis are reported in figure 39.

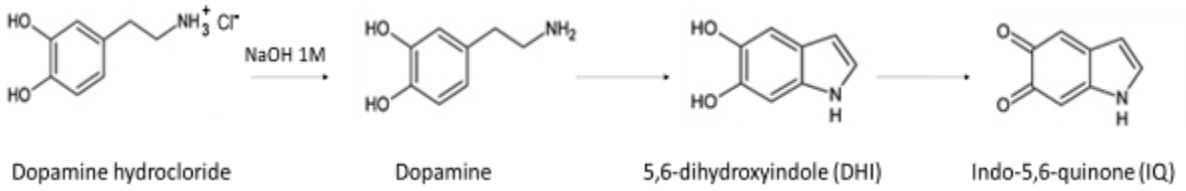

Figure 39. Chemical intermediates that form during the synthesis of MNPs.

The UV-visible and FTIR spectra of MNPs were measured after the nanoparticles purification, to confirm the melanin-like structure. The former spectrum showed a broad absorption band in the UV-visible spectrum, which has been reported in the literature for both synthetic (303;308;332) and natural melanins (303;333;334) (figure 38b).

The FT-IR spectrum of MNPs showed a broad band at 3000-3500 cm^{-1} corresponding to NH and OH stretching of indoles. The signal at 1608 cm^{-1} can be attributed to the C=C stretching vibration of phenolic ring, and those at 1506 cm^{-1} and 1405 cm^{-1} can be assigned to the NH bending and CH_2 bending respectively (figure 38c). These peaks were reported as characteristic of natural melanins (335;336).

4.5.3.2. Analysis of MNPs stability

Morphological analyses of MNPs pointed out that they are uniform, round shaped and well dispersed (figure 40).

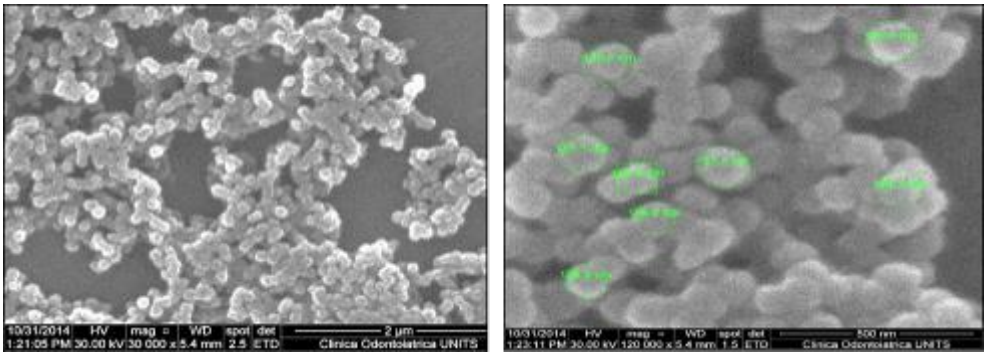

Figure 40. SEM images of MNPs.

The hydrodynamic diameter of the MNPs determined by means of DLS was 222.93 ± 12.29 nm, with a polydispersivity index (PdI) of 0.19, indicating the narrow size distribution. MNPs are negatively charged: the mean ζ-potential value was -26.97 ± 1.25 mV showing that a good nanoparticle dispersion stemmed from electrostatic repulsion. The analysis of the MNPs size pointed out that no significant variation of the mean z-average values occurred up to 80 days: at this time interval, the mean z-average value of the same formulation was 248.07 ± 65.41 nm). The stability of MNPs was also evaluated in the presence of aqueous NaCl at the concentrations of 1.5 mM, 150 mM (which corresponds to the ionic strength of the biological fluids) and 500 mM (figure 41). The result shows that the addition of NaCl 1.5 mM does not significantly modify both the mean z-average and the surface charge values of MNPs. Conversely, when higher concentrations of NaCl are used, the mean dimensions of MNPs increase, indicating their tendency to aggregate. The effect of NaCl on MNPs dimensions is paralleled by the ζ-potential, which points out that the presence of aqueous NaCl at concentrations equal to and higher than 150 mM, the surface potential of MNPs tends to decrease. In these cases, the ions in solution are likely to screen the repulsion forces among surface charges of the MNPs, thus causing their aggregation as confirmed by the increased PdI (0.40 ± 0.04). These results indicate that MNPs display a good stability in water, although in the presence of NaCl at concentrations equal and higher than that of the biological fluids (*i.e.* 150 mM), the tendency to aggregate occurred.

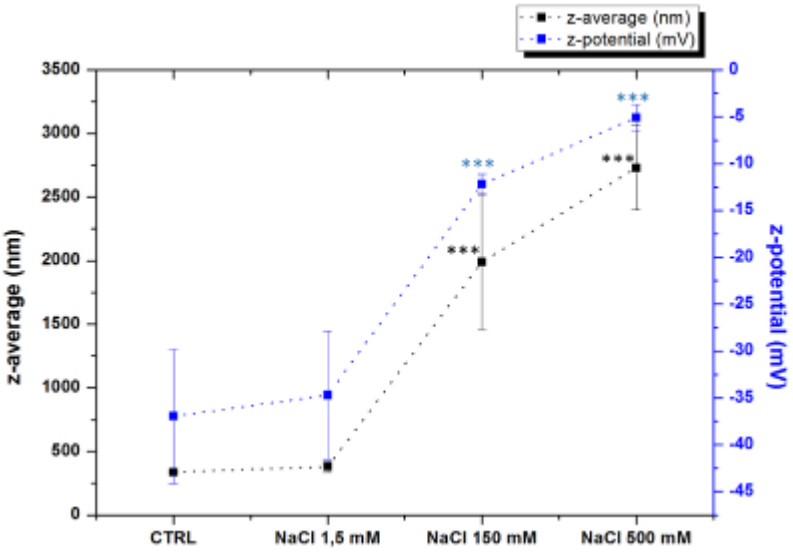

Figure 41. Analysis of MNPs dimension (black squares) and surface potential (blue squares) in water and in NaCl at different concentrations (***: p-value < 0.001).

The stability of MNPs at pH values ranging from 2 to 10 was evaluated by measuring size dimension and surface potential (figure 42). The analysis of the latter shows that a monotonic increase towards negative values of the mean surface charge values occurs upon increasing the pH. In particular, at pH 2 the ζ-potential reaches positive values, while a conversion to negative ones is observed at pH 6, 7, 8, 10.

At pH 5, the ζ-potential approaches the zero value (0.8 ± 0.2 mV), indicating the neutral surface charge of MNPs. At this condition, the dimensions of MNPs significantly increase with respect to the control (*i.e.* MNPs at pH 6), due to the absence of repulsion forces among MNPs, which favors their aggregation as confirmed by both the presence of micrometric structures and the higher PdI (0.41 ± 0.04). Hence, pH 5 has been identified as the least stable condition for MNPs, since in that condition the tendency to aggregate occurs.

At variance, at pH 2, 7 and 10 the particles dimensions do not differ significantly from those of the control. This result matches with the analysis of the surface potential showing that at these conditions MNPs reach a high surface charge density. A slight increase of the mean z-average value was observed at pH 8 (p-value < 0.01); at this conditions, the negative ζ-potential of MNPs indicates the presence of repulsion forces, although the increase of the PdI (0.23 ± 0.02) seems to indicate that small aggregates are formed.

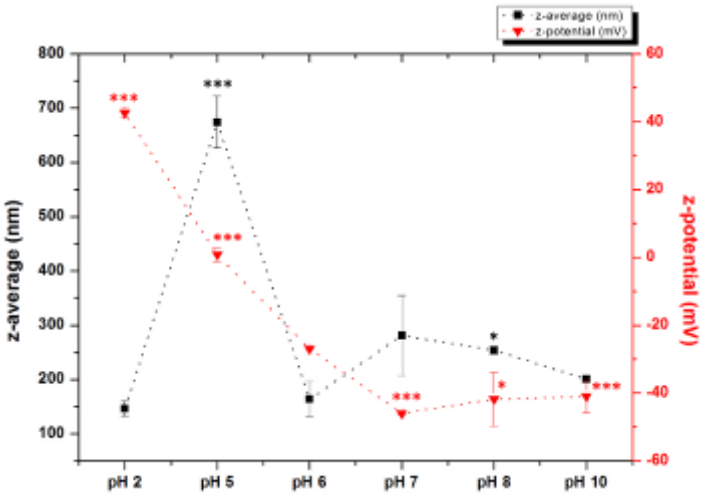

Figure 42. Analysis of MNPs dimension (squares) and surface potential (triangles) at different pH conditions (*: p-value < 0.05; ***: p-value < 0.001).

To explain these results, we hypothesized that at pH 2 the OH and NH groups of catechol moieties of MNPs are protonated, thus conferring a positive charge to the system; at variance, at pH higher than 6, the OH groups are deprotonated, so that MNPs display a negative charge (figure 43).

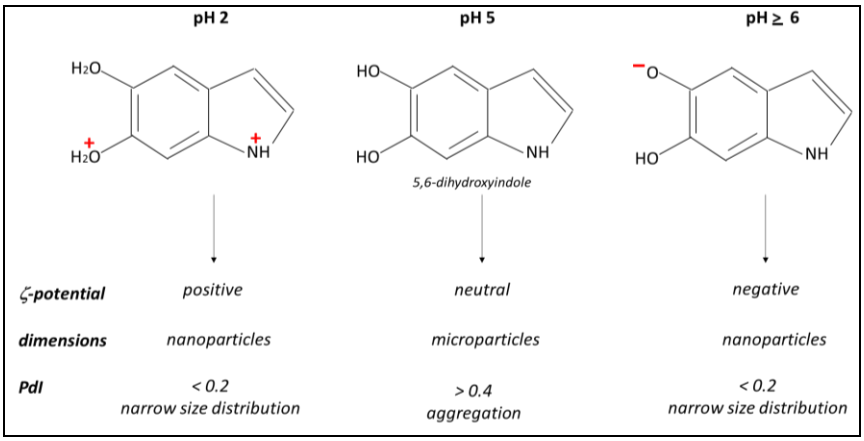

Figure 43. ζ-potential, size dimensions and PdI variations according to the pH.

In both situations, the high positive and negative charges of the system determine the repulsion of the MNPs from each other, leading to a good dispersion of the nanoparticles with no tendency to aggregate. This feature is confirmed by the dimensions of MNPs that do not differ significantly from that of the control, and by the low PdI of the nanoparticle suspensions that ranges from 0.14 ± 0.07 at pH 2 to 0.23 ± 0.02 at pH 8.

Overall, the analyses of the MNP dimensions and surface charge show that MNPs are stable at the selected conditions, except at pH 5 when the neutral surface charge induce the formation of MNPs aggregates.

4.5.3.3. Bioadhesion of MNPs coated membranes

Given the reactivity of MNPs and the exposure of quinones enabling the formation of covalent bonds with nucleophiles such as amino groups of tissue proteins, MNPs were employed for the manufacturing of adhesive coatings, by spreading MNPs on the surface of membranes. SEM analyses showed that MNPs can form a uniform layer on the membrane surface and that they are entrapped on the surface of the membrane (figure 44).

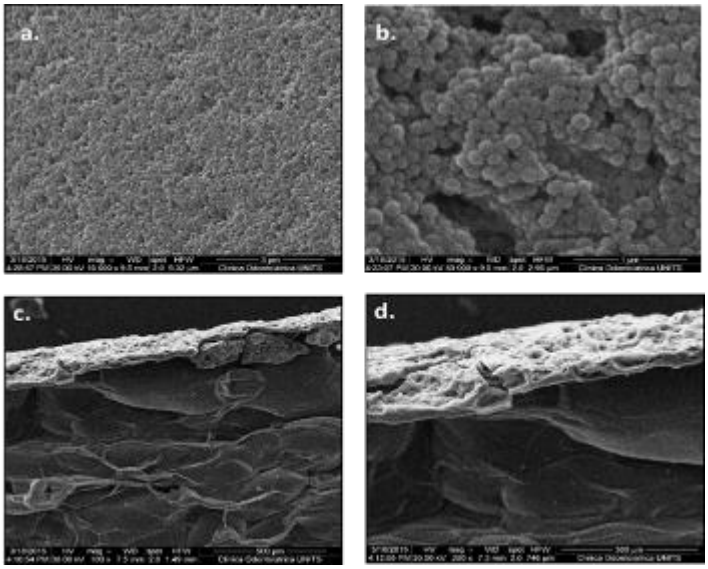

Figure 44. Top view (a. and b.) and cross-section (c. and d.) images of MNPs-coated membranes.

MNPs-coated 4.1.3.6.membranes (Formulation D) were characterized as to their bioadhesive properties to the intestinal tissue, in simulated physiological conditions. These membranes were placed on freshly harvested pig's intestine prior to immersing the system in a HBSS solution. As a control, uncoated membranes (Formulation D) were used and the time required for detachment of the specimens was measured. As shown in figure 45, the detachment kinetic of membranes coated with MNPs is slower than that of the uncoated membranes. Indeed, the latter membranes detached within 90 minutes of incubations. Conversely, in the presence of MNPs-based coating, the bioadhesion to the tissue is significantly increased and it is extended up to 24 hours. Considering the results from the scratch test (see section "*4.1.3.6. In vitro wound healing*"), this time frame is sufficient to achieve a cell gap closure of approximately 85%. Overall, these results demonstrated that MNPs-based coatings increase the adhesion ability of the membranes over time, probably owing to the presence of reactive chemical functionalities exposed on their surface that enabled the formation of covalent bonds with tissue counterparts (334). Moreover, it is worthwhile to note that in the proposed experimental set-up, the tissue-membrane system is completely immersed in a HBSS solution, thus empathizing the *in vivo* conditions. Therefore, as for the detachment of dopamine-containing membranes, in an *in vivo* model the adhesion properties of the coated membranes would be higher.

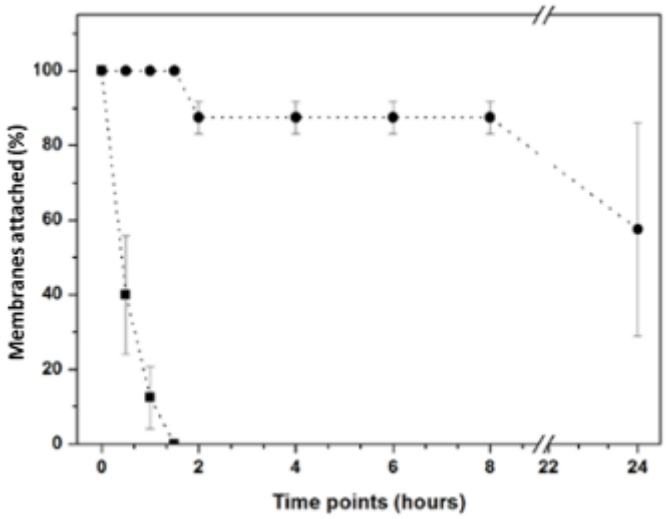

Figure 45. Detachment kinetics of uncoated (squares) and MNPs-coated membranes (rounds).

4.5.3.4. Antimicrobial effect of MNPs

Antimicrobial test were performed on *E. coli* and *S. aureus* strains to evaluate the bactericidal properties of MNPs at different concentrations (figure 46a). The results pointed out that at the highest tested concentrations (200 μg/ml and 50 μg/ml) MNPs display a strong antimicrobial activity on both bacterial strains. The results show that MNPs exert a bactericidal effect in a dose-dependent manner. At the highest tested concentrations (50 μg/ml and 200 μg/ml) the MNPs completely prevent the bacterial growth, whereas at the concentration of 20 μg/ml MNPs had no effect. Thus, MNPs at 50 μg/ml was selected as the lowest concentration of MNPs that effectively kills bacteria. In order to determine whether this effect was related to the MNPs chemical reactivity or to their physical presence causing a mechanical stress on cells, bacteria were treated with latex beads, which do not display any chemical reactivity (figure 46b). Latex beads were added to the bacteria suspension in a number corresponding to the number of MNPs in 50 μg/ml, showing that these nanoparticles do not affect the growth of the treated bacteria, thus proving that the bactericidal mechanism caused by MNPs could be ascribed to their chemical reactivity and not to dimensions.

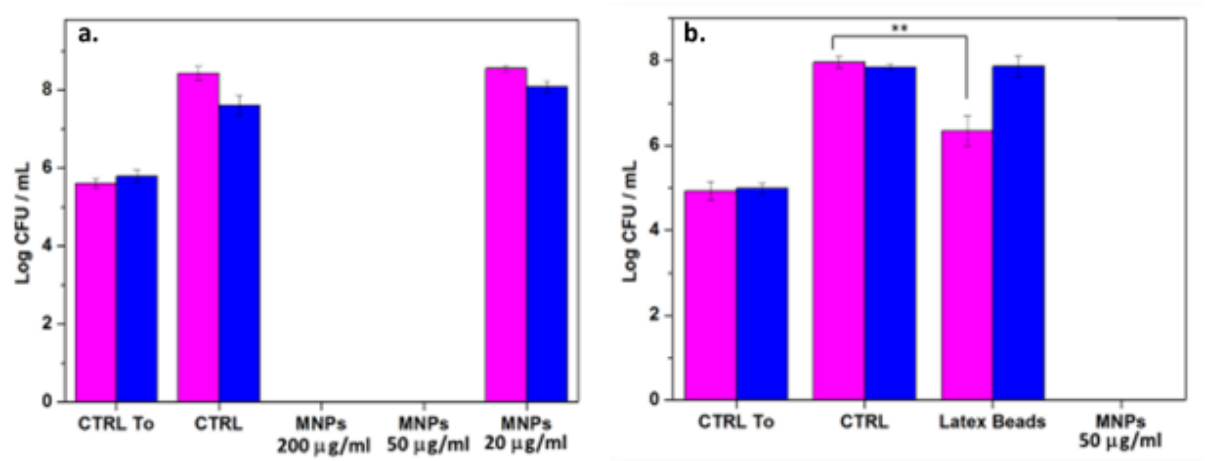

Figure 46. Bacterial growth after 24 hours treatment with MNPs. *E. coli* (pink bars) and *S. aureus* (blue bars) treated with MNPs in suspension at various concentrations (a) and in the presence of latex beads in number corresponding to the number of MNPs in 50 µg/ml (b). (**: p-value < 0.01).

DLS measurement showed that, when resuspended in LB broth, the MNPs tend to aggregate to form micrometric structures (the mean z-average value is 1.595 ± 0.105 µm). Although these aggregates are not able to cross the cell membrane because of their dimension, we hypothesized that after surrounding of bacteria, MNPs can bind to thiol groups of proteins exposed on bacterial membrane through their o-quinone groups. Morphological images of MNPs treated bacteria support this hypothesis showing the interaction of nanoparticles with the cell membrane (figure 47c, 47d, 47e, 47f). These results are consistent with the findings of *Zhao et al* who reported the antibacterial activity of DHI on both gram-positive and gram-negative bacteria: the treatment of bacteria with these compounds leads to the formation of aggregates of bacteria, together with the increased roughness of cell membrane (337). Once the membrane has been damaged, MNPs can cause further damages such as affecting the structure of DNA and of intracellular proteins (338).

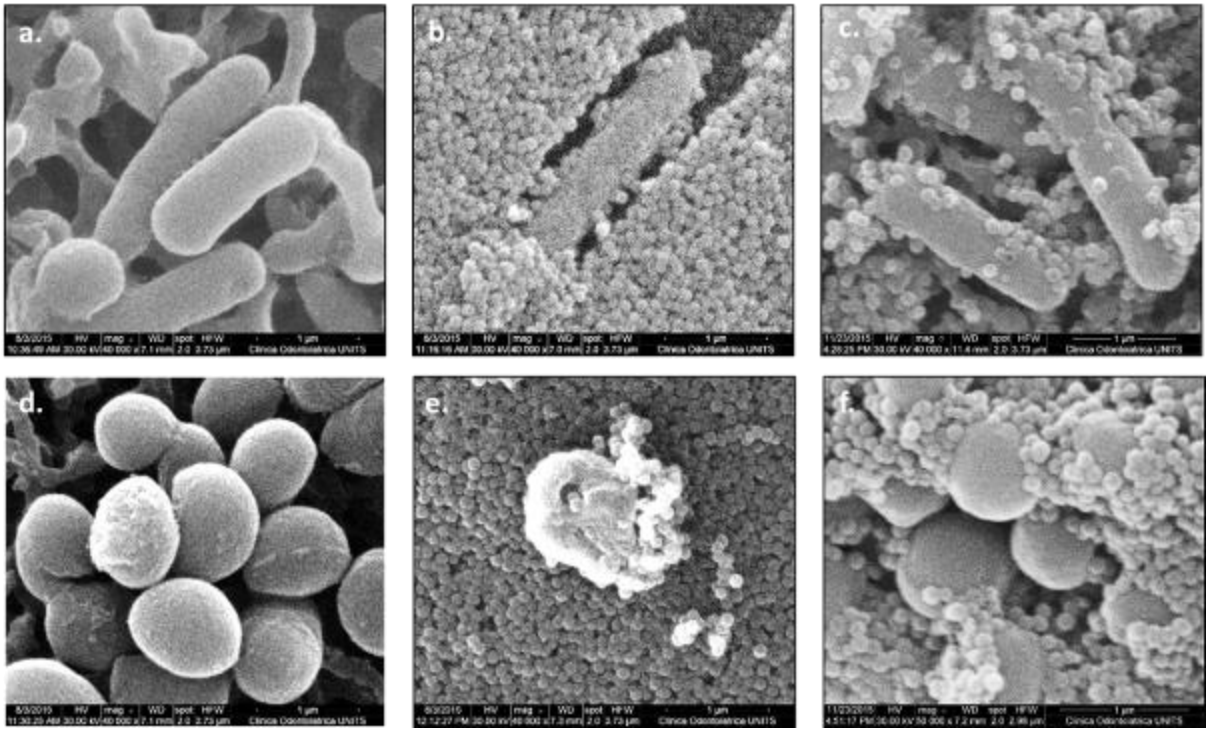

Figure 47. SEM images of untreated *E. coli* (a) and *S. aureus* (d) and *E. coli* treated with MNPs 200 μg/ml (b) or 50 μg/ml (c.) and *S. aureus* treated with MNPs 200 μg/ml (e.) or 50 μg/ml (f.).

Antimicrobial tests were performed on MNPs-coated membranes. The results showed no significant variation in the terms of bacterial growth in the treated samples with respect to the untreated one (data not shown).

We hypothesize that in the case of MNPs-based coatings, the nanoparticles were not able to surround bacterial cells and to cross the membrane, since they were entrapped over the surface of the membrane. In this conformation, the number of reactive species which are effective on bacteria decreases dramatically with respect to the number of reactive groups available on MNPs suspensions. Thus, it is likely that only few bacteria can be recruited by reactive o-quinone of MNPs, resulting in no significant effect on the overall bacterial growth.

4.5.3.5. *In vitro* biocompatibility of MNPs

The LDH assay was performed on fibroblast cells to evaluate the cytotoxic effect of the MNPs suspensions and of MNPs-coated membranes, 24 and 72 hours after treatment (figure 48). The effect of MNPs at the final concentrations of 5 μg/ml and 50 μg/ml was evaluated in terms of LDH release. As a negative control of chemical reactivity induced by nanoparticles, cells treated with latex beads in an equal number as those of MNPs 50 μg/ml were considered.

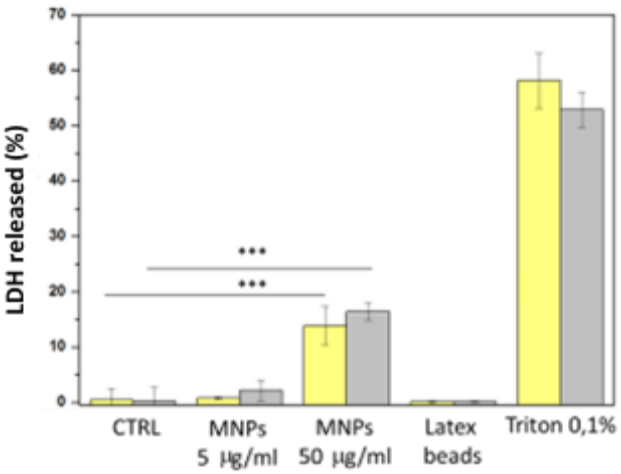

Figure 48. *In vitro* biocompatibility (LDH test) on primary human dermal fibroblasts (HDFa) treated with MNPs 24 hours (yellow bars) and 72 hours (grey bars) after treatment (***: p-value < 0.001).

The results point out that MNPs induce the release of the LDH enzyme in a dose-dependent manner: the higher the concentration of MNPs, the higher the cytotoxic effect on cells. Although at the highest concentration (50 µg/ml) an increased level of cytotoxicity was observed, the cytotoxic response of MNPs-treated cells is far lower than that of the positive control of cell death (Triton X-100) and no enhancement of cell cytotoxicity after 72 hours was observed with respect to 24 hours. It can be hypothesized that, as for the bacterial cells, the cytotoxicity caused by MNPs can be ascribed to their chemical reactivity, since no difference in the terms of LDH release was observed in the presence of latex beads. With respect to the cytotoxic mechanism, it has been reported that catechols can be internalized by cells and undergo redox reactions once inside a biological system. These reactions allow the formation of reactive byproducts that can inactivate enzymes or proteins, trigger the formation of ROS and affect the structure of macromolecules such as DNA (339). All these events can be responsible for the cytotoxic response of cells treated with MNPs. This hypothesis is supported by literature evidences stating that DHI-based compounds display a chemical toxicity to human cells (340-342), although at low concentrations these molecules exert protective effects to retinal cells (340).

4.5.4. CONCLUSIONS

In this study, an adhesive coating based on MNPs was developed to improve the adhesive properties of polysaccharide-based membranes for wound healing applications. These studies

were performed to characterize the features of MNPs and of the MNPs-coated membrane. The test performed pointed out that:

- synthetized MNPs are uniform, well dispersed and round shaped. When resuspended in water, they display a mean diameter of 222.93 ± 12.29 nm, with a polydispersivity index (PdI) of 0.19, indicating the narrow size distribution of the MNPs;
- MNPs are negatively charged particles (ζ-potential is -26.97 ± 1.25 mV);
- MNPs display a good stability in water, although in the presence of NaCl at concentrations higher than that of the biological fluids (*i.e.* 150 mM), aggregation phenomena occur;
- the surface charge of MNPs reaches positive values at acid pH, while negative ones were observed at basic values. At pH 5 the MNPs are unstable, as confirmed by the neutral surface charge and by the formation of larger aggregates;
- MNPs-based coatings confer increased adhesive properties to the membrane in simulated physiological conditions. The adhesion to the intestinal tissue was proved over time and this data can be ascribed to the presence of reactive chemical moieties exposed on the MNPs surface, which enables the formation of covalent bonds with tissue counterparts (proteins);
- MNPs exert an antimicrobial effect on both gram-positive and gram-negative bacteria in a dose dependent manner, through a mechanism that may involve the inactivation of metabolic enzymes and the damage of the cellular structures. No effect in terms of bacterial growth was observed after the treatment with MNPs-coated membranes;
- MNPs induces a low cytotoxic response on cells at high concentrations. The MNPs cytotoxicity can be ascribed to the chemical reactivity of MNPs that can be uptaken by cells, damage the cellular structures and lead to cell death.

5. CONCLUDING REMARKS

Despite the recent efforts in the development of tissue adhesives for biomedical use, novel solutions are required to improve the adhesion ability in the moist environment of the human body. These adhesives can be used as a glue at the biomaterial-tissue interface or embedded within the medical device, thus tailoring the adhesive properties of the system to the final medical application. The present work aimed at the manufacturing of a bioactive, bioadhesive and biodegradable membranes based on polysaccharides, for wound healing applications. Despite a good initial tackiness of the native membrane was proved on *ex vivo* tissue explants, the adhesive properties needed to be implemented in the long term, in order to enable the release of the bioactive component at the wound site. In this regard, the first part of this thesis was focused on the development and characterization of the membranes, while the second part was focused on the adhesion aspects.

In particular, it was demonstrated that:

- polysaccharide-based membranes can be manufactured by freeze-drying alginate-HA hydrogels crosslinked with calcium. The final constructs were proved to be biocompatible and bioactive *in vitro*, thus sustaining and accelerating fibroblasts activity (wound healing);

- the sterilization of the membranes with terminal sterilization techniques (i.e. γ-rays and H_2O_2 gas plasma) affects the properties of the final product. Thus, a sterilization based on $scCO_2$ was successfully employed to limit the impact on the polysaccharide matrix. This method was proved to be the most suitable for the alginate-HA membranes developed in this work;

- the presence of H_2O_2 at the biomaterial-tissue interface enhances the short term adhesiveness of the membrane through a mechanism that mainly involves the structural modification of tissue collagen to adhesive gelatin;

- the implementation of alginate modified at the nanoscale by the grafting of dopamine moieties improved the adhesiveness of the membranes to the intestinal tissue.

Preliminary *in vivo* adhesion test supported the *in vitro* results and indicated the biocompatibility of the dopamine-containing membranes.

- membranes coated with MNPs displayed an enhanced adhesion to tissue explants, providing a powerful tool for the enhancement of the adhesive features of the membranes without modifying the chemical structure of the main components. MNPs were shown to exert a bactericidal effect on both gram-positive and gram-negative bacteria in a dose-dependent fashion, and to induce a low cytotoxic response towards fibroblasts.

6. BIBLIOGRAPHY

(1) World Cancer Research Fund and American Institute for Cancer ResearchFood, Nutrition, Physical Activity, and the Prevention of Cancer: A Global Perspective.Washington, DC: American Institute for Cancer Research. 2007.

(2) Boyle P, Langman JS. ABC of colorectal cancer: Epidemiology. BMJ 2000 Sep 30;321(7264):805-8.

(3) Haggar FA, Boushey RP. Colorectal cancer epidemiology: incidence, mortality, survival, and risk factors. Clin Colon Rectal Surg 2009 Nov;22(4):191-7.

(4) Jemal A, Clegg LX, Ward E, Ries LA, Wu X, Jamison PM, et al. Annual report to the nation on the status of cancer, 1975-2001, with a special feature regarding survival. Cancer 2004 Jul 1;101(1):3-27.

(5) World Health Organization Cancer Incidence in Five Continents. Lyon: The World Health Organization and The International Agency for Research on Cancer. 2002.

(6) Reyes JM, Herretes S, Pirouzmanesh A, Wang DA, Elisseeff JH, Jun A, et al. A modified chondroitin sulfate aldehyde adhesive for sealing corneal incisions. Invest Ophthalmol Vis Sci 2005 Apr;46(4):1247-50.

(7) Fenoglio L, Castagna E, Comino A, Luchino C, Senore C, Migliore E, et al. A shift from distal to proximal neoplasia in the colon: a decade of polyps and CRC in Italy. BMC Gastroenterol 2010;10:139.

(8) Siegel R, DeSantis C, Jemal A. Colorectal cancer statistics, 2014. CA Cancer J Clin 2014 Mar;64(2):104-17.

(9) Janout V, Kollarova H. Epidemiology of colorectal cancer. Biomed Pap Med Fac Univ Palacky Olomouc Czech Repub 2001 Sep;145(1):5-10.

(10) Davies RJ, Miller R, Coleman N. Colorectal cancer screening: prospects for molecular stool analysis. Nat Rev Cancer 2005 Mar;5(3):199-209.

(11) de Jong AE, Morreau H, Nagengast FM, Mathus-Vliegen EM, Kleibeuker JH, Griffioen G, et al. Prevalence of adenomas among young individuals at average risk for colorectal cancer. Am J Gastroenterol 2005 Jan;100(1):139-43.

(12) Grande DA, Pitman MI, Peterson L, Menche D, Klein M. The repair of experimentally produced defects in rabbit articular cartilage by autologous chondrocyte transplantation. J Orthop Res 1989;7:208-18.

(13) Jackson-Thompson J, Ahmed F, German RR, Lai SM, Friedman C. Descriptive epidemiology of colorectal cancer in the United States, 1998-2001. Cancer 2006 Sep 1;107(S5):1103-11.

(14) Wilmink ABM. Overview of the epidemiology of colorectal cancer. Dis Colon Rectum 1997;40(4):483-93.

(15) National Institutes of Health. What you need to know about cancer of the colon and rectum. Bethesda, MD: U.S. Department of Health and Human Services & National Institutes of Health. 2006.

(16) Larsson SC, Wolk A. Meat consumption and risk of colorectal cancer: a meta-analysis of prospective studies. Int J Cancer 2006 Dec 1;119(11):2657-64.

(17) Santarelli RL, Pierre F, orpet DE. Processed meat and colorectal cancer: a review of epidemiologic and experimental evidence. Nutr Cancer 2008;60(2):131-44.

(18) Lee KJ, Inoue M, Otani T, Iwasaki M, Sasazuki S, Tsugane S. Physical activity and risk of colorectal cancer in Japanese men and women: the Japan Public Health Center-based prospective Study. Cancer Causes Control 2007;18(2):199-209.

(19) Tsong WH, Koh WP, Yuan JM, Wang R, Sun CL, Yu MC. Cigarettes and alcohol in relation to colorectal cancer: the Singapore Chinese Health Study. Br J Cancer 2007 Mar 12;96(5):821-7.

(20) Zisman AL, Nickolov A, Brand RE, Gorchow A, Roy HK. Associations between the age at diagnosis and location of colorectal cancer and the use of alcohol and tobacco: implications for screening. Archives of Internal Medicine 2006 Mar 27;166(6):629-34.

(21) Pöschl G, Seitz HK. Alcohol and cancer. Alcohol Alcohol 2004 May;39(3):155-65.

(22) Nelson H, Petrelli N, Carlin A, Couture J, Fleshman J, Guillem J, et al. Guidelines 2000 for Colon and Rectal Cancer Surgery. Journal of the National Cancer Institute 2001 Apr 18;93(8):583-96.

(23) Chang GJ, Rodriguez-Bigas MA, Skibber JM, Moyer VA. Lymph node evaluation and survival after curative resection of colon cancer: systematic review. Journal of the National Cancer Institute 2007 Mar 21;99(6):433-41.

(24) Ho YH, Ashour MA. Techniques for colorectal anastomosis. World J Gastroenterol 2010 Apr 7;16(13):1610-21.

(25) Thornton FJ, Barbul A. Healing in the gastrointestinal tract. Surgical Clinics of North America 1997 Jun 1;77(3):549-73.

(26) Gaertner WB, Hagerman GF, Potter MJ, Karulf RE. Experimental evaluation of a bovine pericardium-derived collagen matrix buttress in ileocolic and colon anastomoses. J Biomed Mater Res B Appl Biomater 2010 Jan;92(1):48-54.

(27) Asteria CR, Gagliardi G, Pucciarelli S, Romano G, Infantino A, La TF, et al. Anastomotic leaks after anterior resection for mid and low rectal cancer: survey of the Italian Society of Colorectal Surgery. Tech Coloproctol 2008 Jun;12(2):103-10.

(28) Alves A, Panis Y, Trancart D, Regimbeau JM, Pocard M, Valleur P. Factors associated with clinically significant anastomotic leakage after large bowel resection: multivariate analysis of 707 patients. World J Surg 2002 Apr;26(4):499-502.

(29) Lindgren R, Hallbook O, Rutegard J, Sjodahl R, Matthiessen P. What is the risk for a permanent stoma after low anterior resection of the rectum for cancer? A six-year follow-up of a multicenter trial. Dis Colon Rectum 2011 Jan;54(1):41-7.

(30) Rullier E, Laurent C, Garrelon JL, Michel P, Saric J, Parneix M. Risk factors for anastomotic leakage after resection of rectal cancer. Br J Surg 1998 Mar 1;85(3):355-8.

(31) den DM, Marijnen CA, Collette L, Putter H, Pahlman L, Folkesson J, et al. Multicentre analysis of oncological and survival outcomes following anastomotic leakage after rectal cancer surgery. Br J Surg 2009 Sep;96(9):1066-75.

(32) Poon RT, Chu KW, Ho JW, Chan CW, Law WL, Wong J. Prospective evaluation of selective defunctioning stoma for low anterior resection with total mesorectal excision. World J Surg 1999 May;23(5):463-7.

(33) Ashwani R, Kelli D.B. Surgical Management of Rectal Cancer. 34 ed. 2007.

(34) Rodriguez-Ramirez SE, Uribe A, Ruiz-Garcia EB, Labastida S, Luna-Perez P. Risk factors for anastomotic leakage after preoperative chemoradiation therapy and low anterior resection with total mesorectal excision for locally advanced rectal cancer. Rev Invest Clin 2006 May;58(3):204-10.

(35) Lipska MA, Bissett IP, Parry BR, Merrie AEH. Anastomotic leakage after lower gastrointestinal anastomosis: men are at a higher risk. ANZ Journal of Surgery 2006 Jul 1;76(7):579-85.

(36) Konishi T, Watanabe T, Kishimoto J, Nagawa H. Risk factors for anastomotic leakage after surgery for colorectal cancer: results of prospective surveillance. Journal of the American College of Surgeons 2006 Mar;202(3):439-44.

(37) Gorissen KJ, Benning D, Berghmans T, Snoeijs MG, Sosef MN, Hulsewe KWE, et al. Risk of anastomotic leakage with non-steroidal anti-inflammatory drugs in colorectal surgery. Br J Surg 2012 May 1;99(5):721-7.

(38) Matthiessen P, Hallbook O, Rutegard J, Simert G, Sjodahl R. Defunctioning stoma reduces symptomatic anastomotic leakage after low anterior resection of the rectum for cancer: a randomized multicenter trial. Ann Surg 2007 Aug;246(2):207-14.

(39) Nesbakken A, Nygaard K, Lunde OC. Outcome and late functional results after anastomotic leakage following mesorectal excision for rectal cancer. Br J Surg 2001 Mar;88(3):400-4.

(40) Koperna T. Cost-effectiveness of defunctioning stomas in low anterior resections for rectal cancer: a call for benchmarking. Arch Surg 2003 Dec;138(12):1334-8.

(41) Rickert A, Willeke F, Kienle P, Post S. Management and outcome of anastomotic leakage after colonic surgery. Colorectal Disease 2010 Oct 1;12(10Online):e216-e223.

(42) Hoeppner J, Wassmuth B, Marjanovic G, Timme S, Hopt UT, Keck T. Anastomotic sealing by extracellular matrices (ECM) improves healing of colonic anastomoses in the critical early phase. J Gastrointest Surg 2010 Jun;14(6):977-86.

(43) de la Fuente SG, Gottfried MR, Lawson DC, Harris MB, Mantyh CR, Pappas TN. Evaluation of porcine-derived small intestine submucosa as a biodegradable graft for gastrointestinal healing. J Gastrointest Surg 2003 Jan;7(1):96-101.

(44) Hoeppner J, Crnogorac V, Marjanovic G, Juttner E, Keck T, Weiser HF, et al. Small intestinal submucosa for reinforcement of colonic anastomosis. Int J Colorectal Dis 2009 May;24(5):543-50.

(45) Ozel SK, Kazez A, Akpolat N. Does a fibrin-collagen patch support early anastomotic healing in the colon? An experimental study. Tech Coloproctol 2006 Oct;10(3):233-6.

(46) Pantelis D, Beissel A, Kahl P, Wehner S, Vilz TO, Kalff JC. The effect of sealing with a fixed combination of collagen matrix-bound coagulation factors on the healing of colonic anastomoses in experimental high-risk mice models. Langenbecks Arch Surg 2010 Nov;395(8):1039-48.

(47) Nordentoft T, Romer J, Sorensen M. Sealing of gastrointestinal anastomoses with a fibrin glue-coated collagen patch: a safety study. J Invest Surg 2007 Nov;20(6):363-9.

(48) Eryilmaz R, Samuk M, Tortum OB, Akcakaya A, Sahin M, Goksel S. The role of dura mater and free peritoneal graft in the reinforcement of colon anastomosis. J Invest Surg 2007 Jan;20(1):15-21.

(49) Thomas P, Massard G, Porte H, Doddoli C, Ducrocq X, Conti M. A new bioabsorbable sleeve for lung staple-line reinforcement (FOREseal): report of a three-center phase II clinical trial. Eur J Cardiothorac Surg 2006 Jun;29(6):880-5.

(50) Maggiori L, Rullier E, Meyer C, Portier G, Faucheron JL, Panis Y. Randomized controlled trial of pelvic calcium alginate following rectal cancer surgery. Br J Surg 2010 Apr;97(4):479-84.

(51) Uzun MA, Koksal N, Ozkan OF, Kayahan M, Gumrukcu G. Salvage repair of anastomotic dehiscence following colon surgery using an expanded polytetrafluoroethylene graft. Tech Coloproctol 2012 Apr;16(2):169-73.

(52) Tang CL, Seow-Choen F, Fook-Chong S, Eu KW. Bioresorbable adhesion barrier facilitates early closure of the defunctioning ileostomy after rectal excision: a prospective, randomized trial. Dis Colon Rectum 2003 Sep;46(9):1200-7.

(53) O'Kane S. Wound remodelling and scarring. J Wound Care 2002 Sep;11(8):296-9.

(54) Velnar T, Bailey T, Smrkolj V. The wound healing process: an overview of the cellular and molecular mechanisms. J Int Med Res 2009 Sep;37(5):1528-42.

(55) Catanzano O, D'Esposito V, Acierno S, Ambrosio MR, De CC, Avagliano C, et al. Alginate-hyaluronan composite hydrogels accelerate wound healing process. Carbohydr Polym 2015 Oct 20;131:407-14.

(56) Choi JH, Jun JH, Kim JH, Sung HJ, Lee JH. Synergistic effect of interleukin-6 and hyaluronic acid on cell migration and ERK activation in human keratinocytes. J Korean Med Sci 2014 Nov;29 Suppl 3:S210-S216.

(57) Doillon CJ, Silver FH. Collagen-based wound dressing: effects of hyaluronic acid and firponectin on wound healing. Biomaterials 1986 Jan;7(1):3-8.

(58) Gomes JA, Amankwah R, Powell-Richards A, Dua HS. Sodium hyaluronate (hyaluronic acid) promotes migration of human corneal epithelial cells in vitro. Br J Ophthalmol 2004 Jun;88(6):821-5.

(59) Inoue M, Katakami C. The effect of hyaluronic acid on corneal epithelial cell proliferation. Invest Ophthalmol Vis Sci 1993 Jun;34(7):2313-5.

(60) Markovsky E, Baabur-Cohen H, Eldar-Boock A, Omer L, Tiram G, Ferber S, et al. Administration, distribution, metabolism and elimination of polymer therapeutics. J Control Release 2012 Jul 20;161(2):446-60.

(61) Balakrishnan B, Mohanty M, Umashankar PR, Jayakrishnan A. Evaluation of an in situ forming hydrogel wound dressing based on oxidized alginate and gelatin. Biomaterials 2005 Nov;26(32):6335-42.

(62) Moseley R, Waddington RJ, Embery G. Hyaluronan and its potential role in periodontal healing. Dent Update 2002 Apr;29(3):144-8.

(63) Renier D, Bellato P, Bellini D, Pavesio A, Pressato D, Borrione A. Pharmacokinetic behaviour of ACP gel, an autocrosslinked hyaluronan derivative, after intraperitoneal administration. Biomaterials 2005 Sep;26(26):5368-74.

(64) Boateng JS, Matthews KH, Stevens HNE, Eccleston GM. Wound healing dressings and drug delivery systems: a review. J Pharm Sci 2008 Aug 1;97(8):2892-923.

(65) Jayakumar R, Prabaharan M, Sudheesh Kumar PT, Nair SV, Tamura H. Biomaterials based on chitin and chitosan in wound dressing applications. Biotechnology Advances 2011 May;29(3):322-37.

(66) Powers JG, Morton LM, Phillips TJ. Dressings for chronic wounds. Dermatol Ther 2013 May 1;26(3):197-206.

(67) Cotrim H, Pereira G. Impact of colorectal cancer on patient and family: implications for care. Eur J Oncol Nurs 2008 Jul;12(3):217-26.

(68) Cakmak A, Aylaz G, Kuzu MA. Permanent stoma not only affects patients' quality of life but also that of their spouses. World J Surg 2010 Dec;34(12):2872-6.

(69) Jung SH, Yu CS, Choi PW, Kim DD, Park IJ, Kim HC, et al. Risk factors and oncologic impact of anastomotic leakage after rectal cancer surgery. Dis Colon Rectum 2008 Jun;51(6):902-8.

(70) Frye J, Bokey EL, Chapuis PH, Sinclair G, Dent OF. Anastomotic leakage after resection of colorectal cancer generates prodigious use of hospital resources. Colorectal Dis 2009 Nov;11(9):917-20.

(71) Baldwin AD, Kiick KL. Polysaccharide-modified synthetic polymeric biomaterials. Biopolymers 2010;94(1):128-40.

(72) Rinaudo M. Main properties and current applications of some polysaccharides as biomaterials. Polym Int 2008 Mar 1;57(3):397-430.

(73) Rinaudo M, Auzely R, Mazeau K. Polysaccharides and carbohydrate polymers, in *Encyclopedia of Polymer Science and Technology*. New York: 2004.

(74) Rinaudo M. Polysaccharides, in *Kirk-Othmer Encyclopedia of Chemical Technology*. 5 ed. 2006.

(75) Rinaudo M. Non-covalent interactions in polysaccharide systems. Macromol Biosci 2006 Aug 7;6(8):590-610.

(76) Spagnoli C, Korniakov A, Ulman A, Balazs EA, Lyubchenko YL, Cowman MK. Hyaluronan conformations on surfaces: effect of surface charge and hydrophobicity. Carbohydr Res 2005 Apr 11;340(5):929-41.

(77) Müller U. In vitro biocompatibility testing of biomaterials and medical devices. Med Device Technol 2008 Mar;19(2):30, 32-0, 34.

(78) Ríhová B. Biocompatibility of biomaterials: hemocompatibility, immunocompatiblity and biocompatibility of solid polymeric materials and soluble targetable polymeric carriers. Advanced Drug Delivery Reviews 1996 Sep 16;21(2):157-76.

(79) Bakoš D, Soldána M, Hernández-Fuentes I. Hydroxyapatite-collagen-hyaluronic acid composite. Biomaterials 1999 Jan;20(2):191-5.

(80) Krause A, Kirschning A, Drager G. Bioorthogonal metal-free click-ligation of cRGD-pentapeptide to alginate. Org Biomol Chem 2012 Aug 7;10(29):5547-53.

(81) Wang L, Khor E, Wee A, Lim LY. Chitosan-alginate PEC membrane as a wound dressing: assessment of incisional wound healing. J Biomed Mater Res 2002 Jan 1;63(5):610-8.

(82) Cheragwandi A, Nieuwenhuis DH, Gagner M, Consten EC. An update of available innovative staple line reinforcement materials in colorectal surgery. Surg Technol Int 2008;17:131-7.

(83) Frenkel JS. The role of hyaluronan in wound healing. Int Wound J 2014 Apr;11(2):159-63.

(84) King SR, Hickerson WL, Proctor KG. Beneficial actions of exogenous hyaluronic acid on wound healing. Surgery 1991 Jan;109(1):76-84.

(85) Lim SH, Hudson SM. Synthesis and antimicrobial activity of a water-soluble chitosan derivative with a fiber-reactive group. Carbohydrate Research 2004 Jan 22;339(2):313-9.

(86) Zheng LY, Zhu JF. Study on antimicrobial activity of chitosan with different molecular weights. Carbohydrate Polymers 2003 Dec 1;54(4):527-30.

(87) Sacco P, Travan A, Borgogna M, Paoletti S, Marsich E. Silver-containing antimicrobial membrane based on chitosan-TPP hydrogel for the treatment of wounds. J Mater Sci Mater Med 2015 Mar;26(3):128.

(88) Yang HS, Shin J, Bhang SH, Shin JY, Park J, Im GI, et al. Enhanced skin wound healing by a sustained release of growth factors contained in platelet-rich plasma. Exp Mol Med 2011 Nov 30;43:622-9.

(89) Scognamiglio F, Travan A, Rustighi I, Tarchi P, Palmisano S, Marsich E, et al. Adhesive and sealant interfaces for general surgery applications. Journal of Biomedical Materials Research Part B: Applied Biomaterials 2015 Apr 1;n/a.

(90) Dornish M, Rauh F. Alginate. In: Guelche S.A., Hollinger O., editors. An introduction to biomaterials. Taylor & Francis; 2006. p. 261-72.

(91) Haug A, Larsen Br, Smidsrød O. Uronic acid sequence in alginate from different sources. Carbohydrate Research 1974;32(2):217-25.

(92) Gorin PAJ, Spencer JFT. Exocellular alginic acid from Azotobacter vinelandii. Can J Chem 1966 May 1;44(9):993-8.

(93) Govan JR, Fyfe JA, Jarman TR. Isolation of alginate-producing mutants of Pseudomonas fluorescens, Pseudomonas putida and Pseudomonas mendocina. J Gen Microbiol 1981 Jul;125(1):217-20.

(94) Smidsrød O, Haug A. Dependence upon the gel-sol state of the ion-exchange properties of alginates. Acta Chem Scand 1972;26(5):2063-74.

(95) Smidsrød O. Molecular basis for some physical properties of alginates in the gel state. Faraday Discuss Chem Soc 1974;57(0):263-74.

(96) Braccini I, Grasso RP, Pérez S. Conformational and configurational features of acidic polysaccharides and their interactions with calcium ions: a molecular modeling investigation. Carbohydrate Research 1999 Apr 30;317(1-4):119-30.

(97) Braccini I, Pérez S. Molecular basis of Ca^{2+}-induced gelation in alginates and pectins: the egg-box model revisited. Biomacromolecules 2001 Dec 1;2(4):1089-96.

(98) Smidsrød O, Glover RM, Whittington SG. The relative extension of alginates having different chemical composition. Carbohydrate Research 1973;27(1):107-18.

(99) Martinsen A, Skjåk-Bræk G, Smidsrød O, Zanetti F, Paoletti S. Comparison of different methods for determination of molecular weight and molecular weight distribution of alginates. Carbohydrate Polymers 1991;15(2):171-93.

(100) Kohn R, Larsen B. Preparation of water-soluble polyuronic acids and their calcium salts, and the determination of calcium ion activity in relation to the degree of polymerization. Acta Chem Scand 1972;26(6):2455-68.

(101) Grant GT, Morris ER, Rees DA, Smith PJC, Thom D. Biological interactions between polysaccharides and divalent cations: the egg-box model. FEBS Letters 1973;32(1):195-8.

(102) Donati I, Synnøve H, Mørch Yrr A., Borgogna M, Dentini M, Skjåk-Bræk G. New hypothesis on the role of alternating sequences in calcium alginate gels. Biomacromolecules 2005 Mar 1;6(2):1031-40.

(103) Smidsrød O, Haug A. Properties of poly(1,4-hexuronates) in the gel state. II. Comparison of gels of different chemical composition. Acta Chemica Scandinavica 1972;26:79-88.

(104) Draget K, Østgaard K, Smidsrød O. Alginate-based solid media for plant tissue culture. Appl Microbiol Biotechnol 1989;31(1):79-83.

(105) Grasdalen H, Larsen B, Smidsrød O. ^{13}C-n.m.r. studies of monomeric composition and sequence in alginate. Carbohydrate Research 1981 Mar 2;89(2):179-91.

(106) Esser E, Tessmar JKV. Preparation of well-defined calcium cross-linked alginate films for the prevention of surgical adhesions. Journal of Biomedical Materials Research Part B: Applied Biomaterials 2013 Jul 1;101B(5):826-39.

(107) Rosellini E, Cristallini C, Barbani N, Vozzi G, Giusti P. Preparation and characterization of alginate/gelatin blend films for cardiac tissue engineering. Journal of Biomedical Materials Research Part A 2009 Nov 1;91A(2):447-53.

(108) Cuadros TR, Skurtys O, Aguilera JM. Mechanical properties of calcium alginate fibers produced with a microfluidic device. Carbohydrate Polymers 2012 Aug 1;89(4):1198-206.

(109) Kang E, Choi YY, Chae SK, Moon JH, Chang JY, Lee SH. Microfluidic spinning of flat alginate fibers with grooves for cell-aligning scaffolds. Adv Mater 2012 Aug 16;24(31):4271-7.

(110) Turco G, Donati I, Grassi M, Marchioli G, Lapasin R, Paoletti S. Mechanical spectroscopy and relaxometry on alginate hydrogels: a comparative analysis for structural characterization and network mesh size determination. Biomacromolecules 2011 Apr 11;12(4):1272-82.

(111) Andersen T, Markussen C, Dornish M, Heier-Baardson H, Melvik JE, Alsberg E, et al. In situ gelation for cell immobilization and culture in alginate foam scaffolds. Tissue Eng Part A 2014 Feb 1;20(3-4):600-10.

(112) Andersen T, Melvik JE, Gåserød O, Alsberg E, Christensen BrE. Ionically gelled alginate foams: physical properties controlled by type, amount and source of gelling ions. Carbohydrate Polymers 2014 Jan 2;99:249-56.

(113) Blair SD, Jarvis P, Salmon M, McCollum C. Clinical trial of calcium alginate haemostatic swabs. Br J Surg 1990 May 1;77(5):568-70.

(114) Sayag J, Meaume S, Bohbot S. Healing properties of calcium alginate dressings. J Wound Care 1996 Sep;5(8):357-62.

(115) Wang N, Adams G, Buttery L, Falcone FH, Stolnik S. Alginate encapsulation technology supports embryonic stem cells differentiation into insulin-producing cells. Journal of Biotechnology 2009 Dec;144(4):304-12.

(116) Hooper SJ, Percival SL, Hill KE, Thomas DW, Hayes AJ, Williams DW. The visualisation and speed of kill of wound isolates on a silver alginate dressing. International Wound Journal 2012 Dec 1;9(6):633-42.

(117) Li X, Chen S, Zhang B, Li M, Diao K, Zhang Z, et al. In situ injectable nano-composite hydrogel composed of curcumin, N,O-carboxymethyl chitosan and oxidized alginate for wound healing application. International Journal of Pharmaceutics 2012 Nov 1;437(1-2):110-9.

(118) Meyer K, Palmer JW. The polysaccharide of the vitreous humor. Journal of Biological Chemistry 1934 Dec 1;107(3):629-34.

(119) Milas M, Rinaudo M. Characterization and properties of hyaluronic acid (hyaluronan). 2 ed. New York: Dekker; 2005.

(120) Necas J, Bartosikova L, Brauner P, Kolar J. Hyaluronic acid (hyaluronan): a review. 2008.

(121) Dechert TA, Ducale AE, Ward SI, Yager DR. Hyaluronan in human acute and chronic dermal wounds. Wound Repair Regen 2006 May;14(3):252-8.

(122) Sato E, Ando T, Ichikawa J, Okita G, Sato N, Wako M, et al. High molecular weight hyaluronic acid increases the differentiation potential of the murine chondrocytic ATDC5 cell line. J Orthop Res 2014 Dec 1;32(12):1619-27.

(123) Seidlits SK, Khaing ZZ, Petersen RR, Nickels JD, Vanscoy JE, Shear JB, et al. The effects of hyaluronic acid hydrogels with tunable mechanical properties on neural progenitor cell differentiation. Biomaterials 2010 May;31(14):3930-40.

(124) Gerecht S, Burdick JA, Ferreira LS, Townsend SA, Langer R, Vunjak-Novakovic G. Hyaluronic acid hydrogel for controlled self-renewal and differentiation of human embryonic stem cells. Proc Natl Acad Sci U S A 2007 Jul 3;104(27):11298-303.

(125) Pardue EL, Ibrahim S, Ramamurthi A. Role of hyaluronan in angiogenesis and its utility to angiogenic tissue engineering. Organogenesis 2008 Oct;4(4):203-14.

(126) Park D, Kim Y, Kim H, Kim K, Lee YS, Choe J, et al. Hyaluronic acid promotes angiogenesis by inducing RHAMM-TGFβ receptor interaction via CD44-PKCδ. Mol Cells 2012 Jun;33(6):563-74.

(127) Jiang D, Liang J, Noble PW. Hyaluronan as an immune regulator in human diseases. Physiol Rev 2011 Jan;91(1):221-64.

(128) Shirali AC, Goldstein DR. Activation of the innate immune system by the endogenous ligand hyaluronan. Curr Opin Organ Transplant 2008 Feb;13(1):20-5.

(129) Arrich J, Piribauer F, Mad P, Schmid D, Klaushofer K, Mullner M. Intra-articular hyaluronic acid for the treatment of osteoarthritis of the knee: systematic review and meta-analysis. CMAJ 2005 Apr 12;172(8):1039-43.

(130) Lo GH, LaValley M, McAlindon T, Felson DT. Intra-articular hyaluronic acid in treatment of knee osteoarthritis: A meta-analysis. JAMA 2003 Dec 17;290(23):3115-21.

(131) Strauss EJ, Hart JA, Miller MD, Altman RD, Rosen JE. Hyaluronic acid viscosupplementation and osteoarthritis: current uses and future directions. The American Journal of Sports Medicine 2009 Aug 1;37(8):1636-44.

(132) Grigolo B, De FL, Roseti L, Cattini L, Facchini A. Down regulation of degenerative cartilage molecules in chondrocytes grown on a hyaluronan-based scaffold. Biomaterials 2005 Oct;26(28):5668-76.

(133) Lisignoli G, Cristino S, Piacentini A, Toneguzzi S, Grassi F, Cavallo C, et al. Cellular and molecular events during chondrogenesis of human mesenchymal stromal cells grown in a three-dimensional hyaluronan based scaffold. Biomaterials 2005 Oct;26(28):5677-86.

(134) Pianigiani E, Andreassi A, Taddeucci P, Alessandrini C, Fimiani M, Andreassi L. A new model for studying differentiation and growth of epidermal cultures on hyaluronan-based carrier. Biomaterials 1999 Sep;20(18):1689-94.

(135) Solchaga LA, Dennis JE, Goldberg VM, Caplan AI. Hyaluronic acid-based polymers as cell carriers for tissue-engineered repair of bone and cartilage. J Orthop Res 1999 Mar 1;17(2):205-13.

(136) Turner NJ, Kielty CM, Walker MG, Canfield AE. A novel hyaluronan-based biomaterial (Hyaff-11) as a scaffold for endothelial cells in tissue engineered vascular grafts. Biomaterials 2004 Dec;25(28):5955-64.

(137) Nyman E, Huss F, Nyman T, Junker J, Kratz G. Hyaluronic acid, an important factor in the wound healing properties of amniotic fluid: in vitro studies of re-epithelialisation in human skin wounds. J Plast Surg Hand Surg 2013 Apr;47(2):89-92.

(138) Olczyk P, Komosinska-Vassev K, Winsz-Szczotka K, Kuznik-Trocha K, Olczyk K. Hyaluronan: structure, metabolism, functions, and role in wound healing. Postepy Hig Med Dosw (Online) 2008;62:651-9.

(139) Donati I, Feresini M, Travan A, Marsich E, Lapasin R, Paoletti S. Polysaccharide-based polyanion-polycation-polyanion ternary systems. A preliminary analysis of interpolyelectrolyte interactions in dilute solutions. Biomacromolecules 2011 Nov 14;12(11):4044-56.

(140) Geremia I, Borgogna M, Travan A, Marsich E, Paoletti S, Donati I. Determination of the composition for binary mixtures of polyanions: the case of mixed solutions of alginate and hyaluronan. Biomacromolecules 2014 Mar 10;15(3):1069-73.

(141) Oerther S, Le GH, Payan E, Lapicque F, Presle N, Hubert P, et al. Hyaluronate-alginate gel as a novel biomaterial: mechanical properties and formation mechanism. Biotechnol Bioeng 1999 Apr 20;63(2):206-15.

(142) Oerther S, Payan E, Lapicque F, Presle N, Hubert P, Muller S, et al. Hyaluronate-alginate combination for the preparation of new biomaterials: investigation of the behaviour in aqueous solutions. Biochim Biophys Acta 1999 Jan 4;1426(1):185-94.

(143) Dausse Y, Grossin L, Miralles G, Pelletier S, Mainard D, Hubert P, et al. Cartilage repair using new polysaccharidic biomaterials: macroscopic, histological and biochemical approaches in a rat model of cartilage defect. Osteoarthritis Cartilage 2003 Jan;11(1):16-28.

(144) Gerard C, Catuogno C, Amargier-Huin C, Grossin L, Hubert P, Gillet P, et al. The effect of alginate, hyaluronate and hyaluronate derivatives biomaterials on synthesis of non-articular chondrocyte extracellular matrix. J Mater Sci Mater Med 2005 Jun;16(6):541-51.

(145) Aulin C, Bergman K, Jensen-Waern M, Hedenqvist P, Hilborn J, Engstrand T. In situ cross-linkable hyaluronan hydrogel enhances chondrogenesis. J Tissue Eng Regen Med 2011 Aug;5(8):e188-e196.

(146) Chung J, Song M, Ha CW, Kim JA, Lee CH, Park YB. Comparison of articular cartilage repair with different hydrogel-human umbilical cord blood-derived mesenchymal stem cell composites in a rat model. Stem Cell Research & Therapy 2014;5(2):39.

(147) Neuman MG, Nanau RM, Oruna-Sanchez L, Coto G. Hyaluronic acid and wound healing. J Pharm Pharm Sci 2015;18(1):53-60.

(148) Foster LC, Arkonac BM, Sibinga NES, Shi C, Perrella MA, Haber E. Regulation of CD44 gene expression by the proinflammatory cytokine interleukin1â in vascular smooth muscle cells. Journal of Biological Chemistry 1998 Aug 7;273(32):20341-6.

(149) Puré E, Cuff CA. A crucial role for CD44 in inflammation. Trends in Molecular Medicine 2001 May 1;7(5):213-21.

(150) Toole BP. Hyaluronan in morphogenesis. Journal of Internal Medicine 1997 Jul 1;242(1):35-40.

(151) Acharya PS, Majumdar S, Jacob M, Hayden J, Mrass P, Weninger W, et al. Fibroblast migration is mediated by CD44-dependent TGFβ activation. J Cell Sci 2008 May 1;121(Pt 9):1393-402.

(152) Choi YS, Lee SB, Hong SR, Lee YM, Song KW, Park MH. Studies on gelatin-based sponges. Part III: a comparative study of cross-linked gelatin/alginate, gelatin/hyaluronate and chitosan/hyaluronate sponges and their application as a wound dressing in full-thickness skin defect of rat. J Mater Sci Mater Med 2001 Jan;12(1):67-73.

(153) Yamane S, Iwasaki N, Majima T, Funakoshi T, Masuko T, Harada K, et al. Feasibility of chitosan-based hyaluronic acid hybrid biomaterial for a novel scaffold in cartilage tissue engineering. Biomaterials 2005 Feb;26(6):611-9.

(154) Matsumoto Y, Arai K, Momose H, Kuroyanagi Y. Development of a wound dressing composed of a hyaluronic acid sponge containing arginine. J Biomater Sci Polym Ed 2009;20(7-8):993-1004.

(155) Woodworth BA, Chandra RK, Hoy MJ, Lee FS, Schlosser RJ, Gillespie MB. Randomized controlled trial of hyaluronic acid/carboxymethylcellulose dressing after endoscopic sinus surgery. ORL J Otorhinolaryngol Relat Spec 2010;72(2):101-5.

(156) Ahmed M, Punshon G, Darbyshire A, Seifalian AM. Effects of sterilization treatments on bulk and surface properties of nanocomposite biomaterials. J Biomed Mater Res B Appl Biomater 2013 Oct 11;101(7):1182-90.

(157) Delgado LM, Pandit A, Zeugolis DI. Influence of sterilisation methods on collagen-based devices stability and properties. Expert Review of Medical Devices 2014 Mar 21;11(3):305-14.

(158) Lambert BJ, Mendelson TA, Craven MD. Radiation and ethylene oxide terminal sterilization experiences with drug eluting stent products. AAPS PharmSciTech 2011 Dec 2;12(4):1116-26.

(159) Phillip E, Murthy NS, Bolikal D, Narayanan P, Kohn J, Lavelle L, et al. Ethylene oxide's role as a reactive agent during sterilization: Effects of polymer composition and device architecture. Journal of Biomedical Materials Research Part B: Applied Biomaterials 2013 May 1;101B(4):532-40.

(160) Karajanagi SS, Yoganathan R, Mammucari R, Park H, Cox J, Zeitels SM, et al. Application of a dense gas technique for sterilizing soft biomaterials. Biotechnol Bioeng 2011 Jul 1;108(7):1716-25.

(161) Marreco PR, Moreira PcdL, Genari SC, Moraes AM. Effects of different sterilization methods on the morphology, mechanical properties, and cytotoxicity of chitosan membranes used as wound dressings. Journal of Biomedical Materials Research Part B: Applied Biomaterials 2004 Nov 15;71B(2):268-77.

(162) Mendes GCC, Brandão T, Silva CLM. Ethylene oxide sterilization of medical devices: A review. American Journal of Infection Control 2007 Nov;35(9):574-81.

(163) Murray KA, Kennedy JE, McEvoy B, Vrain O, Ryan D, Cowman R, et al. Effects of gamma ray and electron beam irradiation on the mechanical, thermal, structural and physicochemical properties of poly (ether-block-amide) thermoplastic elastomers. Journal of the Mechanical Behavior of Biomedical Materials 2013 Jan;17:252-68.

(164) Kanjickal D, Lopina S, Evancho-Chapman MM, Schmidt S, Donovan D. Effects of sterilization on poly(ethylene glycol) hydrogels. Journal of Biomedical Materials Research Part A 2008 Dec 1;87A(3):608-17.

(165) Donati I, Benincasa M, Foulc MP, Turco G, Toppazzini M, Solinas D, et al. Terminal sterilization of BisGMA-TEGDMA thermoset materials and their bioactive surfaces by supercritical CO_2. Biomacromolecules 2012 Apr 9;13(4):1152-60.

(166) Herdegen V, Felix A, Haseneder R, Repke JU, Leppchen-Fröhlich K, ade I, et al. Sterilization of medical products from collagen by means of supercritical CO_2. Chem Eng Technol 2014 Nov 1;37(11):1891-5.

(167) Pasquali I, Bettini R. Are pharmaceutics really going supercritical? Int J Pharm 2008 Dec 8;364(2):176-87.

(168) Spilimbergo S, Dehghani F, Bertucco A, Foster NR. Inactivation of bacteria and spores by pulse electric field and high pressure CO_2 at low temperature. Biotechnol Bioeng 2003 Apr 5;82(1):118-25.

(169) Hemmer JD, Drews MJ, LaBerge M, Matthews MA. Sterilization of bacterial spores by using supercritical carbon dioxide and hydrogen peroxide. Journal of Biomedical Materials Research Part B: Applied Biomaterials 2007 Feb 1;80B(2):511-8.

(170) Zhang J, Burrows S, Gleason C, Matthews MA, Drews MJ, LaBerge M, et al. Sterilizing Bacillus pumilus spores using supercritical carbon dioxide. Journal of Microbiological Methods 2006 Sep;66(3):479-85.

(171) Bernhardt A, Wehrl M, Paul B, Hochmuth T, Schumacher M, Schütz K, et al. Improved sterilization of sensitive biomaterials with supercritical carbon dioxide at low temperature. PLoS One 2015 Jun 12;10(6):e0129205.

(172) Perrut M. Sterilization and virus inactivation by supercritical fluids (a review). The Journal of Supercritical Fluids 2012 Jun;66:359-71.

(173) Russell N, Rives A, Bertollo N, Pelletier MH, Walsh WR. The effect of sterilization on the dynamic mechanical properties of paired rabbit cortical bone. Journal of Biomechanics 2013 Jun 21;46(10):1670-5.

(174) White A, Burns D, Christensen TW. Effective terminal sterilization using supercritical carbon dioxide. Journal of Biotechnology 2006 Jun 10;123(4):504-15.

(175) Zhang J, Davis TA, Matthews MA, Drews MJ, LaBerge M, An YH. Sterilization using high-pressure carbon dioxide. The Journal of Supercritical Fluids 2006 Oct;38(3):354-72.

(176) Qiu QQ, Leamy P, Brittingham J, Pomerleau J, Kabaria N, Connor J. Inactivation of bacterial spores and viruses in biological material using supercritical carbon dioxide with sterilant. Journal of Biomedical Materials Research Part B: Applied Biomaterials 2009 Nov 1;91B(2):572-8.

(177) Shieh E, Paszczynski A, Wai CM, Lang Q, Crawford RL. Sterilization of Bacillus pumilus spores using supercritical fluid carbon dioxide containing various modifier solutions. Journal of Microbiological Methods 2009 Mar;76(3):247-52.

(178) Zhang J, Dalal N, Matthews MA, Waller LN, Saunders C, Fox KF, et al. Supercritical carbon dioxide and hydrogen peroxide cause mild changes in spore structures associated with high killing rate. Journal of Microbiological Methods 2007 Sep 14;70(3):442-51.

(179) Li X, Xu A, Xie H, Yu W, Xie W, Ma X. Preparation of low molecular weight alginate by hydrogen peroxide depolymerization for tissue engineering. Carbohydrate Polymers 2010 Feb 11;79(3):660-4.

(180) Piraino F, Selimovic S. A current view of functional biomaterials for wound care, molecular and cellular therapies. Biomed Res Int 2015;2015:403801.

(181) Bischoff M, Kinzl L, Schmelz A. The complicated wound. Unfallchirurg 1999 Oct;102(10):797-804.

(182) Komarcevic A. The modern approach to wound treatment. Med Pregl 2000 Jul;53(7-8):363-8.

(183) Robson MC, Steed DL, Franz MG. Wound healing: biologic features and approaches to maximize healing trajectories. Curr Probl Surg 2001 Feb;38(2):72-140.

(184) Lazarus GS, Cooper DM, Knighton DR. Definitions and guidelines for assessment of wounds and evaluation of healing. Archives of Dermatology 1994 Apr 1;130(4):489-93.

(185) Szycher M, Lee SJ. Modern wound dressings: a systematic approach to wound healing. J Biomater Appl 1992 Oct;7(2):142-213.

(186) Degreef HJ. How to heal a wound fast. Dermatol Clin 1998 Apr;16(2):365-75.

(187) Jespersen J. Pathophysiology and clinical aspects of fibrinolysis and inhibition of coagulation. Experimental and clinical studies with special reference to women on oral contraceptives and selected groups of thrombosis prone patients. Dan Med Bull 1988 Feb;35(1):1-33.

(188) Pool JG. Normal hemostatic mechanisms: a review. Am J Med Technol 1977 Aug;43(8):776-80.

(189) Koch AE, Polverini PJ, Kunkel SL, Harlow LA, DiPietro LA, Elner VM, et al. Interleukin-8 as a macrophage-derived mediator of angiogenesis. Science 1992 Dec 11;258(5089):1798-801.

(190) Greaves NS, Ashcroft KJ, Baguneid M, Bayat A. Current understanding of molecular and cellular mechanisms in fibroplasia and angiogenesis during acute wound healing. Journal of Dermatological Science 2013 Dec;72(3):206-17.

(191) Ramasastry SS. Acute Wounds. Clinics in Plastic Surgery 2005 Apr;32(2):195-208.

(192) Witte MB, Barbul A. General principles of wound healing. Surgical Clinics of North America 1997 Jun 1;77(3):509-28.

(193) Chen WYJ, Abatangelo GIOV. Functions of hyaluronan in wound repair. Wound Repair and Regeneration 1999 Mar 1;7(2):79-89.

(194) Baum CL, Arpey CJ. Normal cutaneous wound healing: clinical correlation with cellular and molecular events. Dermatol Surg 2005 Jun;31(6):674-86.

(195) Clark RA. Regulation of fibroplasia in cutaneous wound repair. Am J Med Sci 1993 Jul;306(1):42-8.

(196) Greenhalgh DG. The role of apoptosis in wound healing. Int J Biochem Cell Biol 1998 Sep;30(9):1019-30.

(197) Sieggreen MY. Healing of physical wounds. Nurs Clin North Am 1987 Jun;22(2):439-47.

(198) Falanga V. Wound healing and chronic wounds. J Cutan Med Surg 1998 Dec;3 Suppl 1:S1-S5.

(199) Hart J. Inflammation. 2: Its role in the healing of chronic wounds. J Wound Care 2002 Jul;11(7):245-9.

(200) van der Vijver R, van Laarhoven C, de Man B, Lomme R, Hendriks T. The effect of fibrin glue on the early healing phase of intestinal anastomoses in the rat. Int J Colorectal Dis 2012;27(8):1101-7.

(201) Thompson SK, Chang EY, Jobe BA. Clinical review: healing in gastrointestinal anastomoses, Part I. Microsurgery 2006 Jan 1;26(3):131-6.

(202) Bosmans J, Jongen A, Bouvy N, Derikx J. Colorectal anastomotic healing: why the biological processes that lead to anastomotic leakage should be revealed prior to conducting intervention studies. BMC Gastroenterology 2015.

(203) Munireddy S, Kavalukas SL, Barbul A. Intra-abdominal healing: gastrointestinal tract and adhesions. Surgical Clinics of North America 2010 Dec;90(6):1227-36.

(204) Daams F, Monkhorst K, van den Broek J, Slieker JC, Jeekel J, Lange JF. Local ischaemia does not influence anastomotic healing: an experimental study. Eur Surg Res 2013;50(1):24-31.

(205) Braund R, Hook SM, Greenhill N, Medlicott NJ. Distribution of fibroblast growth factor-2 (FGF-2) within model excisional wounds following topical application. J Pharm Pharmacol 2009 Feb;61(2):193-200.

(206) Chen JD, Lapiere JC, Sauder DN, Peavey C, Woodley DT. Interleukin-1α stimulates keratinocyte migration through an epidermal growth factor/transforming growth factor-α-independent pathway. J Invest Dermatol 1995 May;104(5):729-33.

(207) Stynes G, Kiroff GK, Morrison WAJ, Kirkland MA. Tissue compatibility of biomaterials: benefits and problems of skin biointegration. ANZ Journal of Surgery 2008 Aug 1;78(8):654-9.

(208) Williams DF. There is no such thing as a biocompatible material. Biomaterials 2014 Dec;35(38):10009-14.

(209) Qiu Y, Park K. Environment-sensitive hydrogels for drug delivery. Advanced Drug Delivery Reviews 2001 Dec 31;53(3):321-39.

(210) Tokarev I, Minko S. Stimuli-responsive porous hydrogels at interfaces for molecular filtration, separation, controlled release, and gating in capsules and membranes. Adv Mater 2010 Aug 17;22(31):3446-62.

(211) Zhu J. Bioactive modification of poly(ethylene glycol) hydrogels for tissue engineering. Biomaterials 2010 Jun;31(17):4639-56.

(212) Augst AD, Kong HJ, Mooney DJ. Alginate hydrogels as biomaterials. Macromol Biosci 2006 Aug 7;6(8):623-33.

(213) Francesko A, Tzanov T. Chitin, Chitosan and Derivatives for Wound Healing and Tissue Engineering. In: Nyanhongo GS, Steiner W, Gübitz G, editors. Biofunctionalization of Polymers and their Applications. 125 ed. Springer Berlin Heidelberg; 2011. p. 1-27.

(214) Vaissiere G, Chevallay B, Herbage D, Damour O. Comparative analysis of different collagen-based biomaterials as scaffolds for long-term culture of human fibroblasts. Med Biol Eng Comput 2000 Mar;38(2):205-10.

(215) Yu A, Niiyama H, Kondo S, Yamamoto A, Suzuki R, Kuroyanagi Y. Wound dressing composed of hyaluronic acid and collagen containing EGF or bFGF: comparative culture study. J Biomater Sci Polym Ed 2013;24(8):1015-26.

(216) Palacio ML, Bhushan B. Bioadhesion: a review of concepts and applications. Philos Trans A Math Phys Eng Sci 2012 May 28;370(1967):2321-47.

(217) Komatsu F, Mori R, Uchio Y. Optimum surgical suture material and methods to obtain high tensile strength at knots: problems of conventional knots and the reinforcement effect of adhesive agent. J Orthop Sci 2006;11(1):70-4.

(218) Mehdizadeh M, Yang J. Design strategies and applications of tissue bioadhesives. Macromol Biosci 2013 Mar;13(3):271-88.

(219) Pusateri AE, Holcomb JB, Kheirabadi BS, Alam HB, Wade CE, Ryan KL. Making sense of the preclinical literature on advanced hemostatic products. J Trauma 2006 Mar;60(3):674-82.

(220) Mooney DJ, Silva EA. Tissue Engineering: A glue for biomaterials. Nat Mater 2007 May;6(5):327-8.

(221) Dumville JC, Coulthard P, Worthington HV, Riley P, Patel N, Darcey J, et al. Tissue adhesives for closure of surgical incisions. Cochrane Database Syst Rev 2014;11:CD004287.

(222) Lee JH, Kim HL, Lee MH, Taguchi H, Hyon SH, Park JC. Antimicrobial effect of medical adhesive composed of aldehyded dextran and epsilon-Poly(L-Lysine). J Microbiol Biotechnol 2011 Nov;21(11):1199-202.

(223) Martone WJ, Nichols RL. Recognition, prevention, surveillance, and management of surgical site infections: introduction to the problem and symposium overview. Clinical Infectious Diseases 2001 Sep 1;33(Supplement 2):S67-S68.

(224) Lequaglie C, Giudice G, Marasco R, Morte AD, Gallo M. Use of a sealant to prevent prolonged air leaks after lung resection: a prospective randomized study. J Cardiothorac Surg 2012;7:106.

(225) Losi P, Burchielli S, Spiller D, Finotti V, Kull S, Briganti E, et al. Cyanoacrylate surgical glue as an alternative to suture threads for mesh fixation in hernia repair. J Surg Res 2010 Oct;163(2):e53-e58.

(226) Wang Mg, Tian Ml, Zhao Xf, Nie Ys, Chen J, Shen Ym. Effectiveness and safety of n-butyl-2-cyanoacrylate medical adhesive for noninvasive patch fixation in laparoscopic inguinal hernia repair. Surg Endosc 2013;27(10):3792-8.

(227) Matos-Pérez CR, White JD, Wilker JJ. Polymer composition and substrate influences on the adhesive bonding of a biomimetic, cross-linking polymer. J Am Chem Soc 2012 Jun 6;134(22):9498-505.

(228) Lopez C., Facciolo F., Lequaglie C., Rendina E.A., Saita S., Dell'Amore D., et al. Efficacy and safety of fibrin sealant patch in the treatment of air leakage in thoracic surgery. Minerva Chirurgica 2013 Dec.

(229) Minato N., Katayama Y., Yunoki J., Kawasaki H., Satou H. Hemostatic effectiveness of a new application method for fibrin glue, the "rub-and-spray method", in emergency aortic surgery for acute aortic dissection. Ann Thorac Cardiovasc Surg 2009 Aug.

(230) Wheat JC, Wolf JS, Jr. Advances in bioadhesives, tissue sealants, and hemostatic agents. Urol Clin North Am 2009 May;36(2):265-75, x.

(231) Liu Y, Kopelman D, Wu LQ, Hijji K, Attar I, Preiss-Bloom O, et al. Biomimetic sealant based on gelatin and microbial transglutaminase: an initial in vivo investigation. Journal of Biomedical Materials Research Part B: Applied Biomaterials 2009 Oct 1;91B(1):5-16.

(232) Jallali N, Haji A, Watson CJ. A prospective randomized trial comparing 2-octyl cyanoacrylate to conventional suturing in closure of laparoscopic cholecystectomy incisions. J Laparoendosc Adv Surg Tech A 2004 Aug;14(4):209-11.

(233) Switzer EF, Dinsmore RC, North JH, Jr. Subcuticular closure versus Dermabond: a prospective randomized trial. Am Surg 2003 May;69(5):434-6.

(234) Gilbert TW, Badylak SF, Gusenoff J, Beckman EJ, Clower DM, Daly P, et al. Lysine-derived urethane surgical adhesive prevents seroma formation in a canine abdominoplasty model. Plast Reconstr Surg 2008 Jul;122(1):95-102.

(235) Walgenbach K, Bannasch H, Kalthoff S, Rubin JP. Randomized, prospective study of TissuGlu® surgical adhesive in the management of wound drainage following abdominoplasty. Aesth Plast Surg 2012;36(3):491-6.

(236) D'Andrilli A, Andreetti C, Ibrahim M, Ciccone AM, Venuta F, Mansmann U, et al. A prospective randomized study to assess the efficacy of a surgical sealant to treat air leaks in lung surgery. European Journal of Cardio-Thoracic Surgery 2009 May 1;35(5):817-21.

(237) Lee BP, Dalsin JL, Messersmith PB. Synthesis and gelation of DOPA-modified poly(ethylene glycol) hydrogels. Biomacromolecules 2002 Sep;3(5):1038-47.

(238) Brubaker CE, Kissler H, Wang LJ, Kaufman DB, Messersmith PB. Biological performance of mussel-inspired adhesive in extrahepatic islet transplantation. Biomaterials 2010 Jan 6;31(3):420-7.

(239) Geim AK, Dubonos SV, Grigorieva IV, Novoselov KS, Zhukov AA, Shapoval SY. Microfabricated adhesive mimicking gecko foot-hair. Nat Mater 2003 Jul;2(7):461-3.

(240) Chen K, Xu X, Guo J, Zhang X, Han S, Wang R, et al. Enhanced intracellular delivery and tissue retention of nanoparticles by mussel-inspired surface chemistry. Biomacromolecules 2015 Nov 9;16(11):3574-83.

(241) Lee BP, Chao CY, Nunalee FN, Motan E, Shull KR, Messersmith PB. Rapid gel formation and adhesion in photocurable and biodegradable block copolymers with high dopa content. Macromolecules 2006 Mar 1;39(5):1740-8.

(242) Guvendiren M, Messersmith PB, Shull KR. Self-assembly and adhesion of dopa-modified methacrylic triblock hydrogels. Biomacromolecules 2008 Jan 1;9(1):122-8.

(243) Li Y, Qin M, Li Y, Cao Y, Wang W. Single molecule evidence for the adaptive binding of dopa to different wet surfaces. Langmuir 2014 Apr 22;30(15):4358-66.

(244) Autumn K, Liang YA, Hsieh ST, Zesch W, Chan WP, Kenny TW, et al. Adhesive force of a single gecko foot-hair. Nature 2000 Jun 8;405(6787):681-5.

(245) Pennisi E. Biomechanics. Geckos climb by the hairs of their toes. Science 2000 Jun 9;288(5472):1717-8.

(246) Autumn K, Sitti M, Liang YA, Peattie AM, Hansen WR, Sponberg S, et al. Evidence for van der Waals adhesion in gecko setae. Proc Natl Acad Sci U S A 2002 Sep 17;99(19):12252-6.

(247) Sun W, Neuzil P, Kustandi TS, Oh S, Samper VD. The nature of the gecko lizard adhesive force. Biophys J 2005 Aug 24;89(2):L14-L17.

(248) Jeong HE, Lee JK, Kim HN, Moon SH, Suh KY. A nontransferring dry adhesive with hierarchical polymer nanohairs. Proc Natl Acad Sci U S A 2009 Apr 7;106(14):5639-44.

(249) Kustandi TS, Samper VD, Ng WS, Chong AS, Gao H. Fabrication of a gecko-like hierarchical fibril array using a bonded porous alumina template. Journal of Micromechanics and Microengineering 2007;17(10):N75.

(250) Murphy MP, Kim S, Sitti M. Enhanced Adhesion by Gecko-inspired hierarchical fibrillar adhesives. ACS Appl Mater Interfaces 2009 Apr 29;1(4):849-55.

(251) Kwak MK, Jeong HE, Suh KY. Rational design and enhanced biocompatibility of a dry adhesive medical skin patch. Adv Mater 2011 Sep 8;23(34):3949-53.

(252) Cheung E, Karagozler ME, Sukho P, Byungkyu K, Sitti M. A new endoscopic microcapsule robot using beetle inspired microfibrillar adhesives. 2005 p. 551-7.

(253) Glass P, Cheung E, Sitti M. A Legged Anchoring Mechanism for Capsule Endoscopes Using Micropatterned Adhesives. Biomedical Engineering, IEEE Transactions on 2008 Dec;55(12):2759-67.

(254) Lee H, Lee BP, Messersmith PB. A reversible wet/dry adhesive inspired by mussels and geckos. Nature 2007 Jul 19;448(7151):338-41.

(255) Mahdavi A, Ferreira L, Sundback C, Nichol JW, Chan EP, Carter DJ, et al. A biodegradable and biocompatible gecko-inspired tissue adhesive. Proc Natl Acad Sci U S A 2008 Feb 19;105(7):2307-12.

(256) Bre LP, Zheng Y, Pego AP, Wang W. Taking tissue adhesives to the future: from traditional synthetic to new biomimetic approaches. Biomater Sci 2013;1(3):239-53.

(257) Waite JH. Reverse engineering of bioadhesion in marine mussels. Ann N Y Acad Sci 1999 Jun 18;875:301-9.

(258) Rzepecki LM, Hansen KM, Waite JH. Characterization of a cystine-rich polyphenolic protein family from the blue mussel Mytilus edulis L. The Biological Bulletin 1992 Aug 1;183(1):123-37.

(259) Papov VV, Diamond TV, Biemann K, Waite JH. Hydroxyarginine-containing polyphenolic proteins in the adhesive plaques of the marine mussel mytilus edulis. Journal of Biological Chemistry 1995 Aug 25;270(34):20183-92.

(260) Waite JH, Qin X. Polyphosphoprotein from the adhesive pads of Mytilus edulis. Biochemistry 2001 Mar 1;40(9):2887-93.

(261) Warner SC, Waite JH. Expression of multiple forms of an adhesive plaque protein in an individual mussel, Mytilus edulis. Marine Biology 1999;134(4):729-34.

(262) Anderson TH, Yu J, Estrada A, Hammer MU, Waite JH, Israelachvili JN. The contribution of dopa to substrate-peptide adhesion and internal cohesion of mussel-inspired synthetic peptide films. Adv Funct Mater 2010 Dec 8;20(23):4196-205.

(263) Silverman HG, Roberto FF. Understanding marine mussel adhesion. Mar Biotechnol (NY) 2007 Dec 8;9(6):661-81.

(264) Zhao H, Robertson NB, Jewhurst SA, Waite JH. Probing the adhesive footprints of mytilus californianus byssus. Journal of Biological Chemistry 2006 Apr 21;281(16):11090-6.

(265) Liu C, Glantz G, Livingston E. Fibrin glue as a sealant for high-risk anastomosis in surgery for morbid obesity. OBES SURG 2003;13(1):45-8.

(266) Sapala J, Wood M, Schuhknecht M. Anastomotic leak prophylaxis using a vapor-heated fibrin sealant: report on 738 gastric bypass patients. Obes Surg 2004;14(1):35-42.

(267) Yilmaz HG, Odabasi M, Buyukbayram H, Bac B. Effectiveness of fibrin tissue adhesive for colocolic anastomosis reliability. Ulus Travma Derg 2001 Apr;7(2):87-90.

(268) Krishnamoorthy B, Najam O, Khan UA, Waterworth P, Fildes JE, Yonan N. Randomized prospective study comparing conventional subcuticular skin closure with dermabond skin glue after saphenous vein harvesting. The Annals of Thoracic Surgery 2009 Nov;88(5):1445-9.

(269) Burzio LA, Waite JH. Cross-linking in adhesive quinoproteins: studies with model decapeptides. Biochemistry 2000 Sep 1;39(36):11147-53.

(270) Olmi S, Scaini A, Erba L, Bertolini A, Croce E. Use of fibrin glue (Tissucol) as a hemostatic in laparoscopic conservative treatment of spleen trauma. Surg Endosc 2007;21(11):2051-4.

(271) Yu M, Hwang J, Deming TJ. Role of l-3,4-dihydroxyphenylalanine in mussel adhesive proteins. J Am Chem Soc 1999 Jun 1;121(24):5825-6.

(272) Waite JH. Nature's underwater adhesive specialist. International Journal of Adhesion and Adhesives 1987;7(1):9-14.

(273) Deacon MP, Davis SS, Waite JH, Harding SE. Structure and mucoadhesion of mussel glue protein in dilute solution. Biochemistry 1998 Oct 1;37(40):14108-12.

(274) Huang K, Lee BP, Ingram DR, Messersmith PB. Synthesis and characterization of self-assembling block copolymers containing bioadhesive end groups. Biomacromolecules 2002 Mar 1;3(2):397-406.

(275) Schnurrer J, Lehr CM. Mucoadhesive properties of the mussel adhesive protein. International Journal of Pharmaceutics 1996 Sep 6;141(1-2):251-6.

(276) Karabulut E, Pettersson T, Ankerfors M, Wågberg L. Adhesive layer-by-layer films of carboxymethylated cellulose nanofibril-dopamine covalent bioconjugates inspired by marine mussel threads. ACS Nano 2012 Jun 26;6(6):4731-9.

(277) Kim JH, Lee M, Park CB. Polydopamine as a biomimetic electron gate for artificial photosynthesis. Angew Chem Int Ed 2014 Jun 16;53(25):6364-8.

(278) Lee BP, Messersmith PB, Israelachvili JN, Waite JH. Mussel-inspired adhesives and coatings. Annu Rev Mater Res 2011 Aug 1;41:99-132.

(279) Lee H, Scherer NF, Messersmith PB. Single-molecule mechanics of mussel adhesion. Proc Natl Acad Sci U S A 2006 Aug 29;103(35):12999-3003.

(280) Lee H, Dellatore SM, Miller WM, Messersmith PB. Mussel-inspired surface chemistry for multifunctional coatings. Science 2007 Oct 19;318(5849):426-30.

(281) Wang J, Tahir MN, Kappl M, Tremel W, Metz N, Barz M, et al. Influence of binding-site density in wet bioadhesion. Adv Mater 2008 Oct 17;20(20):3872-6.

(282) Chung H, Glass P, Pothen JM, Sitti M, Washburn NR. Enhanced adhesion of dopamine methacrylamide elastomers via viscoelasticity tuning. Biomacromolecules 2011 Feb 14;12(2):342-7.

(283) Liu Y, Meng H, Konst S, Sarmiento R, Rajachar R, Lee BP. Injectable dopamine-modified poly(ethylene glycol) nanocomposite hydrogel with enhanced adhesive property and bioactivity. ACS Appl Mater Interfaces 2014 Oct 8;6(19):16982-92.

(284) Murphy JL, Vollenweider L, Xu F, Lee BP. Adhesive performance of biomimetic Adhesive-coated biologic scaffolds. Biomacromolecules 2010 Nov 8;11(11):2976-84.

(285) Min Y, Hammond PT. Catechol-modified polyions in layer-by-layer assembly to enhance stability and sustain release of biomolecules: a bioinspired approach. Chem Mater 2011 Dec 27;23(24):5349-57.

(286) Nishida J, Kobayashi M, Takahara A. Light-triggered adhesion of water-soluble polymers with a caged catechol group. ACS Macro Lett 2013 Feb 19;2(2):112-5.

(287) Wang J, Liu C, Lu X, Yin M. Co-polypeptides of 3,4-dihydroxyphenylalanine and l-lysine to mimic marine adhesive protein. Biomaterials 2007 Aug;28(23):3456-68.

(288) Yamamoto H. Synthesis and adhesive studies of marine polypeptides. J Chem Soc , Perkin Trans 1 1987;(0):613-8.

(289) Podsiadlo P, Liu Z, Paterson D, Messersmith PB, Kotov NA. Fusion of seashell nacre and marine bioadhesive analogs: High-strength nanocomposite by layer-by-layer assembly of clay and L-3,4- dihydroxyphenylalanine polymer. 2007;19(7):949-55.

(290) Westwood G, Horton TN, Wilker JJ. Simplified polymer mimics of cross-linking adhesive proteins. Macromolecules 2007 May 1;40(11):3960-4.

(291) White JD, Wilker JJ. Underwater bonding with charged polymer mimics of marine mussel adhesive proteins. Macromolecules 2011 Jul 12;44(13):5085-8.

(292) Yu M, Deming TJ. Synthetic polypeptide mimics of marine adhesives. Macromolecules 1998 Jul 1;31(15):4739-45.

(293) Lee Y, Chung HJ, Yeo S, Ahn CH, Lee H, Messersmith PB, et al. Thermo-sensitive, injectable, and tissue adhesive sol-gel transition hyaluronic acid/pluronic composite hydrogels prepared from bio-inspired catechol-thiol reaction. Soft Matter 2010;6(5):977-83.

(294) Ryu JH, Lee Y, Kong WH, Kim TG, Park TG, Lee H. Catechol-functionalized chitosan/pluronic hydrogels for tissue adhesives and hemostatic materials. Biomacromolecules 2011 Jul 11;12(7):2653-9.

(295) Hoffmann B, Volkmer E, Kokott A, Augat P, Ohnmacht M, Sedlmayr N, et al. Characterisation of a new bioadhesive system based on polysaccharides with the potential to be used as bone glue. J Mater Sci: Mater Med 2009;20(10):2001-9.

(296) Mehdizadeh M, Weng H, Gyawali D, Tang L, Yang J. Injectable citrate-based mussel-inspired tissue bioadhesives with high wet strength for sutureless wound closure. Biomaterials 2012 Nov;33(32):7972-83.

(297) Rose S, Prevoteau A, Elziere P, Hourdet D, Marcellan A, Leibler L. Nanoparticle solutions as adhesives for gels and biological tissues. Nature 2014 Jan 16;505(7483):382-5.

(298) Zhang M, Liu M, Bewick S, Suo Z. Nanoparticles to increase adhesive properties of biologically secreted materials for surface affixing. J Biomed Nanotechnol 2009 Jun;5(3):294-9.

(299) Ju KY, Lee Y, Lee S, Park SB, Lee JK. Bioinspired polymerization of dopamine to generate melanin-like nanoparticles having an excellent free-radical-scavenging property. Biomacromolecules 2011 Feb 14;12(3):625-32.

(300) d'Ischia M, Napolitano A, Pezzella A, Meredith P, Sarna T. Chemical and structural diversity in eumelanins. Unexplored Bio-Optoelectronic Materials. Angew Chem Int Ed Engl 2009;48(22):3914-21.

(301) Lawrie KJ, Meredith P, McGeary RP. Synthesis and polymerization studies of organic-soluble eumelaninsGÇá. Photochemistry and Photobiology 2008 May 1;84(3):632-8.

(302) Postma A, Yan Y, Wang Y, Zelikin AN, Tjipto E, Caruso F. Self-polymerization of dopamine as a versatile and robust technique to prepare polymer capsules. Chem Mater 2009 Jul 28;21(14):3042-4.

(303) Yu X, Fan H, Liu Y, Shi Z, Jin Z. Characterization of carbonized polydopamine nanoparticles suggests ordered supramolecular structure of polydopamine. Langmuir 2014 May 20;30(19):5497-505.

(304) Jiang J, Zhu L, Zhu L, Zhu B, Xu Y. Surface characteristics of a self-polymerized dopamine coating deposited on hydrophobic polymer films. Langmuir 2011 Dec 6;27(23):14180-7.

(305) Wu TF, Hong JD. Dopamine-melanin nanofilms for biomimetic structural coloration. Biomacromolecules 2015 Feb 9;16(2):660-6.

(306) Araújo M, Viveiros R, Correia TR, Correia IdJ, Bonifácio VDB, Casimiro T, et al. Natural melanin: A potential pH-responsive drug release device. International Journal of Pharmaceutics 2014 Jul 20;469(1):140-5.

(307) Zhang R, Fan Q, Yang M, Cheng K, Lu X, Zhang L, et al. Engineering melanin nanoparticles as an efficient drug-delivery system for imaging-guided chemotherapy. Adv Mater 2015 Sep 1;27(34):5063-9.

(308) Rageh MM, El-Gebaly RH, Abou-Shady H, Amin DG. Melanin nanoparticles (MNPs) provide protection against whole-body -irradiation in mice via restoration of hematopoietic tissues. Mol Cell Biochem 2015 Jan;399(1-2):59-69.

(309) Kohri M, Nannichi Y, Taniguchi T, Kishikawa K. Biomimetic non-iridescent structural color materials from polydopamine black particles that mimic melanin granules. J Mater Chem C 2015;3(4):720-4.

(310) Xiao M, Li Y, Allen MC, Deheyn DD, Yue X, Zhao J, et al. Bio-inspired structural colors produced via self-assembly of synthetic melanin nanoparticles. ACS Nano 2015 May 26;9(5):5454-60.

(311) Ju KY, Lee JW, Im GH, Lee S, Pyo J, Park SB, et al. Bio-inspired, melanin-like nanoparticles as a highly efficient contrast agent for T1-weighted magnetic resonance imaging. Biomacromolecules 2013 Oct 14;14(10):3491-7.

(312) Liopo A, Su R, Oraevsky AA. Melanin nanoparticles as a novel contrast agent for optoacoustic tomography. Photoacoustics 2015 Mar;3(1):35-43.

(313) Chassepot A, Ball V. Human serum albumin and other proteins as templating agents for the synthesis of nanosized dopamine-eumelanin. Journal of Colloid and Interface Science 2014 Jan 15;414:97-102.

(314) Vold IM, Kristiansen KA, Christensen BE. A study of the chain stiffness and extension of alginates, in vitro epimerized alginates, and periodate-oxidized alginates using size-exclusion chromatography combined with light scattering and viscosity detectors. Biomacromolecules 2006 Jul;7(7):2136-46.

(315) Lee C, Shin J, Lee JS, Byun E, Ryu JH, Um SH, et al. Bioinspired, calcium-free alginate hydrogels with tunable physical and mechanical properties and improved biocompatibility. Biomacromolecules 2013 Jun 10;14(6):2004-13.

(316) Kastrup CJ, Nahrendorf M, Figueiredo JL, Lee H, Kambhampati S, Lee T, et al. Painting blood vessels and atherosclerotic plaques with an adhesive drug depot. Proceedings of the National Academy of Sciences 2012 Dec 26;109(52):21444-9.

(317) Lee H, Dellatore SM, Miller WM, Messersmith PB. Mussel-Inspired Surface Chemistry for Multifunctional Coatings. Science 2007 Oct 19;318(5849):426-30.

(318) Bernkop-Schnürch A, Steininger S. Synthesis and characterisation of mucoadhesive thiolated polymers. International Journal of Pharmaceutics 2000 Jan 25;194(2):239-47.

(319) Grasdalen H, Larsen B, Smidsrød O. A p.m.r. study of the composition and sequence of uronate residues in alginates. Carbohydrate Research 1979 Jan;68(1):23-31.

(320) Zhang Y, Zhang X, Shi B, Miron R. Membranes for guided tissue and bone regeneration. Annals of Oral and Maxillofacial Surgery 2013 Feb 01;1(1):10.

(321) Khil MS, Cha DI, Kim HY, Kim IS, Bhattarai N. Electrospun nanofibrous polyurethane membrane as wound dressing. Journal of Biomedical Materials Research Part B: Applied Biomaterials 2003 Nov 15;67B(2):675-9.

(322) Sionkowska A. Current research on the blends of natural and synthetic polymers as new biomaterials: Review. Progress in Polymer Science 2011 Sep;36(9):1254-76.

(323) Coda A, Lamberti R, Martorana S. Classification of prosthetics used in hernia repair based on weight and biomaterial. Hernia 2012;16(1):9-20.

(324) Birkenfeld F, Behrens E, Kern M, Gassling V, Wiltfang J. Mechanical properties of collagen membranes: are they sufficient for orbital floor reconstructions? J Craniomaxillofac Surg 2015 Mar;43(2):260-3.

(325) Lindenhayn K, Perka C, Spitzer RS, Heilmann HH, Pommerening K, Mennicke J, et al. Retention of hyaluronic acid in alginate beads: Aspects for in vitro cartilage engineering. J Biomed Mater Res 1999 Feb 1;44(2):149-55.

(326) Ikarashi Y, Tsuchiya T, Nakamura A. Cytotoxicity of medical materials sterilized with vapour-phase hydrogen peroxide. Biomaterials 1995;16(3):177-83.

(327) Shahab U, Ahmad S, Moinuddin, Dixit K, Habib S, Alam K, et al. Hydroxyl radical modification of collagen type II increases its arthritogenicity and immunogenicity. PLoS One 2012 Feb 3;7(2):e31199.

(328) Draye JP, Delaey B, Van de Voorde A, Van Den Bulcke A, De Reu B, Schacht E. In vitro and in vivo biocompatibility of dextran dialdehyde cross-linked gelatin hydrogel films. Biomaterials 1998 Sep;19(18):1677-87.

(329) Sokolsky-Papkov M, Domb AJ, Golenser J. Impact of aldehyde content on Amphotericin B-Dextran imine conjugate toxicity. Biomacromolecules 2006 May 1;7(5):1529-35.

(330) Bilic G, Brubaker C, Messersmith PB, Mallik AS, Quinn TM, Haller C, et al. Injectable candidate sealants for fetal membrane repair: bonding and toxicity in vitro. American Journal of Obstetrics and Gynecology 2010 Jan;202(1):85.

(331) Donati I, Draget KI, Borgogna M, Paoletti S. Tailor-made alginate bearing galactose moieties on mannuronic residues: selective modification achieved by a chemoenzymatic strategy. Biomacromolecules 2005 Jan 1;6(1):88-98.

(332) Costa TG, Younger R, Poe C, Farmer PJ, Szpoganicz B. Studies on synthetic and natural melanin and its affinity for Fe(III) Ion. Bioinorg Chem Appl 2012;2012:712840.

(333) Apte M, Girme G, Bankar A, RaviKumar A, Zinjarde S. 3, 4-dihydroxy-L-phenylalanine-derived melanin from Yarrowia lipolytica mediates the synthesis of silver and gold nanostructures. Journal of Nanobiotechnology 2013;11(1):2.

(334) Centeno SA, Shamir J. Surface enhanced Raman scattering (SERS) and FTIR characterization of the sepia melanin pigment used in works of art. Journal of Molecular Structure 2008 Feb 17;873(1-3):149-59.

(335) Sajjan S, Kulkarni G, Yaligara V, Kyoung L, Karegoudar TB. Purification and physiochemical characterization of melanin pigment from Klebsiella sp. GSK. J Microbiol Biotechnol 2010 Nov;20(11):1513-20.

(336) Tu Yg, Sun Yz, Tian Yg, Xie My, Chen J. Physicochemical characterisation and antioxidant activity of melanin from the muscles of Taihe Black-bone silky fowl (Gallus gallus domesticus Brisson). Food Chemistry 2009 Jun 15;114(4):1345-50.

(337) Zhao P, Zhu KY, Jiang H. Heterologous expression, purification, and biochemical characterization of a greenbug (Schizaphis graminum) acetylcholinesterase encoded by a paralogous gene (ace-1). J Biochem Mol Toxicol 2010 Jan;24(1):51-9.

(338) Schweigert N, Zehnder AJB, Eggen RIL. Chemical properties of catechols and their molecular modes of toxic action in cells, from microorganisms to mammals. Environmental Microbiology 2001 Feb 1;3(2):81-91.

(339) Schweigert N, Zehnder AJB, Eggen RIL. Chemical properties of catechols and their molecular modes of toxic action in cells, from microorganisms to mammals. Environmental Microbiology 2001 Feb 1;3(2):81-91.

(340) Heiduschka P, Blitgen-Heinecke P, Tura A, Kokkinou D, Julien S, Hofmeister S, et al. Melanin precursor 5,6-dihydroxyindol: protective effects and cytotoxicity on retinal cells in vitro and in vivo. Toxicol Pathol 2007 Dec;35(7):1030-8.

(341) PAWELEK JM, LERNER AB. 5,6-Dihydroxyindole is a melanin precursor showing potent cytotoxicity. Nature 1978 Dec 7;276(5688):627-8.

(342) Urabe K, Aroca P, Tsukamoto K, Mascagna D, Palumbo A, Prota G, et al. The inherent cytotoxicity of melanin precursors: a revision. Biochim Biophys Acta 1994 Apr 28;1221(3):272-8.